Polarized light - host location and selection cue in phytophagous insects?

by

Adam James Blake

M.Sc. (Ecology), University of Alberta, 2010

B.Sc. (ENCS), University of Alberta, 2006

Thesis Submitted in Partial Fulfillment of the
Requirements for the Degree of
Doctor of Philosophy

in the
Department of Biological Sciences
Faculty of Science

© Adam James Blake 2020

SIMON FRASER UNIVERSITY

Fall 2020

Copyright in this work rests with the author. Please ensure that any reproduction or re-use is done in accordance with the relevant national copyright legislation.

Declaration of Committee

Name:	**Adam Blake**
Degree:	**Doctor of Philosophy**
Title:	**Polarized light - host location and selection cue in phytophagous insects?**
Committee:	**Chair:** **Ronald Ydenberg** Professor, Biological Sciences
	Gerhard Gries Supervisor Professor, Biological Sciences
	Iñigo Novales Flamarique Committee Member Professor, Biological Sciences
	Almut Kelber Committee Member Professor, Biology Lund University
	Leithen M'Gonigle Examiner Assistant Professor, Biological Sciences
	Martin How External Examiner Royal Society University Research Fellow with Proleptic Lectureship School of Biological Sciences University of Bristol

Abstract

Insect herbivores exploit plant cues to discern host and non-host plants. Studies of visual plant cues have focused on color despite the inherent polarization sensitivity of insect photoreceptors and the information carried by polarization of foliar reflectance, most notably the degree of linear polarization (*DoLP*; 0-100%). The *DoLP* of foliar reflection was hypothesized to be a host plant cue for insects but was never experimentally tested. I investigated the use of these polarization cues by the cabbage white butterfly, *Pieris rapae* (Pieridae). This butterfly has a complex visual system with several different polarization-sensitive photoreceptors, as characterized with electrophysiology and histology. I applied photo polarimetry revealing large differences in the *DoLP* of leaf-reflected light among plant species generally and between host and non-host plants of *P. rapae* specifically. As polarized light cues are directionally dependent, I also tested, and modelled, the effect of approach trajectory on the polarization of plant-reflected light and the resulting attractiveness to *P. rapae,* showing that certain approach trajectories are optimal for discriminating among plants based on these cues. I then demonstrated that *P. rapae* exploit the *DoLP* of foliar reflections to discriminate among plants. In experiments with paired digital plant images that allowed for independent control of polarization, color and intensity, *P. rapae* females preferred images of the host plant cabbage with a low *DoLP* (31%) to images of the non-host plant potato with a high DoLP (50%). These results indicated that the *DoLP* had a greater effect on foraging decisions than the differential color, intensity or shape of the two plant images. To investigate potential neurological mechanisms, I designed behavioral bioassays presenting choices between images that differed in color, intensity and/or *DoLP*. The combined results of these bioassays suggest that several photoreceptor classes are involved and that *P*. *rapae* females process and interpret polarization reflections in a way different from that described for other polarization-sensitive taxa. My work has focused on *P. rapae* and its host plants but there is every reason to believe that the *DoLP* of foliar reflection is an essential plant cue that may commonly be exploited by foraging insect herbivores

Keywords: Behaviour; Insect Vision; Polarization Vision; Photo Polarimetry; Degree of Linear Polarization; *Pieris rapae*

Acknowledgements

I have to thank Dr. Gerhard Gries for taking me on as a student and giving me the opportunity to pursue a “career that will keep [me] entertained all [my] life”. Your enthusiasm for my project findings and for science in general was unwavering even when my own enthusiasm faltered.

I would like to thank Drs. Iñigo Novales Flamarique and Almut Kelber for having agreed to serve on my advisory committee and for having provided expert advice and constructive feedback throughout my study. I thank Dr. Martin J. How and Dr. Leithen M'Gonigle for having agreed to serve as the External Examiner and the Internal Examiner, respectively, of my thesis defense. I also thank Dr. Ronald Ydenberg for chairing the defense.

I must thank Dr. Kentaro Arikawa (Graduate University for Advanced Studies, SOKENDAI) for hosting me in his laboratory and for being so generous with his time and expertise. The brief time I spent in his lab was invaluable for my PhD research and my growth as a vision scientist. I must thank Atsuko Matsushita for assistance and instruction with microscopy and histology, Dr. Doekele G. Stavenga for his immense expertise on the optics of butterfly eyes, and Dr. Primož Pirih for his tireless instruction on epi-illumination light microscopy.

I gratefully acknowledge financial support from Contech, Scotts Canada, BASF Canada, the Natural Sciences and Engineering Research Council of Canada, and Simon Fraser University. Without this support none of this work would have been possible.

My research has benefited greatly from the hard work, dedication, and intellectual contributions of my coauthors and former research assistants Samuel Couture, Dr. Matthew C. Go, Gina S. Hahn, Hayley Grey, Shelby A. Kwok, and Deby McIntosh. You are the most talented group of research assistants I’ve had the pleasure of working with, and I am sure you will have great success in whatever you choose to undertake.

I must recognize the Gries lab. I can think of no better environment to learn, hone my skills, and broaden my understanding. The comradery, conversation, and collaborations have made me a far better scientist. Regine Gries is truly the linchpin of

this group; it is her hard work that paves the way for all of our success. I thank Drs. Sean McCann, Catherine Scott and Bekka Brodie, you at times set an intimidatingly high bar of success for me when I first entered the lab. I would also specifically like to thank current and former lab-mates Sebastian Ibarra, Dr. Daniel Peach, Nathan Derstine, Josh Pol, Asim Renyard, Elton Ko, Yonathan Uriel, and Jaime Chalissery. I cherish the times we've spent together even those spent in "Glorious" distraction.

I thank my friend, colleague, coauthor and bubble-mate Dan Peach for his advice, kindness and for also "being such an all-around fantastic person". The passion for science you inspire in others is truly admirable. The friendship of you and Grace have been a boon in these "interesting" times.

I must thank my parents Lorrie and Tony, and my brother Brendan. I would not be on the path I find myself on today without you.

Lastly, I must thank my wonderful wife Sara. Without her love, understanding, support, and (sometimes not so) gentle encouragement, I would not have reached the end of this PhD. She was always a willing sounding board, and has assisted with more lab and field work than I can ever truly repay. I count myself truly lucky to share this and all my accomplishments with her.

Table of Contents

List of Tables

List of Figures

List of Acronyms

λ	Wavelength
AoP	Axis of polarization (0-180°)
DoLP	Degree of linear polarization (0-100%)
I	intensity
R	Red (575-700 nm, see Fig. 2.2c)
G	Green (450-625 nm, see Fig. 2.2c)
B	Blue (400-525 nm, see Fig. 2.2c)
UV	Ultraviolet (325-400 nm, see Fig. 2.2c)
ϕ	angle between the azimuth of the observer and the light source (see Fig. 2.1)
θ	elevation of light source (see Fig. 2.1)
ω	angle between observer and light source with the plant at its vertex (see Fig. 2.1)
ψ	2-dimensional component of ω perpendicular to the plane passing through both the observer and plant (see Fig. 2.1)
ζ	Elevation of the observer (see Fig. 2.1)
ϕ_{max}	Preferred e-vector of a photoreceptor or *AoP* that is maximally absorbed by a photoreceptor
PS	Polarization sensitivity. Ratio of sensitivity at ϕ_{max} and perpendicular to ϕ_{max}

Chapter 1.

Introduction

Phytophagous insects must locate and select suitable host plants for feeding and oviposition to maximize their fitness (Jaenike 1990). While searching for, evaluating, and eventually accepting host plants, insects exploit diverse plant cues including visual, infrared, olfactory, tactile, and gustatory characteristics (Prokopy and Owens 1983; Renwick and Chew 1994; Finch and Collier 2000; Takács et al. 2008). Visual cues are thought to primarily mediate insect alightment on (host) plants (Prokopy and Owens 1983). Most studies of visual host plant cues have focused on the color or intensity of foliar reflectance, or on leaf shape (Prokopy and Owens 1983; Reeves 2011). Despite this focus, the polarization of foliage reflections has been hypothesized to be an important host plant cue (Kelber et al. 2001).

1.1. Polarized Light

1.1.1. Physics of Polarized Light

Electromagnetic radiation in the ultraviolet (UV), human visible, and the entire electromagnetic spectrum can be viewed as a wave or oscillation in the electric field (Johnsen 2011). As a result, each photon of light can be described with respect to its wavelength and the orientation of this oscillation. The direction of this oscillation is known as the e-vector or axis of polarization (*AoP*). The *AoP* is expressed as an angle relative to the vertical between 0-180°. The *AoP* is limited to 180° as the displacement of the wave is in two opposite directions, and a *AoP* of *X* and 180°+*X* are equivalent. The *AoP* can be decomposed into two perpendicular directional components, for simplicity referred to horizontal and vertical. If the horizontal and the vertical component are in phase with each other, the direction of oscillation does not change as the wave propagates forward and the light is linearly polarized. However, if these two components are out of phase, the resultant *AoP* will change as the wave moves forward. If the components are out of phase by ¼ wavelength (λ), the *AoP* will trace out a circle through one period and the light is circularly polarized. Other phase differences between the

horizontal and the vertical component will result in elliptically polarized light, where the direction of oscillation will trace out an ellipse rather than a circle. Depending on the direction of the phase shift, the polarization of the light will be either right- or left-handed.

The above descriptions apply to single photons but in nature, light is composed of multiple photons and represents a mixture of many different oscillations (Johnsen 2011). When measured over time, the oscillations of photons composing a beam of light from the sun and most other light sources are essentially random and cancel each other out resulting in no net polarization. In this case, the light is said to be unpolarized. However, if the *AoP* of photons is anisotropic or not randomly distributed, we can detect an overall *AoP* of a beam of light (Fig 4.1b). This light is partially polarized and can be viewed as a mixture of light oscillating in the direction of the overall *AoP* and light oscillating in all directions (unpolarized). The strength of this anisotropy in light *AoP* is referred as the degree of polarization. This degree of polarization can be calculated for both circularly and linearly polarized light (*DoLP*; see also section 1.1.3). In an analogy with color, linear polarization can be described by three distinct aspects (Bernard and Wehner 1977; Cronin et al. 2014). *AoP* can be viewed as corresponding with hue, *DoLP* is synonymous with saturation, and both color and polarization share the aspect of intensity (*I*).

While there are some biological sources of circularly polarized light (Cronin et al. 2014), only stomatopods have been demonstrated to detect the handedness of polarization (Templin et al. 2017). Other arthropod photoreceptors perceive elliptically polarized light as linear polarized light with a lower *DoLP*. As polarization of elliptically polarized light approaches circular, the *DoLP* decreases with circularly polarized light being indistinguishable from unpolarized light (Johnsen 2011). Thus for the remainder of my thesis, polarization will refer to linear polarization, unless otherwise noted.

1.1.2. Measuring Polarized Light

Polarimetry is the quantification of the polarization of light (Horváth and Varjú 2004; Foster et al. 2018). At its most basic, polarimetry entails taking and comparing measurements of the intensity of a light source with different orientations of a polarizing filter (a λ/4 retarder may also be involved if characterizing circularly polarized light). Most methods use polarizing filters, light guiding optics, and some form of light detector. By

comparing measurements with a set of formulas, we can determine a set of Stokes parameters (or Stokes vector) which describe the polarization of a given beam of light.

Three measurements of intensity at different orientations of a polarized filter are needed to determine the three Stokes parameters relevant for linearly polarized light (Johnsen 2011). However, most commonly measurements are taken with the filter's transmission axis (orientation with maximum transmission) at 0°, 45°, 90° and 135°. The Stokes parameters, and from them the *AoP* and *DoLP*, can be calculated with these equations below (Eq. 1-5; Horváth and Varjú 2004).

$$I = I_0 + I_{90} = I_{45} + I_{135} \tag{1}$$

$$Q = I_0 - I_{90} \tag{2}$$

$$U = I_{45} - I_{135} \tag{3}$$

$$AoP = \frac{1}{2}\arctan\left(\frac{Q}{U}\right) \tag{4}$$

$$DoLP = \frac{\sqrt{Q^2 + U^2}}{I} \tag{5}$$

Photographic polarimetry is the most commonly used technique for quantifying the intensity measurements required to estimate Stokes parameters (Foster et al. 2018). This technique was initially dubbed video polarimetry because a video camera was used to capture the images used for analyses (Horváth and Varjú 1997). The current method uses multiple exposures taken with a digital camera to measure polarization across a scene. The *DoLP* and *AoP* are then typically depicted through false color images (Foster et al. 2018), however polarization depicting overlays added to a typical photograph offers several advantages such as greater ease of depicting ellipticity, greater ease of distinguishing small differences in *AoP*, and all information can be depicted in a single panel (Gagnon and Marshall 2016). A lack of spectral resolution is a disadvantage of using digital cameras, because color is limited to the typical red, green and blue (RGB) color channels (Foster et al. 2018). Using a spectrometer instead of a camera gives greater spectral resolution but at the cost of spatial resolution. The various methods of polarimetry are extensively reviewed in Horváth and Varjú (2004, Chpt. 1) and Foster et

al. (2018). A more detailed description of the photographic polarimetry methods used in my thesis is presented in Chapter 2.

1.1.3. Sources of Polarized Light

Natural and artificial light are generally unpolarized (Cronin et al. 2014). Polarized light in nature is a consequence of scattering (Johnsen 2011). Whether it be scattering by small particles, or reflections from shiny objects (which are a form of coherent scattering), the underlying optical mechanism is the same. Both types of scattering are common, so while most light sources are unpolarized, partially polarized light is very common in nature (Cronin et al. 2014). There are other sources of polarized light in the natural world (see Können 1985) but they are beyond the scope of this thesis.

When a ray of light is scattered by a particle small in size relative to the incident (original) wavelength, light scattered at 90° to the original direction of travel becomes highly polarized, with a *AoP* perpendicular to a plane including both the original ray and the scattered ray (see Fig. 8.2A and 8.3A in Cronin et al. 2014). For skylight, these small particles are air molecules and their light scattering results in a band of strongly polarized light 90° from the sun (overhead at sunrise or sunset). The *DoLP* is approximately 80% and diminishes as one approaches the sun and the anti-solar point (Johnsen 2011). Multiple scattering prevents this band of light from approaching 100% *DoLP*. Scattering of light is also responsible for the polarization of light underwater, although this generally does not exceed a *DoLP* of 30% (Johnsen 2011). As most light underwater is downwelling from the surface, unless the observer is near the surface during the crepuscular period, the greatest polarization will be seen when looking horizontally through the water column (90° from the main direction of light propagation) and will have a roughly horizontally *AoP*.

Specular reflections from shiny (and not so shiny) surfaces are another mechanism of producing polarization of light in nature (Cronin et al. 2014; Fig. 4.1ab). This mechanism is highly dependent upon the incident angle of the reflected light, with the *DoLP* being maximized when this angle approaches the Brewster's angle (Johnsen 2011). The Brewster's angle is dependent upon the index of refraction of the surface and the surrounding medium. In the case of leaf tissue (1.5) and air (1) this gives an approximate Brewster's angle of 55° (Vanderbilt and Grant 1985; Grant et al. 1993). The

angle of incidence affects the reflections of light in accordance with its *AoP* relative to the surface (see Fig. 8.4 in Johnsen 2011). At the Brewster's angle, only light with an *AoP* parallel to the surface is reflected, resulting in light polarized parallel to that surface. However, this is only one component of the reflection, and typically the diffuse component (see section 1.1.4) lowers the overall *DoLP* (Horváth and Varjú 2004), with natural scenes having *DoLPs* typically ranging between 0-50% (Foster et al. 2018).

1.1.4. Polarized Reflections from Plant Surfaces

Like other shiny surfaces, leaves polarize light through specular reflection (see section 1.1.3) which is strongly directionally dependant (Foster et al. 2018). As inflorescences are generally less shiny than leaves and typically reflect only weakly polarized light (Horváth et al. 2002; van der Kooi et al. 2019), I focus here on reflections from leaves. The reflected *DoLP* depends upon how closely the light's incident angle approximates the Brewster's angle (Johnsen 2011). The incident angle itself is dependent on the solar and observer elevation and azimuth, resulting in shifts in polarization with observer position and time of day (Hegedüs and Horváth 2004; see Fig. 2.1). Reflections from a leaf are polarized in a direction parallel to the surface. However, groups of leaves with many orientations will be polarized tangentially with respect to the sun (Können 1985). Also worth noting is that as this specular reflection occurs at the leaf surface, the incident light does not interact with the interior of the leaf, and the reflected light has a spectral composition similar to that of the incident light (Grant et al. 1993).

In addition to these directional effects, the *DoLP* is affected by surface characteristics of leaves across many spatial scales (Grant 1987). Generally, leaf characteristics that increase surface roughness decrease the *DoLP*, making matte leaves less polarized than shiny leaves (Grant et al. 1993). The cuticle is the first "obstacle" encountered by a light ray striking a leaf (Grant 1987), and accounts for most of the surface detail on small scales (less than 10% of λ). Being extracellular and multilayered, the cuticle forms a protective barrier at the plant-air interface. Its uppermost layer is composed of epicuticular waxes of various chemical compositions that are genetically determined and species-specific. These waxes scatter light, but unlike coherent scattering, the resulting *AoP* of the light is random (Grant et al. 1993; Johnsen 2011). Moreover, undulations, pubescence and other large leaf features affect how light reflects from a leaf surface (Grant et al. 1993). These large features lower the overall

DoLP of a leaf since the differently oriented surfaces will result in specular reflections that are spread across a wider range of directions (Grant et al. 1993).

The *DoLP* of a leaf (or other objects) is also affected by the largely unpolarized diffuse reflection. This diffuse reflectance is produced by light that enters the leaf and is multiply scattered by the tissue, effectively randomizing the polarization of the light (Grant 1987). This light does interact with the internal structure of the leaf, and the absorption of light by pigments can reduce diffuse reflections at certain wavelengths. This lower diffuse reflectance, when taken with the spectrally flat specular reflectance, results in a relatively higher *DoLP* from darker-colored objects (Horváth and Varjú 1997). For this reason, green leaves have a lower *DoLP* in the green range of the human-visible spectrum than in the red and blue range.

1.2. Arthropod Photoreceptors

1.2.1. Rhabdomeric Photoreceptors

To begin the cascade of chemical reactions underlying vision, the chromophore of a visual pigment must first absorb a photon (Johnsen 2011; Cronin et al. 2014). The largely linear molecular structure of these chromophores gives them an inherent dichroism, allowing preferential absorption of photons with an *AoP* parallel to the molecules' long axis. Visual pigments are confined to cellular membranes and the chromophores are held roughly parallel to the cellular membrane. As a result, the polarization sensitivity of a photoreceptor largely depends upon the orientation of these cellular membranes.

In arthropod photoreceptors, these membranes are ordered into finger-like projections known as microvilli which are tightly packed forming the central light guide, or rhabdom, of each ommatidium (Cronin et al. 2014; Fig. 4.1). These microvilli are transverse to the long axis of the ommatidium and the light path (Johnsen 2011). The tubular structure of these microvilli results in the long axis of the chromophores aligning along the long axis of the microvilli in the portions of the membrane parallel to the light path (see Fig 16.1 in Horváth and Varjú 2004). This alignment results in a greater sensitivity to light with an *AoP* parallel to the long axis of the microvilli (Johnsen 2011). Even with a random-distribution photopigment alignments, this form dichroism will result

in light with an *AoP* parallel to the long axis of the microvilli (referred to as the preferred e-vector or ϕ_{max}) being absorbed twice as much than light with an *AoP* perpendicular to this axis. This polarization sensitivity (PS) is expressed as a ratio, with PS being ~2 in the example above. Given the high PS observed in some insect species, it seems that the orientations of these chromophores are constrained in some way to enhance their alignment with the long axis of the microvilli (Horváth and Varjú 2004; Roberts et al. 2011; Cronin et al. 2014).

As visual responses occur at the level of the photoreceptor, these responses are sensitive to polarized light only if the microvilli of a photoreceptor are also aligned. In order to have photoreceptors with high absolute sensitivity to light, the microvilli must be densely packed into the rhabdom. Aligning the microvilli is the most efficient way to achieve this high density (Cronin et al. 2014). Many photoreceptors do have straight microvilli, but many others have microvilli oriented in two different directions, or microvilli that splay out like a fan (Johnsen 2011). In these cases the PS of the photoreceptor is degraded. Twisting of the microvillar axis along the photoreceptor can also reduce PS (see section 1.2.3; Wehner and Bernard 1993; Horváth and Varjú 2004).

1.2.2. Dorsal Rim Area

In many insects, there is a specialized section of the compound eye termed the 'dorsal rim area'. This area faces upwards at a small part of the sky (Cronin et al. 2014), viewing the polarization pattern therein (see section 1.1.3). Many species of insects utilize skylight polarization information during navigation (Labhart and Meyer 1999). The rhabdoms in the dorsal rim area – unlike their counterparts in all other areas of the eye – are short in length (thus enhancing PS), have a large cross-sectional area, and have a wide field of view. Invariably, these ommatidia also possess two photoreceptors with orthogonal microvilli and similar spectral sensitivity, allowing for opponent processing (Cronin et al. 2014; Labhart 2016). The ommatidia of the dorsal rim are arranged in a fan like pattern so that these orthogonal photoreceptors present a variety of ϕ_{max}. The signals originating from ommatidia with similar ϕ_{max} are processed and pooled in POL-neurons of the optic lobe, describing the strength of the polarization signal at *AoP* near 0, 60 and 120°. Comparisons between these three POL-neurons then allow for the determination of skylight *AoP* independent of *DoLP* and intensity, similar to the process of photo

polarimetry described above (see section 1.1.2). This information is used in several navigation-related behaviors linked to polarized light (see section 1.3.1).

1.2.3. Photoreceptor Twist

In many insects, rhabdoms outside of the dorsal rim area are twisted along their longitudinal axis reducing or even demolishing PS (Horváth and Varjú 2004; Labhart 2016). For example, the microvillar direction in honey bees, *Apis mellifera*, shifts by 1°/µm resulting in a twist of ~180° over the length of the rhabdom. Among different insect species, the amount of this twist varies throughout the length of the eye but this twisting greatly reduces the PS of photoreceptors (Horváth and Varjú 2004). A highly polarization-sensitive photoreceptor with microvilli aligned along its length absorbs less unpolarized light, a process known as self-screening. The distal portion of the photoreceptor absorbs most of the light with an *AoP* at or near it's ϕ_{max}, resulting in most of the light available to the proximal portion of the photoreceptor having an AoP perpendicular to it's ϕ_{max} (Cronin et al. 2014). This twisting along the length of the rhabdom nullifies this effect (Horváth and Varjú 2004) and is thought to be an adaptation by diurnal floral foragers enabling them to accurately perceive colors by avoiding the potentially confounding effects of polarization-induced false colors (see section 1.2.5). Although photoreceptor twists are known only from bees, ants, flies and odonates, other insects have other means of degrading PS (see section 1.2.1; Horváth and Varjú 2004; Johnsen 2011).

1.2.4. Ventral Polarization Vision

While there are several prominent examples of insects (most notably the honeybee) with low PS in the ventral compound eye (Horváth and Varjú 2004), it has been recently shown there are many other insects with such PS (Heinloth et al. 2018). However photoreceptor twist remains the default assumption for uncharacterized compound eyes, despite examples of photoreceptor twisting being limited to the Hymenoptera, Odonata and Diptera (Horváth and Varjú 2004; Heinloth et al. 2018). Ventral polarization vision or PS in the ventral eye region ('ventral PS') is well known among aquatic insects that are attracted to horizontally polarized light which is used as a cue for bodies of water (see section 1.3.2; Horváth and Varjú 2004; Heinloth et al. 2018). For example, common backswimmers, *Notonecta glauca* (Hemiptera: Notonoctidae),

possess a specialized region in their ventral eye for detection of polarized light. Other insects associated with aquatic environments with behavioral evidence for ventral PS include members of the Ephemeroptera, Odonata, Diptera, Coleoptera, Trichoptera, and other members of Hemiptera (Horváth and Varjú 2004; Horváth et al. 2014b).

Ventral PS also occurs in terrestrial insects across several taxonomic orders. In Orthoptera, desert locusts, *Schistocerca gregaria*, are known to avoid large bodies of water during migratory flights due to their polarized reflections (see section 1.3.2; Shashar et al. 2005). The eyes of cockroaches (Blattodea) are polarization sensitive outside the dorsal rim area, as demonstrated through a combination of electrophysiological, behavioral and morphological studies (Hegedüs and Horváth 2004; Mishra and Meyer-Rochow 2008). There is a mixture of behavioral and morphological evidence for ventral PS in several hemipteran families (Wakakuwa et al. 2014; Mishra 2015; Paris et al. 2017). Morphological studies have shown photoreceptors with microvilli arrangement suggesting PS in many families of beetles (Wachmann 1977; Gokan and Hosobuchi 1979; Lin 1993; Mishra and Meyer-Rochow 2006; Meyer-Rochow and Mishra 2009), and electrophysiological recordings have demonstrated PS in Curculionidae and Buprestidae (Ilić et al. 2016; Meglič et al. 2020). While not all lepidopterans show evidence for ventral PS (Horváth and Varjú 2004), some have extreme PS (Belušič et al. 2017). Butterflies, in particular, are sensitive to polarized light throughout their compound eyes, with *Papilio* butterflies being particularly well studied (see sections 1.2.5, 1.3.3, 1.4.4; Cronin et al. 2014; Mathejczyk and Wernet 2017; Heinloth et al. 2018). While photoreceptor twisting is known from several higher dipterans, behavioral and electrophysiological investigations have demonstrated PS in the ventral compound eye (Horváth and Varjú 2004; Heinloth et al. 2018). These dipterans seem to be reliant on populations of low-twist photoreceptors in the ventral compound eye, as demonstrated in *Drosophila* (Wernet et al. 2012). Even in the Hymenoptera where examples of photoreceptor twist and low ventral PS can be found, little is known about ventral polarization vision (Zeil et al. 2014) and further examination of the ventral compound eye may yet discover groups with ventral PS. Given these widespread examples among insects and the PS inherent in rhabdomeric photoreceptors, it seems that polarization sensitivity throughout the insect compound eye should be assumed unless proven otherwise.

1.2.5. Perception of Polarized Light

Depending on the number and spectral sensitivity of photoceptors involved, there are several possible ways polarized light might be perceived by an arthropod visual system (Labhart 2016). Just as a single class of photoreceptor is insufficient for color vision (Cronin et al. 2014), comparisons between signals from photoreceptors with the same ϕ_{max} (1D system) are unable to glean any specific information about *DoLP* and *AoP* (see Fig. 2b in Labhart 2016). Even though photoreceptor responses are affected by polarization, these differences are indistinguishable from changes in responses caused by stimulus color or intensity. Opponent processing between two photoreceptors that differ in ϕ_{max} (2D system) in a polarization-opponent (polop) interneuron can allow some discrimination between *DoLP* and *AoP.* However, as photoreceptor responses can be affected by both *DoLP* and *AoP*, there is significant ambiguity among them (How and Marshall 2014; see Fig. 3 in Labhart 2016). Despite this ambiguity, these 2D systems underly many of the polarization-mediated behaviors (see section 1.3), and can allow for "true" polarization vision (perception of *AoP* independent of intensity). Based on theory, a visual system would require three photoreceptors with different ϕ_{max} (3D system) to unambiguously determine *AoP*, *DoLP*, and intensity (Bernard and Wehner 1977; see Fig. 2d in Labhart 2016). Processing of polarization information by polop neurons in the dorsal rim area is the best known example of a 3D system (see Section 1.2.2), however signals from these neurons have a low spatial acuity and are not independent of intensity and color (Labhart 2016).

True polarization vision requires that the response to polarized light is unaffected by the spectral makeup or the intensity of the stimulus light (Labhart 2016). If the photoreceptors compared in opponent processing differ in their spectral sensitivity, this difference results in polarization-induced false colours, where photoreceptor response is dependent on both stimulus color and polarization. The perception of false colors has been demonstrated in *Papilio* butterflies, however the photoreceptors are only moderately sensitive to polarized light (PS~2) (Kelber et al. 2001). False colors should allow butterflies to discriminate between matte and shiny surfaces (Hegedüs and Horváth 2004). Vertebrate host-finding in horseflies and phototaxis in *Daphnia* have also been shown to be dependent upon both color and polarization (Flamarique and Browman 2000; Meglič et al. 2019). The perception of intensity may also be dependent on polarization, as has been shown in foraging *Papilio* (Kinoshita et al. 2011) and in

target detection by fiddler crabs (How et al. 2015). These examples suggest that the visual systems of arthropods combine intensity, color and/or polarization information in ways suited to the biotic and abiotic characteristics of their particular habitats.

One additional aspect of polarized light perception worth mentioning is the distinction between simultaneous and successive mechanisms (Kirschfeld 1972). The mechanisms discussed thus far have focused on simultaneous mechanisms. Successive mechanisms entail comparisons of multiple observations over time after the alignment of *AoP* from an object and the ϕ_{max} of the photoceptor have changed either through rotation of the eye or movement of the arthropod through the environment. Such a mechanism requires only a single polarization-sensitive photoreceptor (Horváth and Varjú 2004) and is functionally similar to photographic polarimetry (see section 1.1.2). This behavior has been demonstrated in stomatopod crustaceans where these organism use torsional movements of their eyes to maximize polarization contrast (Daly et al. 2016). Compared to other visual subsystems, successive mechanisms require a greater degree of neural processing and integration making them a less parsimonious explanation (Labhart 2016).

1.3. Polarization-Related Behaviors

1.3.1. Navigation

As mentioned previously (see section 1.2.3), many insects use skylight polarization (see section 1.1.3) as a navigational cue (Horváth and Varjú 2004; Mathejczyk and Wernet 2017). Skylight navigation is prevalent among central-place foragers such as bees, ants and wasps that return to their nest after foraging bouts (Zeil et al. 2014; Mathejczyk and Wernet 2017). This navigation was first demonstrated in honey bees that integrate celestial polarization and solar position as a direction reference in their in-hive “waggle dance” which informs nestmates about the location of a food source. Desert ants, *Cataglyphis bicolor,* are perhaps best suited to investigate the use of skylight polarization as a navigational cue (Mathejczyk and Wernet 2017). Returning to their nest without the aid of landmarks, these ants – using “path integration” – chart a direct straight line path relying heavily on celestial polarization (Horváth and Varjú 2004; Zeil et al. 2014; Mathejczyk and Wernet 2017). Polarized light navigation also occurs in other species of bees and ants (Zeil et al. 2014).

Unlike ants and bees (Hymenoptera), most insects do not repeatedly travel back and forth to a central location (Mathejczyk and Wernet 2017). Behavioral experiments with these non-hymenopterans are typically based on observations of spontaneous behaviors (i.e., turning) in response to rotations of a polarized filter. These “polarotactic” behavioral responses have been noted in many insects including monarch butterflies (*Danaus plexippus*), flies (*Drosophila, Musca*), crickets, locusts and scarab beetles (Horváth and Varjú 2004; Mathejczyk and Wernet 2017). Anatomical investigations of the dorsal rim area in many taxa suggests that the use of polarized light as a navigational cue is common among insects (Labhart and Meyer 1999).

1.3.2. Water Location and Avoidance

Insects living in or near aquatic habitats are commonly attracted to sources of horizontally polarized light (Horváth and Varjú 2004; Mathejczyk and Wernet 2017; Heinloth et al. 2018). Light reflecting off the water surface becomes horizontally polarized, often to a high degree (see section 1.1.3), and can be a useful cue for insects seeking bodies of water (Wehner 2001). The backswimmer, *Notonecta glauca*, exemplifies this mode of resource location but this mode has also been noted in a myriad of other water associated insects (see section 1.2.4; Horváth and Varjú 2004). This attraction results in many dark shiny man-made surfaces such as wet asphalt, cars, and glass buildings becoming ecological traps, as they are mistaken for water bodies during oviposition and other behaviors since they produce horizontally polarized light. This phenomenon is known as polarized light pollution (Horváth et al. 2009, 2014b). For certain insects living at or near the water-air interface polarized reflections could interfere with other visual tasks (Heinloth et al. 2018), and it seems that in water striders (*Gerris lacustris*) their ventral eye is adapted to filter out these reflections (Horváth and Varjú 2004). Horizontally polarized light can also be used as a cue to avoid water (Wehner 2001), as shown for flying locust swarms that alter course to avoid crossing large water bodies (see section 1.2.4, Shashar et al. 2005).

1.3.3. Intraspecific Polarization Signaling

The body structures of many arthropods produce polarized light patterns which likely function in intraspecific signaling (Cronin 2018). This possibly covert communication channel is especially intriguing but its investigation can lead to erroneous

conclusions (Marshall et al. 2014) since polarization is difficult to manipulate independent of color and intensity (Foster et al. 2018). Nonetheless, there are examples among insects and other arthropods suggesting the use of polarized light as a communication signal. For example, the wings of many butterflies produce highly polarized light through iridescence which likely has a signal function for polarization-sensitive conspecifics (Mathejczyk and Wernet 2017). In the nymphalid butterfly *Heliconius cydno*, a depolarizing filter altered the preference of approaching males (Sweeney et al. 2003). However these shifts in mate preference may have been due to filter-related changes in light intensity or color (Horváth and Varjú 2004). Further supporting polarized light as a intraspecific signal is findings that the wings of butterflies living in forests, where polarized light is rare, are far more likely to reflect polarized light than the wings of butterflies living in open habitats (Douglas et al. 2007). Crustaceans are also known to use polarized structures in courtship displays (Marshall et al. 2019). Stomatopod crustaceans, known for their polarization vision, possess a number of polarized-light producing structures used during courtship. Experimentally reducing the *DoLP* of this presumed signal alters mate-choice, however the effects of *DoLP* and color could not be completely disentangled (Chiou et al. 2011). Fiddler crabs too have polarized light-producing body structures and are known to be sensitive to *AoP* and *DoLP* (Zeil and Hofmann, 2001), but in this case polarization may just be a component of a crab's contrast with the background (Marshall et al. 2019).

1.3.4. Object Detection

Polarized light (or the lack thereof) can be used for detecting and evaluating objects in the environment, whether they be predators, prey, or hosts. Several crustaceans are known to react to a looming stimulus, thought to mimic the approach of a predator, which is visible only via polarization sensitivity (Cronin et al. 2014; Cronin 2018). These types of stimuli are typically presented via a LCD monitor with its front polarizer removed, with increasing pixel values generating increasing shifts in *AoP* from baseline (Foster et al. 2018). The pure-polarization contrasts and the highly polarized light (100% *DoLP*) of these stimuli are atypical of those that these animals would naturally encounter in their habitat (Cronin et al. 2014). However, effects of both *DoLP* and *AoP* on predator avoidance responses by fiddler crabs have been demonstrated in a natural setting (How et al. 2015). At least in fiddler crabs, this response to the object

seems to be driven by both intensity and polarization contrast which are processed separately (Smithers et al. 2019). The polarization contrast of objects may also be a useful cue for prey detection, and could be exploited by aquatic and other water associated insects and their larvae (Marshall et al. 2019). However, polarization contrast requires the rather uniform background found in aquatic environments and moist mudflats but not in terrestrial environments with their complex mosaic of polarized reflections (Marshall et al. 2019; see section 1.1.3).

Animals in terrestrial environments use polarized light to locate both plant and animal hosts. Horseflies in search for bodies of water or vertebrate hosts respond to polarized surfaces (Horváth et al. 2014a). Horseflies seeking vertebrate hosts are attracted to surface reflections with a high *DoLP* regardless of *AoP*, likely because the various parts of an animal host produce different *AoP*s (Egri et al. 2012b). Even though dark- and light-colored hosts are equally suitable for blood feeding, horseflies seek hosts with darker pelage as they have a higher *DoLP* (Horváth et al. 2010; Egri et al. 2012a). It should also be noted that black and white patterns, most notably the zebra stripes, can make host less attractive to horseflies and other blood feeding flies (Egri et al. 2012a; Blahó et al. 2012).

Insect herbivores may also use polarized light as a cue to help them locate and evaluate potential host plants. This use has been best demonstrated with *Papilio* butterflies, where polarization-induced false colors should allow these butterflies to discriminate between shiny and matte leaves (Kelber et al. 2001; Horváth et al. 2002; Hegedüs and Horváth 2004). However, the test stimuli presented in these experiments, had a *DoLP* much higher than that of plant-reflected light. Discrimination among real plants has yet to be demonstrated (but see Chapters 4 and 5). As polarization sensitivity in the ventral compound eye is quite common among insects (see section 1.2.4), groups other than *Papilio* butterflies can be expected to exploit the polarization of plant-reflected light as a host plant cue (Kelber et al. 2001).

1.4. Cabbage White Butterfly

1.4.1. Geographic Origin and Global Spread

The cabbage white butterfly, *Pieris rapae* (Linnaeus, 1758), also known as the small white, small cabbage white, or imported cabbageworm, is present on all continents with the exception of South America and Antarctica. Its global spread has followed human movements and the domestication and cultivation of *Brassica* crops (Ryan et al. 2019). The two recognized subspecies *P. rapae rapae* (Linnaeus, 1758) and *P. rapae crucivora Boisduval* 1836 correspond to the European and Asian populations, respectively. The most notable difference between the two subspecies is the greater UV wing reflectance of *P. r. crucivora* females relative to both male conspecifics and *P. r. rapae* females (Fig. 3.2; see section 1.4.2; Obara and Majerus 2000). As cabbage white butterflies have the greatest genetic diversity in the eastern Mediterranean and Levant region, this is likely their ancestral range where both subspecies originated (Fukano et al. 2012; Ryan et al. 2019). According to genetic analysis, divergence between the two subspecies occurred ~800 CE, likely related to trade along the Silk Road and diversification of *Brassica* crops (Ryan et al. 2019; see Fig. 2). Greater trade between China and Russia facilitated the expansion of *P. r. crucivora* to Siberia in ~1700 CE. European colonization then led to the introduction of European *P. rapae rapae* to North Africa in ~1800 CE, and to eastern North America in ~1860 CE. The completion of rail lines across North America in the 1870s likely then resulted in an introduction of butterflies from eastern North America to central California. Members of this western population were inadvertently introduced into New Zealand in ~1924 CE, further spreading to Australia in ~1932 CE.

1.4.2. Life History

The cabbage white butterfly, along with other *Pieris* butterflies (Pieridae: Lepidoptera), has a long evolutionary history with plants in the order Brassicales (Edger et al. 2015). Cabbage white butterflies exploit host plants in the family Brassicaceae, and other plants from the Brassicales (Chew and Renwick 1995). The cabbage white butterfly can be an economic pest of "*Brassica*" vegetables (Maltais et al. 1998). It is multivoltine through much of its range, overwintering as pupae. Eggs are laid singly on host plants, and progress through five larval instars before pupation (Jones 1977), with

the full lifecycle being complete in approximately four weeks depending on temperature (Webb and Shelton 1988). Larvae are well adapted to the glucosinolate defenses of their host plants, even requiring their ingestion to complete development (Renwick and Lopez 1999). Early instars are unlikely to survive migrating to new host plants, and rely upon maternal host plant choice (Courtney 1986). While egg mortality is low, early instars have high mortality. Subsequent instars are more likely to survive but final instar larvae and pupae suffer extensive mortality from parasitoids (Courtney 1986). Larvae are also attacked by generalist insect predators, vertebrate predators and micro-parasites such bacteria, fungi, and viruses, most notably the trans-ovarially transmitted granulosis virus, which also hampers colony rearing (Courtney 1986).

Behavioural activities of cabbage white butterflies such as dispersal (see section 1.4.3), oviposition (see section 1.4.3), feeding and mating are well documented (Courtney 1986). In pierids, adults feed mainly opportunistically as they rely on energy reserves from larval feeding (Courtney 1986). When searching for females, males generally disperse to areas with a high chance of mate encounters such as patches of flowers or host plants (Courtney 1986). Adult females generally mate within one day of emergence, with peak oviposition occurring 3-10 days post emergence (Jones 1977; Webb and Shelton 1988). Males initially recognize females through sexually dimorphic wings, with the wings of female *P. r. crucivora* having relatively high UV reflectance relative to males (Fig. 3.2). Males also engage in “flutter responses” to deter the incorrect approaches of other males (Obara 1970; Obara and Majerus 2000; Giraldo and Stavenga 2007). Females first evaluate males during flight displays, with visual cues from the dorsal wing surface being most important (Morehouse and Rutowski 2010). Following the flight display the pair lands and the male approaches the female, with mate acceptance being primarily mediated by volatile chemical cues (McQueen and Morehouse 2018). Both males and females mate multiple times (Wedell and Cook 1999) over their three to four week lifespan (Webb and Shelton 1988).

1.4.3. Host Finding

Dispersal flights in search of suitable host plant habitat represent the first stage of host plant finding by female cabbage white butterflies (Hern et al. 1996). Females searching for host plants disperse in a linear direction, with the move length and number of eggs laid decreasing with increased host plant density (Jones 1977; Hern et al. 1996).

This type of behavioral response to host plant density results in longer residency time in dense patches and fewer eggs being laid on any one host plant. The strategy is thought to better “spread the risk”, and may be an adaptation to host plants occurring in ephemeral habitats. Cabbage white butterflies can disperse 250-600 m over the course of a day, with one general direction being preferred (Jones et al. 1980). These “oviposition flights” occur only in sunny warm weather, with most eggs being laid in the late morning to early afternoon (Hern et al. 1996).

The second stage of host finding involves the approach towards, and the alighting on plants. While foraging females are unable to orient to host plants at distances beyond 1 m (Fahrig and Paloheimo 1987), below 1 m their approach seems to be guided primarily by visual plant cues, primarily color (Hern et al. 1996). Leaf size or shape did not affect the females’ preference when other variables were held constant (Renwick and Radke 1988). Green objects are preferred both during approach (Hern et al. 1996) and oviposition (Kelber 2001), but female can learn to associate hosts with different colors (Snell-Rood and Papaj 2009). Leaf color can be indicative of host plant suitability, with bluer cabbage plants containing fewer chemical defenses and allowing for better larval performance (Green et al. 2015). While gravid females prefer green objects, they do not visually discriminate between host plants (Ikeura et al. 2010; Green et al. 2015).

Volatile olfactory cues are also thought to play some role in host plant location in pierids (Hern et al. 1996) but there is little evidence for volatile plant odorants attracting cabbage white butterflies (Chew and Renwick 1995; Hern et al. 1996). While several host plant odorants, including isothiocyanates, elicit antennal responses, these responses do not seem to affect behavior (Chew and Renwick 1995). In a lab setting, females deprived of host plant odor failed to discriminate between hosts, but this failure has not been linked to any particular chemicals (Ikeura et al. 2010). Conversely, odorants from damaged cabbage plants and non-host odorants are deterrent (Hern et al. 1996). The role of olfaction for host plant location by cabbage white butterflies remains largely unknown.

Better understood is the role of tactile cues or contact chemical cues in host plant acceptance by cabbage white butterflies (Chew and Renwick 1995; Hern et al. 1996). Host plants contact chemicals can both stimulate or deter oviposition by female

butterflies. Glucosinolates of *Brassica* host plants are major oviposition stimulants (see Table 6.1 in Chew and Renwick 1995), with aromatic glucosinolates being more stimulatory than aliphatic ones (Chew and Renwick 1995; Hern et al. 1996). Glucobrassicin, in particular, has been noted to be a powerful oviposition stimulant. The effects of oviposition stimulants are countered by effects of oviposition deterrents. These deterrents included coumarin and rutin from non-brassicaceous plants (Hern et al. 1996), as well as various glycosides from non-acceptable brassicaceous hosts (see Table 6.2 in Chew and Renwick 1995). Female cabbage white butterflies also deposit an oviposition deterring pheromone during egg laying, but it seems to play a minor role in host plant acceptance relative to other stimulants and deterrents (Hern et al. 1996).

1.4.4. Visual System

The compound eye of cabbage white butterflies is made up of a mosaic of three ommatidial types which in the ventral eye are easily identified by the trapezoidal (I), square (II), or rectangular (III) arrangement of pigment clusters bordering the rhabdom (Qiu et al. 2002; Chapter 3; Table 3.1). Like other pierid and papilionid butterflies (Wakakuwa et al. 2007), cabbage whites have a 3-tiered fused rhabdom (Shimohigashi and Tominaga 1991). In the distal and proximal portions of the rhabdom, photoreceptors R1-4 and R5-8 contribute microvilli, respectively. The R9 cell body is located basally and it is only in this very basal portion that the R9 photoreceptor contributes to the rhabdom (Figs. 3.1, 3.4). Intracellular recordings of photoreceptors in the ventral compound eye of *P. r. crucivora* have revealed at least eight spectral classes (Qiu and Arikawa 2003ab; Arikawa et al. 2005), however only four opsins (PrUV, PrV, PrB, PrL) are expressed (Wakakuwa et al. 2004; Arikawa et al. 2005; Table 3.1).

Photoreceptors R1,2 express different shortwave opsins depending on ommatidial type (Table 3.1; Fig. 3.10; Arikawa et al. 2005). In type I ommatidia, one of these two photoreceptors expresses the blue-light-absorbing PrB and the other the UV-light-absorbing PrUV. In type III ommatidia, both of these photoreceptors express PrUV. The violet-light-absorbing PrV is expressed in R1,2 in both male and female *P. rapae*, but there is a sexual dimorphism in the spectral sensitivity of these receptors (Fig. 3.2b; Qiu and Arikawa 2003b).This sexual dimorphism can be explained by the absorbance of a fluorescing pigment in the R1,2 photoreceptors of male butterflies. Fluorescence microscopy with blue-violet excitation reveals the presence of this pigment in type II

ommatidia of males but not of females. This pigment acts as a violet-absorbing filter on the PrV-expressing R1 and R2 photoreceptors (Arikawa et al. 2005). This filtering, or lack thereof, results in violet-sensitive photoreceptors in females, and in a double-peaked blue (dB) photoreceptors in males.

Photoreceptors R3-8 (and presumably R9) express PrL, which absorbs maximally in the green-yellow range (Wakakuwa et al. 2004). However, single cell recordings reveal multiple spectral classes of red-sensitive photoreceptors (Table 3.1; Fig. 3.10; Qiu and Arikawa 2003a). Observations from live butterflies under epi-illumination light microscopy show ommatidia with pale-red and deep-red eyeshine (Qiu et al. 2002). Microspectrophotometry on histological sections revealed pale-red pigment clusters in type I and III ommatidia, and deep-red pigments in type II ommatidia, corresponding well with the colour of the eyeshine (Stavenga and Arikawa 2011). As a portion of the light propagating down the rhabdom travels outside the rhabdom boundary (Stavenga 2006), these perirhabdomal pigment clusters filter the light reaching photoreceptors R5-8 and shift their spectral sensitivity towards the red end of the spectrum, with the pale-red and deep-red pigments shifting peak sensitivity to 620 and 640 nm, respectively (Qiu and Arikawa 2003a; Stavenga and Arikawa 2011).

Like in most butterflies, the photoreceptors of the cabbage white do not twist along their length and the microvillar axis is aligned along the length of the rhabdom (Ribi 1978; Shimohigashi and Tominaga 1991; Qiu et al. 2002). This alignment should result in PS, however the microvilli of some photoreceptors are arranged in a fan-like pattern which degrades PS. The PS of cabbage white photoreceptors have been confirmed through single cell recordings (Qiu and Arikawa 2003; Chapter 3).

1.5. Hypotheses and Objectives

In Chapter 2, I use photographic polarimetry (see section 1.1.2) to characterize *AoP* and *DoLP* of foliar reflections. If *DoLP* were to be an important host plant cue, at least for female *P. rapae*, host and non-host plants should have different *DoLP*. Foliar polarization of whole plants are affected by the position of the observer and the light source but these effects are not well understood. The objectives of chapter 2 were to: (1) compare polarization measurement among host and non-hosts of the cabbage white butterfly, and (2) measure select plant species under different light source and observer

positions allowing for modeling of the effect of approach trajectory on plant attractiveness to host-plant-seeking cabbage white females (see Chapter 4 for explanation of attractive polarization cues).

In Chapter 3, I tested the hypothesis that the sexually dimorphic dB photoreceptors (see section 1.4.4) are an adaptation to enhance discrimination of UV light reflected from the wings of females (see section 1.4.2). If the dB photoreceptor were to be such an adaptation, eyes of the ancestral *P. r. rapae* subspecies (see section 1.4.1) should lack this photoreceptor type. I performed a comparative study of *P. r. rapae* and *P. r. crucivora* compound eyes analyzing genetic, spectrophotometric, microscopic, and *in vivo* eyeshine observations. I took new measurements for *P. r. rapae* but used existing data for *P. r. crucivora*. I also re-examined previously obtained electrophysiological recordings of *P. r. crucivora* photoreceptors to refine estimates of spectral and polarization sensitivities.

In Chapter 4, I tested the long-standing hypothesis that phytophagous insects discriminate between host plants on the basis of their polarized light reflections (Kelber et al. 2001). To test this hypothesis, I developed a novel display system (Fig. 4.3) to create identical plant images with divergent *DoLP* or *AoP* as test stimuli for behavioral bioassays. The objectives of this chapter were to (1) demonstrate that cabbage white females discriminate between host plants on the basis of *DoLP*, and to characterize the attractive range of host plant *DoLP* and *AoP*.

In Chapter 5, again making use of my novel stimulus display system for behavioral bioassays (Fig. 4.3), I designed experiments to characterize the neurological mechanism(s) that allow(s) *P. rapae* to discriminate between stimuli with divergent *DoLP*. Emulating the work of Kinoshita et al. (2011), my first objective was to determine whether cabbage white females perceive differential *DoLP* as differences in stimulus intensity or color by investigating the effect of differential stimulus intensity on color and polarization preferences. My second objective was to identify the photoreceptors involved in this *DoLP* discrimination by presenting a series of choices between stimuli divergent in *DoLP* but with their color manipulated to minimize the stimulation of the butterflies' blue, red, or blue and red photoreceptors. I also modeled the catch of all photoreceptors aiming to explain observed behavioral responses.

1.6. References

Arikawa K, Wakakuwa M, Qiu X, et al (2005) Sexual dimorphism of short-wavelength photoreceptors in the small white butterfly, *Pieris rapae crucivora*. J Neurosci 25:5935–5942. https://doi.org/10.1523/JNEUROSCI.1364-05.2005

Belušič G, Šporar K, Meglič A (2017) Extreme polarisation sensitivity in the retina of the corn borer moth *Ostrinia*. J Exp Biol 220:2047–2056. https://doi.org/10.1242/jeb.153718

Bernard GD, Wehner R (1977) Functional similarities between polarization vision and color vision. Vision Res 17:1019–1028. https://doi.org/10.1016/0042-6989(77)90005-0

Blahó M, Egri Á, Bahidszki L, et al (2012) Spottier targets are less attractive to tabanid flies: On the tabanid-repellency of spotty fur patterns. PLoS ONE 7:e41138. https://doi.org/10.1371/journal.pone.0041138

Chew FS, Renwick JAA (1995) Host plant choice in *Pieris* butterflies. In: Chemical ecology of insects 2. Springer, Boston, MA, pp 214–238

Chiou T-H, Marshall NJ, Caldwell RL, Cronin TW (2011) Changes in light-reflecting properties of signalling appendages alter mate choice behaviour in a stomatopod crustacean *Haptosquilla trispinosa*. Mar Freshw Behav Phy 44:1–11. https://doi.org/10.1080/10236244.2010.546064

Courtney SP (1986) The ecology of pierid butterflies: Dynamics and interactions. In: Advances in Ecological Research. Elsevier, pp 51–131

Cronin TW (2018) A different view: sensory drive in the polarized-light realm. Curr Zool 64:513–523. https://doi.org/10.1093/cz/zoy040

Cronin TW, Johnsen S, Marshall NJ, Warrant EJ (2014) Visual Ecology. Princeton University Press, Princeton, New Jersey

Daly, I.M., How, M.J., Partridge, J.C., Temple, S.E., Marshall, N.J., Cronin, T.W. & Roberts, N.W. 2016. Dynamic polarization vision in mantis shrimps. Nat Commun 7:12140. https://doi.org/10.1038/ncomms12140

Douglas JM, Cronin TW, Chiou T-H, Dominy NJ (2007) Light habitats and the role of polarized iridescence in the sensory ecology of neotropical nymphalid butterflies (Lepidoptera: Nymphalidae). J Exp Biol 210:788–799. https://doi.org/10.1242/jeb.02713

Edger PP, Heidel-Fischer HM, Bekaert M, et al (2015) The butterfly plant arms-race escalated by gene and genome duplications. Proc Natl Acad Sci 112:8362–8366. https://doi.org/10.1073/pnas.1503926112

Egri A, Blaho M, Kriska G, et al (2012a) Polarotactic tabanids find striped patterns with brightness and/or polarization modulation least attractive: an advantage of zebra stripes. J Exp Biol 215:736–745. https://doi.org/10.1242/jeb.065540

Egri Á, Blahó M, Sándor A, et al (2012b) New kind of polarotaxis governed by degree of polarization: attraction of tabanid flies to differently polarizing host animals and water surfaces. Naturwissenschaften 99:407–416. https://doi.org/10.1007/s00114-012-0916-2

Fahrig L, Paloheimo JE (1987) Interpatch dispersal of the cabbage butterfly. Can J Zool 65:616–622. https://doi.org/10.1139/z87-096

Finch S, Collier RH (2000) Host-plant selection by insects – a theory based on "appropriate/inappropriate landings" by pest insects of cruciferous plants. Entomol Exp Appl 96:91–102. https://doi.org/10.1046/j.1570-7458.2000.00684.x

Flamarique IN, Browman HI (2000) Wavelength-dependent polarization orientation in *Daphnia*. J Comp Physiol A 186:1073–1087. https://doi.org/10.1007/s003590000162

Foster JJ, Temple SE, How MJ, et al (2018) Polarisation vision: overcoming challenges of working with a property of light we barely see. Sci Nat 105:27. https://doi.org/10.1007/s00114-018-1551-3

Fukano Y, Satoh T, Hirota T, et al (2012) Geographic expansion of the cabbage butterfly (*Pieris rapae*) and the evolution of highly UV-reflecting females: European origin of UV reflecting *Pieris* butterfly. Insect Sci 19:239–246. https://doi.org/10.1111/j.1744-7917.2011.01441.x

Gagnon YL, Marshall NJ (2016) Intuitive representation of photopolarimetric data using the polarization ellipse. J Exp Biol 219:2430–2434. https://doi.org/10.1242/jeb.139139

Giraldo MA, Stavenga DG (2007) Sexual dichroism and pigment localization in the wing scales of *Pieris rapae* butterflies. Proc R Soc B Biol Sci 274:97–102. https://doi.org/10.1098/rspb.2006.3708

Gokan N, Hosobuchi K (1979) Fine structure of the compound eyes of longicorn beetles (Coleoptera: Cerambycidae). Appl Entomol Zool 14:12–27. https://doi.org/10.1303/aez.14.12

Grant L (1987) Diffuse and specular characteristics of leaf reflectance. Remote Sens Environ 22:309–322. https://doi.org/10.1016/0034-4257(87)90064-2

Grant L, Daughtry CST, Vanderbilt VC (1993) Polarized and specular reflectance variation with leaf surface features. Physiol Plant 88:1–9. https://doi.org/10.1111/j.1399-3054.1993.tb01753.x

Green JP, Foster R, Wilkins L, et al (2015) Leaf colour as a signal of chemical defence to insect herbivores in wild cabbage (*Brassica oleracea*). PLoS One 10:e0136884. https://doi.org/10.1371/journal.pone.0136884

Hegedüs R, Horváth G (2004) Polarizational colours could help polarization-dependent colour vision systems to discriminate between shiny and matt surfaces, but cannot unambiguously code surface orientation. Vision Res 44:2337–2348. https://doi.org/10.1016/j.visres.2004.05.004

Heinloth T, Uhlhorn J, Wernet MF (2018) Insect responses to linearly polarized reflections: orphan behaviors without neural circuits. Front Cell Neurosci 12:50. https://doi.org/10.3389/fncel.2018.00050

Hern A, Edwards-Jones G, Mckinlay RG (1996) A review of the pre-oviposition behaviour of small cabbage white butterfly, *Pieris rapae* (Lepidoptera: Pieridae). Ann Appl Biol 128:349–371. https://doi.org/10.1111/j.1744-7348.1996.tb07328.x

Horváth G, Blahó M, Kriska G, et al (2010) An unexpected advantage of whiteness in horses: the most horsefly-proof horse has a depolarizing white coat. Proc R Soc B Biol Sci 277:1643–1650. https://doi.org/10.1098/rspb.2009.2202

Horváth G, Egri Á, Blahó M (2014a) Linearly Polarized Light as a Guiding Cue for Water Detection and Host Finding in Tabanid Flies. In: Horváth G (ed) Polarized Light and Polarization Vision in Animal Sciences. Springer Berlin Heidelberg, Berlin, Heidelberg, pp 525–559

Horváth G, Gál J, Labhart T, Wehner R (2002) Does reflection polarization by plants influence colour perception in insects? Polarimetric measurements applied to a polarization-sensitive model retina of *Papilio* butterflies. J Exp Biol 205:3281–3298

Horváth G, Kriska G, Malik P, Robertson B (2009) Polarized light pollution: a new kind of ecological photopollution. Front Ecol Environ 7:317–325. https://doi.org/10.1890/080129

Horváth G, Kriska G, Robertson B (2014b) Anthropogenic Polarization and Polarized Light Pollution Inducing Polarized Ecological Traps. In: Horváth G (ed) Polarized Light and Polarization Vision in Animal Sciences. Springer Berlin Heidelberg, Berlin, Heidelberg, pp 443–513

Horváth G, Varjú D (1997) Polarization pattern of freshwater habitats recorded by video polarimetry in red, green and blue spectral ranges and its relevance for water detection by aquatic insects. J Exp Biol 200:1155–1163

Horváth G, Varjú D (2004) Polarized Light in Animal Vision: Polarization Patterns in Nature. Springer, New York

How MJ, Christy JH, Temple SE, et al (2015) Target detection is enhanced by polarization vision in a fiddler crab. Curr Biol 25:3069–3073. https://doi.org/10.1016/j.cub.2015.09.073

How MJ, Marshall NJ (2014) Polarization distance: a framework for modelling object detection by polarization vision systems. Proc R Soc B Biol Sci 281:20131632. https://doi.org/10.1098/rspb.2013.1632

Ikeura H, Kobayashi F, Hayata Y (2010) How do *Pieris rapae* search for Brassicaceae host plants? Biochem Syst Ecol 38:1199–1203. https://doi.org/10.1016/j.bse.2010.12.007

Ilić M, Pirih P, Belušič G (2016) Four photoreceptor classes in the open rhabdom eye of the red palm weevil, *Rynchophorus ferrugineus* Olivier. J Comp Physiol A 202:203–213. https://doi.org/10.1007/s00359-015-1065-9

Jaenike J (1990) Host specialization in phytophagous insects. Annu Rev Ecol Syst 21:243–273. https://doi.org/10.1146/annurev.es.21.110190.001331

Johnsen S (2011) The Optics of Life. Princeton University Press, New Jersey

Jones RE (1977) Movement patterns and egg distribution in cabbage butterflies. J Anim Ecol 46:195. https://doi.org/10.2307/3956

Jones RE, Gilbert N, Guppy M, Nealis V (1980) Long-distance movement of *Pieris rapae*. J Anim Ecol 49:629. https://doi.org/10.2307/4268

Kelber A (2001) Receptor based models for spontaneous colour choices in flies and butterflies. Entomol Exp Appl 99:231–244. https://doi.org/10.1046/j.1570-7458.2001.00822.x

Kelber A, Thunell C, Arikawa K (2001) Polarisation-dependent colour vision in *Papilio*. J Exp Biol 204:2469–2480

Kinoshita M, Yamazato K, Arikawa K (2011) Polarization-based brightness discrimination in the foraging butterfly, *Papilio xuthus*. Philos Trans R Soc B Biol Sci 366:688–696. https://doi.org/10.1098/rstb.2010.0200

Kirschfeld K (1972) Notizen: Die notwendige Anzahl von Rezeptoren zur Bestimmung der Richtung des elektrischen Vektors linear polarisierten Lichtes / The number of receptors necessary for determining the position of the E-vector of linearly polarized light. Z Naturforsch B 27:578–579. https://doi.org/10.1515/znb-1972-0524

Können GP (1985) Polarized Light in Nature. Cambridge University Press, New York, NY

Labhart T (2016) Can invertebrates see the e-vector of polarization as a separate modality of light? J Exp Biol 219:3844–3856. https://doi.org/10.1242/jeb.139899

Labhart T, Meyer EP (1999) Detectors for polarized skylight in insects: a survey of ommatidial specializations in the dorsal rim area of the compound eye. Microsc Res Tech 47:368–379. https://doi.org/10.1002/(SICI)1097-0029(19991215)47:6<368::AID-JEMT2>3.0.CO;2-Q

Lin J-T (1993) Identification of photoreceptor locations in the compound eye of *Coccinella septempunctata* Linnaeus (Coleoptera, Coccinellidae). J Insect Physiol 39:555–562. https://doi.org/10.1016/0022-1910(93)90037-R

Maltais PM, Nuckle JR, Leblanc PV (1998) Economic threshold for three lepidopterous larval pests of fresh-market cabbage in southeastern New Brunswick. J Econ Entomol 91:9. https://doi.org/10.1093/jee/91.3.699

Marshall J, Roberts N, Cronin T (2014) Polarisation Signals. In: Horváth G (ed) Polarized Light and Polarization Vision in Animal Sciences. Springer Berlin Heidelberg, Berlin, Heidelberg, pp 407–442

Marshall NJ, Powell SB, Cronin TW, et al (2019) Polarisation signals: a new currency for communication. J Exp Biol 222:jeb134213-21. https://doi.org/10.1242/jeb.134213

Mathejczyk TF, Wernet MF (2017) Sensing Polarized Light in Insects. In: Oxford Research Encyclopedia of Neuroscience. Oxford University Press

McQueen EW, Morehouse NI (2018) Rapid divergence of wing volatile profiles between subspecies of the butterfly *Pieris rapae* (Lepidoptera: Pieridae). J Insect Sci 18:March 2018, 33. https://doi.org/10.1093/jisesa/iey026

Meglič A, Ilić M, Pirih P, et al (2019) Horsefly object-directed polarotaxis is mediated by a stochastically distributed ommatidial subtype in the ventral retina. Proc Natl Acad Sci 116:21843–21853. https://doi.org/10.1073/pnas.1910807116

Meglič A, Ilić M, Quero C, et al (2020) Two chiral types of randomly rotated ommatidia are distributed across the retina of the flathead oak borer, *Coraebus undatus* (Coleoptera: Buprestidae). J Exp Biol jeb.225920. https://doi.org/10.1242/jeb.225920

Meyer-Rochow VB, Mishra M (2009) A six-rhabdomere, open rhabdom arrangement in the eye of the chrysanthemum beetle *Phytoecia rufiventris*: Some ecophysiological predictions based on eye anatomy. Biocell 33:115–120

Mishra M (2015) An eye ultrastructure investigation of a plant pest *Acyrthosiphon pisum* (Harris) (Insecta: Hemiptera: Aphididae). Open Access Insect Physiol 5:41–46. https://doi.org/10.2147/OAIP.S84633

Mishra M, Meyer-Rochow VB (2008) Fine structural description of the compound eye of the Madagascar 'hissing cockroach' *Gromphadorhina portentosa* (Dictyoptera: Blaberidae). Insect Sci 15:179–192. https://doi.org/10.1111/j.1744-7917.2008.00199.x

Mishra M, Meyer-Rochow VB (2006) Fine structure of the compound eye of the fungus beetle *Neotriplax lewisi* (Coleoptera, Cucujiformia, Erotylidae). Invertebr Biol 125:265–278. https://doi.org/10.1111/j.1744-7410.2006.00059.x

Morehouse NI, Rutowski RL (2010) In the eyes of the beholders: Female choice and avian predation risk associated with an exaggerated male butterfly color. Am Nat 176:768–784. https://doi.org/10.1086/657043

Obara Y (1970) Studies on the mating behavior of the white cabbage butterfly, *Pieris rapae crucivora* Boisduval. J Comp Physiol A 69:99–116. https://doi.org/10.1007/BF00340912

Obara Y, Majerus MEN (2000) Initial mate recognition in the British cabbage butterfly, *Pieris rapae rapae*. Zoolog Sci 17:725–730. https://doi.org/10.2108/zsj.17.725

Paris TM, Allan SA, Udell BJ, Stansly PA (2017) Evidence of behavior-based utilization by the Asian citrus psyllid of a combination of UV and green or yellow wavelengths. PLoS One 12:e0189228-18. https://doi.org/10.1371/journal.pone.0189228

Prokopy R, Owens E (1983) Visual detection of plants by herbivorous insects. Annu Rev Entomol 28:337–364. https://doi.org/10.1146/annurev.en.28.010183.002005

Qiu X, Arikawa K (2003a) Polymorphism of red receptors: sensitivity spectra of proximal photoreceptors in the small white butterfly *Pieris rapae crucivora*. J Exp Biol 206:2787–2793. https://doi.org/10.1242/jeb.00493

Qiu X, Arikawa K (2003b) The photoreceptor localization confirms the spectral heterogeneity of ommatidia in the male small white butterfly, *Pieris rapae crucivora*. J Comp Physiol A 189:81–88. https://doi.org/10.1007/s00359-002-0380-0

Qiu X, Vanhoutte K, Stavenga DG, Arikawa K (2002) Ommatidial heterogeneity in the compound eye of the male small white butterfly, *Pieris rapae crucivora*. Cell Tissue Res 307:371–379. https://doi.org/10.1007/s00441-002-0517-z

Reeves JL (2011) Vision should not be overlooked as an important sensory modality for finding host plants. Environ Entomol 40:855–863. https://doi.org/10.1603/EN10212

Renwick JAA, Chew F (1994) Oviposition behavior in Lepidoptera. Annu Rev Entomol 39:377–400

Renwick JAA, Lopez K (1999) Experience-based food consumption by larvae of *Pieris rapae*: Addiction to glucosinolates? Entomol Exp Appl 91:51–58. https://doi.org/10.1046/j.1570-7458.1999.00465.x/full

Renwick JAA, Radke CD (1988) Sensory cues in host selection for oviposition by the cabbage butterfly, *Pieris rapae*. J Insect Physiol 34:251–257. https://doi.org/10.1016/0022-1910(88)90055-8

Ribi WA (1978) Ultrastructure and migration of screening pigments in the retina of *Pieris rapae* L. (Lepidoptera, Pieridae). Cell Tissue Res 191:57–73. https://doi.org/10.1007/BF00223215

Roberts NW, Porter ML, Cronin TW (2011) The molecular basis of mechanisms underlying polarization vision. Philos Trans R Soc B Biol Sci 366:627–637. https://doi.org/10.1098/rstb.2010.0206

Ryan SF, Lombaert E, Espeset A, et al (2019) Global invasion history of the agricultural pest butterfly *Pieris rapae* revealed with genomics and citizen science. Proc Natl Acad Sci 116:20015–20024. https://doi.org/10.1073/pnas.1907492116

Shashar N, Sabbah S, Aharoni N (2005) Migrating locusts can detect polarized reflections to avoid flying over the sea. Biol Lett 1:472–475. https://doi.org/10.1098/rsbl.2005.0334

Shimohigashi M, Tominaga Y (1991) Identificaton of UV, green and red receptors, and their projection to lamina in the cabbage butterfly, *Pieris rapae*. Cell Tissue Res 263:49–59. https://doi.org/10.1007/BF00318399

Smithers SP, Roberts NW, How MJ (2019) Parallel processing of polarization and intensity information in fiddler crab vision. Sci Adv 5:eaax3572. https://doi.org/10.1126/sciadv.aax3572

Snell-Rood EC, Papaj DR (2009) Patterns of phenotypic plasticity in common and rare environments: a study of host use and color learning in the cabbage white butterfly *Pieris rapae*. Am Nat 173:615–631. https://doi.org/10.1086/597609

Stavenga DG (2006) Invertebrate Photoreceptor Optics. In: Nilsson D-E, Warrant EJ (eds) Invertebrate Vision. Cambridge University Press, pp 1–42

Stavenga DG, Arikawa K (2011) Photoreceptor spectral sensitivities of the small white butterfly *Pieris rapae crucivora* interpreted with optical modeling. J Comp Physiol A 197:373–385. https://doi.org/10.1007/s00359-010-0622-5

Sweeney A, Jiggins C, Johnsen S (2003) Insect communication: Polarized light as a butterfly mating signal. Nature 423:31–32. https://doi.org/10.1038/423031a

Takács S, Bottomley H, Andreller I, et al (2008) Infrared radiation from hot cones on cool conifers attracts seed-feeding insects. Proc R Soc B Biol Sci 276:649–655. https://doi.org/10.1098/rspb.2008.0742

Templin RM, How MJ, Roberts NW, et al (2017) Circularly polarized light detection in stomatopod crustaceans: a comparison of photoreceptors and possible function in six species. J Exp Biol 220:3222–3230. https://doi.org/10.1242/jeb.162941

van der Kooi CJ, Dyer AG, Kevan PG, Lunau K (2019) Functional significance of the optical properties of flowers for visual signalling. Ann Bot 123:263–276. https://doi.org/10.1093/aob/mcy119

Vanderbilt V, Grant L (1985) Plant canopy specular reflectance model. IEEE Trans Geosci Remote Sens GE-23:722–730. https://doi.org/10.1109/TGRS.1985.289390

Wachmann E (1977) Vergleichende Analyse der feinstrukturellen Organisation offener Rhabdome in den Augen der Cucujiformia (Insecta, Coleoptera), unter besonderer Berücksichtigung der Chrysomelidae. Zoomorphologie 88:95–131. https://doi.org/10.1007/BF01880649

Wakakuwa M, Stavenga DG, Arikawa K (2007) Spectral organization of ommatidia in flower-visiting insects. Photochem Photobiol 83:27–34. https://doi.org/10.1562/2006-03-03-IR-831

Wakakuwa M, Stavenga DG, Kurasawa M, Arikawa K (2004) A unique visual pigment expressed in green, red and deep-red receptors in the eye of the small white butterfly, *Pieris rapae crucivora*. J Exp Biol 207:2803–2810. https://doi.org/10.1242/jeb.01078

Wakakuwa M, Stewart F, Matsumoto Y, et al (2014) Physiological basis of phototaxis to near-infrared light in *Nephotettix cincticeps*. J Comp Physiol A 200:527–536. https://doi.org/10.1007/s00359-014-0892-4

Webb S, Shelton AM (1988) Laboratory rearing of the imported cabbageworm. New Yorks Food Life Sci Bull 122:1–6

Wedell N, Cook PA (1999) Strategic sperm allocation in the Small White butterfly *Pieris rapae* (Lepidoptera: Pieridae). Funct Ecol 13:85–93. https://doi.org/10.1046/j.1365-2435.1999.00286.x

Wehner R (2001) Polarization vision – a uniform sensory capacity? J Exp Biol 204:2589–2596

Wehner R, Bernard GD (1993) Photoreceptor twist: a solution to the false-color problem. Proc Natl Acad Sci 90:4132–4135. https://doi.org/10.1073/pnas.90.9.4132

Wernet MF, Velez MM, Clark DA, et al (2012) Genetic dissection reveals two separate retinal substrates for polarization vision in *Drosophila*. Curr Biol 22:12–20. https://doi.org/10.1016/j.cub.2011.11.028

Zeil J, Hofmann M (2001) Signals from 'crabworld': cuticular reflections in a fiddler crab colony. J Exp Biol 204:2561–2569

Zeil J, Ribi WA, Narendra A (2014) Polarisation Vision in Ants, Bees and Wasps. In: Horváth G (ed) Polarized Light and Polarization Vision in Animal Sciences. Springer Berlin Heidelberg, Berlin, Heidelberg, pp 41–60

Chapter 2.

Approach trajectory and solar position affect host plant attractiveness to the small white butterfly[1]

[1]The corresponding manuscript is available as a preprint in *BioRxiv* (2020, doi.org/10.1101/2020.10.04.325639) and is under review in *Vision Research* with the following authors: Blake AJ, Couture C, Go MC, Gries G

2.1. Abstract

While it is well documented that insects exploit polarized sky light for navigation, their use of reflected polarized light for object detection has been less well studied. Recently, we have shown that the small white butterfly, *Pieris rapae,* distinguishes between host and non-host plants based on the degree of linear polarization (*DoLP*) of light reflected from their leaves. To determine how polarized light cues affect host plant foraging by female *P. rapae* across their entire visual range including the ultraviolet (300-650 nm), we applied photo polarimetry demonstrating large differences in the *DoLP* of leaf-reflected light among plant species generally and between host and non-host plants specifically. As polarized light cues are directionally dependent, we also tested, and modelled, the effect of approach trajectory on the polarization of plant-reflected light and the resulting attractiveness to *P. rapae*. Using photo polarimetry measurements of plants under a range of light source and observer positions, we reveal several distinct effects when polarized reflections are examined on a whole-plant basis rather than at the scale of pixels or of entire plant canopies. Most notably from our modeling, certain approach trajectories are optimal for foraging butterflies, or insects generally, to discriminate between plant species on the basis of the *DoLP* of leaf-reflected light.

2.2. Introduction

Many insects exploit polarized skylight to aid in navigation (Labhart and Meyer 1999) but their use of reflected polarized light for host plant detection and selection has hardly been studied (Heinloth et al. 2018). Recently, the small white butterfly, *Pieris rapae* (Linnaeus, 1758), which uses cabbage and other crucifers as host plants (Chew and Renwick 1995), has been shown to discriminate among host and non-host plants based on the degree of linear polarization (0-100%, *DoLP*) of foliar reflections (Blake et al., 2019a). Similar to many other insects (Ilić et al. 2016; Mishra 2015; Wachmann 1977), the rhabdom of *P. rapae* photoreceptors is untwisted with uncurved microvilli that are aligned along the rhabdom's length (Blake et al., 2019b; Qiu et al., 2002). Rhabdomeric photoreceptors have an inherent dichroism due to the tubular structure of the microvilli (Stockhammer 1956; Moody and Parriss 1961; Laughlin et al. 1975). In the ventral compound eye of other insects such as honey bees, *Apis mellifera*, desert ants, *Cataglyphis bicolor*, crickets, *Gryllus campestris*, and cockchafers, *Melolontha melolontha*, the photoreceptors along with the microvilli composing the rhabdom twist along the photoreceptor's longitudinal axis (Wehner and Bernard 1993). This twist serves to disrupt the alignment of microvilli along the rhabdom, preventing preferential absorption of light oscillating in a direction, or with an axis of polarization (0-180°, *AoP*), parallel to the microvillar orientation, as shown in *P. rapae* and other insects. Polarization can result in perceived shifts in color and/or intensity as compared to polarization-blind visual systems (Kelber et al. 2001; Kinoshita et al. 2011).

Shiny surfaces like water, glass or plant foliage can polarize light through specular reflection (Foster et al. 2018). These reflections are polarized in a direction so that their *AoP* is parallel to the surface. The strength of this polarization (*DoLP*) is dependent on the incident angle, with maximal polarization occurring at the Brewster's angle (approximately 55° for foliage; Grant et al., 1993; Johnsen, 2011). The polarization of this light is consequently dependent upon the angle (ω) formed between the sun, the reflecting leaf surface, and the observer (i.e., a camera or insect; Fig. 2.1). This angle is itself dependent upon the solar and observer elevation and azimuth, making these aspects important predictors of foliar polarization (Hegedüs and Horváth 2004). As it is only the specular component of the reflection that is polarized, leaf surface characteristics that increase surface roughness and diffuse reflectance, such as

pubescence, epicuticular waxes or undulations, also affect the *DoLP* (Grant et al. 1993). The *DoLP* can also be altered by reducing diffuse reflectance through pigmentation absorption (Horváth & Varjú, 1997), resulting in an increased foliar *DoLP* in the red and blue relative to green. The type and directionality of the celestial illumination can also affect the polarization of the reflection, with reflections dominated by skylight or overcast skies differing from those dominated by the strong point source of the sun (Horváth et al. 2002, Száz et al. 2016).

As *DoLP* is an important host plant cue, at least for female *P. rapae* (Blake et al., 2019a), it would be informative to compare the *DoLP* and *AoP* of multiple host and non-host plants. While the polarization of select plant species has previously been examined (Grant et al. 1993), and photo polarimetry has been used to examine plant surfaces (Horváth et al., 2002), photo polarimetry has not yet been used to compare foliar reflected polarized light among different plant species. Moreover, polarization characteristics of foliage in the ultraviolet range (UV, 320-400 nm) have been predicted to resemble those in the human-visible range (400-700 nm) (Horváth et al., 2002), but this prediction has never been experimentally tested. Therefore, our first objective was to use photo polarimetry to characterize the *DoLP* and *AoP* of foliar reflections from host and non-host plants of *P. rapae* and to compare polarization characteristics of foliage in both the UV and human-visible range.

Further knowledge gaps pertain to the question as to how interspecific differences in foliar polarization are affected by the position of the observer and the light source. Positional effects have been investigated in relation to single leaves (Hegedüs & Horváth, 2004; Horváth et al., 2002) but not whole plants. Therefore, our second objective was to use photo polarimetry to measure select plant species under a series of light source and observer positions in order to model how approach trajectory affects foliar *AoP* and *DoLP,* and thus plant attractiveness, to host-plant-seeking female *P. rapae*.

2.3. Methods

2.3.1. Plant material

Within a greenhouse, we grew plants in pots (12.7 cm diam), thinning to one plant per pot except for fall rye and oregano. In these species, multiple plants per pot generated a leaf area more comparable to that of the other species examined (Table 2.1). Plants selected for photography in experiments were 10-20 cm tall with 4-6 fully expanded true leaves (BBCH 14-16).

2.3.2. Polarimetry of Experimental Plants

We used photo polarimetry (Foster et al., 2018; Horváth & Varjú, 2004) to measure the intensity (*I*), *DoLP* and *AoP* of the selected plants. To obtain these measurements, we used a modified Olympus E-PM1 camera (Olympus, Tokyo, Japan) with expanded sensitivity in the UV (320-400 nm) (Fig 2.2c; Dr. Klaus Schmitt, Weinheim, Germany, uvir.eu) and an ultra-broadband linear polarizing filter (68-751, Edmund Optics, USA). We narrowed sensitivity to the human-visible range (400-700 nm) and the UV range with a UV/IR filter (Baader Plantarium, Mammendorf, Germany) and a U-filter (Baader Plantarium), respectively. To calculate the *DoLP* and the *AoP,* we took four images with the polarizing filter positioned at 0°, 45°, 90° and 135°.

We kept the white-balance, aperture, and other exposure controls constant between exposures, with all images captured in a raw image format. Within the image-analysis software platform Fiji (Schindelin et al. 2012), we used a series of custom-created macros for image analysis and measurement (Blake et al., 2020a). We decoded images with DCRAW (Coffin 2019) as a 16-bit linear bitmap, persevering sensor linearity. We determined color corrections necessary to ensure accurate color representation through photographing a 99% Spectralon reflectance standard (SRS-99-010, Labsphere, NH, USA) under similar lighting conditions as the experimental plants (Blake et al., 2020a). We aligned all images (0°, 45°, 90°, 135°) from each plant using TurboReg (Thévenaz et al. 1998) and separated the plant in each image from the background (see below). We then calculated Stokes parameters (including *I*), *DoLP,* and *AoP* for each pixel in the red (575-700 nm), green (455-610 nm), blue (410-530 nm) and UV (330-395 nm) bands of the electromagnetic spectrum (Fig. 2.2c) and averaged all

pixel values to give a whole-plant mean for both the intensity (*I*) and the *DoLP,* and a modal value for the *AoP*.

2.3.3. Interspecific comparisons of foliar reflectance (Exp. 1)

We photographed plants upright inside a black velvet-lined box lit by a 400 W Hortilux® Blue metal halide lamp (MT400D/BUD/HTL-BLUE, EYE Lighting Int., Mentor, OH, USA; Fig. 2.2b) suspended 75-80 cm above the box (Fig. 2.3). Light was directed onto a plant by a white-cardstock tube (12.5 × 21.6 cm), thus minimizing reflections from the box walls. The camera was positioned 75-80 cm from the plant at approximately the same height as the plant canopy (Fig. 2.3).

In all exposures (0°, 45°, 90°, 135°) and color bands (UV, blue, green, red), we used a background mask to isolate the plant from the background. We created the background mask using areas above ~2.3% of the maximum pixel value in the green band. To eliminate possible effects of shading or unequal areas of the plants being directly lit, we limited estimations of *DoLP* and *AoP* to areas of the image above 5% of the maximum pixel value in each color band. We further limited estimates of *AoP*, in this and subsequent experiments, to areas with a *DoLP* greater than 15%, as below this *DoLP* estimates of *AoP* have little meaning (Horváth & Varjú, 1997).

2.3.4. Effect of light source azimuth and elevation on foliar polarization (Exp. 2)

To photograph plants in various light source elevation and azimuth combinations (Fig. 2.1abce), we used scaffolding to precisely vary the height of the metal halide lamp and a movable platform to keep the camera and plant in orientation. Subtle variations in plant height did result in some variation in light source elevation but these variations and those of related angles were incorporated into the analyses. We positioned a black velvet background behind the plant in each image to enable optimal separation of the plant from the background, however this background did not block reflected light illumination from the room's walls and ceiling originating from the metal halide lamp. We took these measurements using a subset of the species we examined in the previous experiment, selecting plants with shiny leaves (potato, white mustard), matte leaves (cabbage, rutabaga) and fall rye, which holds its leaves in a more vertical orientation. We omitted

UV polarimetry in this and the subsequent experiment because plants would shift position due to positive phototropism (Koller 2000) during the extended time frame needed for several long UV exposures. Omitting UV polarimetry in experiment 2 was further justified given the strong correlation (R^2 = 75%) between *DoLP* in the UV and blue found in experiment 1 (see Results).

As the intensity of the black velvet background varied considerably with the position of the metal halide lamp, we could not specify a single intensity threshold to separate the plant from the background as we had in the previous experiment. We therefore used a combination of all three human visual color bands to manually create a background mask. As we wanted to compare the plant in different light source positions, we estimated *DoLP* from the same subset of pixels specified by the background mask rather than limiting *DoLP* to areas with a specific intensity, as in the previous experiment.

2.3.5. Effect of observer elevation on foliar polarization (Exp. 3)

Using cabbage and white mustard, we applied the same procedure as described above to examine the effect of observer elevation (camera in this case). At each observer elevation (14°, 0°, -14°), we photographed the plant at a subset of the combinations of elevation and azimuth mentioned above (Fig. 2.1de).

2.3.6. Statistical analysis

We compared foliar reflection among species (Exp. 1), using a linear model with post-hoc Tukey's test (Table 2.2; Blake et al., 2020a). We analyzed the effects of light source and observer positions (Exps. 2, 3) on foliar polarization, using mixed models with plant included as a random effect (Table 2.2; Bates et al., 2015). We incorporated ψ into models of *DoLP* as the square of its cosine, whereas ω was incorporated in these models via $p(\omega)$ as described in the Fresnel equations below (1-3), with n_1 being the refractive index of air (1.00) and n_2 being the refractive index of the leaf surface (1.34-1.79, depending on color band). For each color band, we chose the leaf surface refractive index that minimized model deviance (Blake et al., 2020a). In modeling the effect of observer elevation (Exp. 3), we incorporated ζ into existing models from Exp. 2 as its arctangent, and scaled ζ by a factor of 16 so its effect would quickly reach an asymptote as ζ moved away from 0 (Table 2.2; Blake et al., 2020a).

$$R_s(\omega) = \left| \frac{\left(n_1 \cos\frac{\omega}{2}\right) - n_2\sqrt{1 - \left(\frac{n_1}{n_2}\sin\frac{\omega}{2}\right)}}{\left(n_1 \cos\frac{\omega}{2}\right) + n_2\sqrt{1 - \left(\frac{n_1}{n_2}\sin\frac{\omega}{2}\right)}} \right|^2 \quad (1)$$

$$R_p(\omega) = \left| \frac{n_1\sqrt{1 - \left(\frac{n_1}{n_2}\sin\frac{\omega}{2}\right)} - \left(n_2 \cos\frac{\omega}{2}\right)}{n_1\sqrt{1 - \left(\frac{n_1}{n_2}\sin\frac{\omega}{2}\right)} + \left(n_2 \cos\frac{\omega}{2}\right)} \right|^2 \quad (2)$$

$$p(\omega) = 1 - \frac{R_s(\omega)}{R_p(\omega)} \quad (3)$$

2.3.7. Modeling the effect of solar elevation and azimuth on host attractiveness to *Pieris rapae*

Utilizing the models for *DoLP* and *AoP* from Exp. 3 (Table 2.2), we predicted *DoLP* and *AoP* across most possible values of ζ (-15–90°), all possible values of ϕ (0–360°), and a selection of θ values (15, 45, 75°; Blake et al., 2020a). These predictions were limited to the blue color channel as there were insufficient data to fit *AoP* models for the red and green color bands. Then using the ranges of *DoLP* and *AoP* shown to be unattractive to *P. rapae* (Blake et al., 2019a), we modeled approach trajectories that would result in attractive and unattractive polarization characteristics, as well as low *DoLP* (<10%, moderately attractive).

2.4. Results

2.4.1. Interspecific comparisons of foliar reflectance (Exp. 1)

There were statistically significant differences in both intensity and *DoLP* among plant species in all color bands (Figs. 2.4ab, 2.5ab, 2.6ab, 2.7ab; Table 2.2). In contrast, we found minimal, although sometimes statistically significant, differences in *AoP* among plant species (Figs. 2.4c, 2.5c, 2.6c, 2.7c; Table 2.2). Differences in intensity and *DoLP* were comparably large in the UV and blue color bands. The comparatively shiny-leaved

species had a much higher *DoLP* than the matt-leaved species, but only in the blue and UV bands (Figs. 2.4b, 2.7b), where most *P. rapae* host plants grouped together.

2.4.2. Effect of light source azimuth and elevation on foliar polarization (Exp. 2)

For all three color bands, there was a strong relationship between ω and *DoLP* (Figs. 2.8, 2.9, 2.10; Table 2.2), with *DoLP* increasing as ω approached double the Brewster's angle (53-60°). This relationship was less pronounced when the plants were lit more from the side (larger ψ angle). Fall rye with mostly vertical leaf orientation showed a different and weaker relationship between ω and *DoLP* (Figs. 2.8a, 2.9a, 2.10a).

There was an approximately proportional negative relationship between the ψ angle and *AoP* in all color bands (Figs. 2.11, 2.12, 2.13; Table 2.2). The slope of this relationship was steepest when the light source was behind the observer ($\phi = 0$).

2.4.3. Effect of observer elevation on foliar polarization (Exp. 3)

The effect of ω on *DoLP* increased with the elevation of the observer (ζ; Figs. 2.14, 2.15, 2.16; Table 2.2). The elevation of the observer also affected *AoP* (Fig. 2.17). The slope of the relationship between the ψ angle and *AoP* was shallower at lower observer elevations, while the effect of the ϕ angle on the relationship been ψ angle and *AoP* was more pronounced at higher observer elevations. These effects were all relatively subtle in comparison to the effects of light source position.

2.4.4. Modeling the effect of solar elevation and azimuth on host plant attractiveness to *Pieris rapae*

As indicated by our modeling, the greatest *DoLP* of foliage is realized when the light source is located directly behind the plant (Figs 2.18a-c, 2.19a-c). Effects of solar elevation (θ) on *DoLP* could be compensated for, in part, by shifting the observer elevation (ζ) but lower observer elevation reduced overall *DoLP*.

Our model predicts that the greatest range of *AoP* across all ϕ angles tested is found when solar elevation (θ) is low, with ϕ angles at or near 180° always yielding an

AoP near 90°. We also note that smaller shifts in *AoP* occur with ϕ angle at lower observer angles (ζ), but this effect is relatively small.

When we modeled ζ, ϕ and θ values resulting in combinations of *DoLP* and *AoP* attractive and unattractive to *P. rapae* (Figs. 2.18, 2.19), there was consistently a window of attractive *DoLP*s at a ϕ angle of 180°, and a moderately attractive low *DoLP* area opposite it at a ϕ angle of 0°. All other combinations of ϕ and ζ resulted in unattractive *DoLP*s. Increasing solar elevation (θ) shifted the attractive window downward and the low *DoLP* area upwards. Increased solar elevation (θ) also decreased the size of the attractive window, while increasing the size of the low *DoLP* area. The *AoP* had little effect on these windows outside of a small narrowing of the attractive window at low solar elevations (θ).

2.5. Discussion

Our study confirms earlier work demonstrating large differences in *DoLP* among plant species (Blake et al., 2019a; Grant et al., 1993) and refines our understanding of polarized reflections from plant foliage. Unlike previous studies that examined polarized reflections of single leaves, models of leaves, or plant canopies (Grant et al., 1993; Hegedüs & Horváth, 2004; Horváth et al., 2002; Horváth & Hegedüs, 2014; Maignan et al., 2009; Raven, 2002; Rondeaux & Herman, 1991; Vanderbilt & Grant, 1985; Woolley, 1971), we recorded reflections from entire plants thereby revealing several emergent phenomena. Most importantly, our modeling suggests that certain approach trajectories are optimal for foraging insects to discriminate among plant species based on the *DoLP* of foliar reflections.

Our measurements of polarization of foliar reflections are consistent with point-source polarimetry data (Grant et al. 1993), and other photo polarimetry of plant surfaces (Fig. 2.4, 2.5, 2.6, 2.7; Hegedüs and Horváth, 2004; Horváth et al., 2002). As predicted by Horváth et al. (2002), our UV polarimetry data closely resemble those of the human-visible color bands, especially blue, and are consistent with previous measurements in the human-visible range. Similar to previous measurements (Grant et al., 1993; Horváth et al., 2002), glossy, flat and/or dark leaf surfaces have an increased ratio of specular to diffuse reflection and greater *DoLP* than matte, undulating, and/or bright leaf surfaces. As leaves have high reflectance in the green and red color bands, the *DoLP*s in the blue

and UV color bands expectedly exceeded those in the green and red bands. Moreover, plants with leaves that tend to be held more vertically (e.g., fall rye, onions), and provide little horizonal surface for specular reflections, had low *DoLP* values. Despite large differences in leaf shape (simple *vs* compound) and growth form (all basal leaves *vs* basal and cauline leaves), there were only small, albeit statistically significant, differences in *AoP* between plant species (Table 2.2). These findings in combination with the smaller interspecific differences in intensity relative to *DoLP* (Table 2.2), further support the conclusion that foliar *DoLP* is *the* visual cue that conveys the most host plant information, especially information about the foliar surface (waxes, pubescence, undulations).

The angle between light source, plant and observer (ω) strongly predicted the foliar *DoLP* (Figs. 2.8, 2.9, 2.10) for all color bands, with the strongest polarization at twice the Brewster's angle (53-60°). These data are consistent with both theoretical predictions and other experimental measurements of the effect of viewing angles on *DoLP* (Horváth et al., 2002; Raven, 2002; Rondeaux & Herman, 1991; Woolley, 1971). However, the phenomenon of lowering the *DoLP* with increasing ψ had not previously been noted and emerges here through whole-plant measurements incorporating multiple leaf surfaces. As the orientation of plant leaves is typically more horizontal than vertical, plants lit more from the side than from above (greater ψ) have a relatively smaller leaf area that is positioned in such a way to specularly reflect light in the direction of the observed. These areas without specular reflection have a lower *DoLP,* lowering the plants' overall *DoLP*. Of course, this relationship was absent in fall rye (at least at the growth stage examined) with primarily vertically held leaves. When plants were photographed at or below the level of the leaf canopy (lower ζ), the *DoLP* was reduced (Figs. 2.14, 2.15, 2.16). Similar to the effect of ψ, lower ζ results in a smaller leaf surface reflecting light at the observer, and a larger leaf surface being in shadow or showing light transmitted through the leaves. Light transmitted through leaves has a low *DoLP* due to diffuse scattering by plant tissue, as previously observed in single leaf measurements (Horváth et al., 2002; Vanderbilt & Grant, 1985).

In agreement with prior examinations of foliar polarization, the *AoP* of all color bands was largely a function of ψ (Figs. 2.11, 2.13, 2.14), with values of *AoP* moving away from 90° as the light source was less aligned with the line between the observer and the plant (see Fig. 2.1a). This relation between *AoP* and ψ is consistent with

previous observations (Horváth et al., 2002; Können, 1985). Although the *AoP* of a particular plant area did not change much in relation to the light source position, the variety of leaf orientations within a single plant and the curvature of leaf surfaces ensured that at least a portion of the plant showed a specular reflection regardless of the light source's position relative to the plant. Invariably, these areas of specular reflection showed a greater *DoLP* accounting for much of the observed relationship between *AoP* and ψ. The variety of leaf surface orientations and the resultant *AoP*s also explains why the relationship between *AoP* and ψ is shallower than the inversely proportional relationship one could expect. When plants were viewed with the light source directly in front of the observer ($\phi = 180°$; Figs. 2.11, 2.13, 2.14), the relationship between *AoP* and ψ had a reduced slope, a phenomenon being more pronounced when the plant was observed from a higher angle ($\zeta > 0$; Fig. 2.18). In both cases ($\phi = 180°$, $\zeta > 0$), this resulted in plants having a higher overall *DoLP* (Figs. 2.8, 2.14), and consequently less leaf surface area (with a < 15% *DoLP*) being excluded from estimations of *AoP*. Given that less polarized leaf surface areas showed a weaker relationship between *AoP* and ψ, the overall lower *DoLP* resulted in a stronger relationship between *AoP* and ψ as only leaf areas with highest *DoLP* were above the cutoff. All these effects of ψ on *AoP* could potentially have biological relevance if a host plant foraging insect were to weigh observations of *AoP* by their *DoLP* when determining a plant's overall *AoP*. Nonetheless, in our modeling, these specific effects on *AoP,* and the effects of *AoP* in general, on host plant attractiveness to *P. rapae* seem to be subtle in comparison to the effects of *DoLP* (Figs. 2.18, 2.19).

Our modeling of the effect of approach trajectory on visual attractiveness of plants to *P. rapae* revealed that *DoLP* is a much more important determinant of plant attractiveness than *AoP* (Fig. 2.18). Approach trajectories resulting in *AoP* unattractive to *P. rapae* were also unattractive due to low *DoLP*. It follows that the effect of *AoP* on plant attractiveness can largely be discounted. The key determinant of an attractive *DoLP* was the azimuth of an approach trajectory relative to the light source (ϕ). This was due to its effect on ψ, as plants obliquely lit even at the Brewster's angle showed a much lower *DoLP*. In fact, the only attractive approach trajectories were those where the light source was located behind the target plant. *DoLP* and attractiveness were also affected by how close the angle between observer, plant and light source (ω) was to twice the Brewster's angle, which is affected by light source elevation (θ), observer elevation (ζ),

and azimuth (ϕ). However, when the light source was behind the plant, there was always a combination of θ and ζ allowing for foliar reflections approaching the Brewster's angle. Although high solar elevations (>75°) – constrained to times near solar noon and limited to latitudes near the equator – are relatively rare, they would require much lower approach angles for accurate assessment of foliar *DoLP*. It is the key result of our modelling that for most solar positions there is a single optimal approach trajectory that would best enable a foraging insect to assess foliar *DoLP*. However, this conclusion applies only to settings where foliar reflections are dominated by the specular reflections of sunlight (or another single strong unpolarized light source), as we took measurements indoors and did not incorporate possible effects of polarized skylight (Hegedüs & Horváth, 2004; Horváth et al., 2002). The greater direction spread in the illumination of skylight should increase the *DoLP* of foliar reflection outside of the optimum approach trajectory that we have identified, however this type of illumination would likely also reduce the difference in shiny and matte surfaces (Száz et al. 2016).

We have every reason to predict that our polarization modeling is applicable to the foliar reflectance of many plant species. However, the data we have obtained with herbaceous flowering plants may not be applicable to graminoids, such as fall rye, or other plants with more vertically held leaves. Moreover, due to the size of trees and large shrubs, foraging insects more often approach them from below, and do not view them in their entirety, complicating the applicability of our modeling. It would therefore be intriguing to model whether approach trajectories have similar effects on polarized light cues that may be used by insect herbivores of trees and shrubs.

While this work focused on *P. rapae*, our *DoLP* and *AoP* modeling should be applicable to other polarization-sensitive visual systems. Furthermore, our prediction of a single optimal approach trajectory for the discrimination of *DoLP* should hold true for other polarization-sensitive insects such as *Papilio* butterflies (Kelber et al. 2001; Kinoshita et al. 2011), where increased *DoLP* of foliar reflections would be expected to have a linear effect on attractiveness (Blake et al., 2020b). The approach of butterflies to host plants has not yet been well documented and – accordingly – no stereotyped approach has been noted, as one would anticipate based on our predictions of polarized reflections. Reminiscent of the plunge responses of *Notonecta* backswimmers (Schwind 1984), one might expect an approach where the butterflies' trajectory is constrained so that at least a portion of the compound eyes are viewing the plant at or near the

Brewster's angle. Alternatively, butterflies might circle plants before landing, thereby shifting their azimuth relative to sun, and entering and exiting the attractive window we identified. Circling plants would also allow for sequential comparison of visual information from the plant surface, aiding in *DoLP* assessment through differences in color and/or intensity (Horváth & Varjú, 2004). Mapping the position of butterflies in a 3-dimensional space during approaches to host plants would give insight into how these insects perceive and use the plants' polarized light cues.

In conclusion, using photo polarimetry to examine polarized reflections from entire plants, we show that host and non-host plants of *P. rapae* differ in the *DoLP* of foliar reflections, with UV measurements closely resembling those of blue. Our photo polarimetry further reveals that there is a single optimal approach trajectory that would enable a foraging insect (or other observers) to best discriminate among these interspecific differences in polarization. This optimal approach trajectory is always in the direction of the light source but its inclination is dependent upon the elevation of the light source (θ). It would now be intriguing to determine whether the trajectories of polarization-sensitive insects towards host plants match those predicted by our models.

2.6. References

Bates D, Mächler M, Bolker B, Walker S (2015) Fitting linear mixed-effects models using **lme4**. J Stat Soft 67:1–48. https://doi.org/10.18637/jss.v067.i01

Blake AJ, Go MC, Hahn GS, Grey H, Couture S, Gries G (2019a) Polarization of foliar reflectance: novel host plant cue for insect herbivores. Proc R Soc B 286:20192198. https://doi.org/10.1098/rspb.2019.2198

Blake AJ, Pirih P, Qiu X, Arikawa K, Gries G (2019b) Compound eyes of the small white butterfly *Pieris rapae* have three distinct classes of red photoreceptors. J Comp Physiol A 205:553–565. https://doi.org/10.1007/s00359-019-01330-8

Blake AJ, Couture S, Go MC, Gries G (2020a), Polarimetry data, ImageJ/FIJI macros, R modeling code, and other data from: Approach trajectory and solar position affect host plant attractiveness to the small white butterfly. Mendeley Data, V1. http://doi.org/10.17632/5bh5mhmvrk.1

Blake AJ, Hahn GS, Grey H, Kwok SA, McIntosh D, Gries G (2020b) Polarized light sensitivity in *Pieris rapae* is dependent on both color and intensity. J Exp Biol 223:jeb220350. https://doi.org/10.1242/jeb.220350

Chew FS, Renwick JAA (1995) Host plant choice in *Pieris* butterflies. In: Chemical ecology of insects 2. Springer, Boston, MA, pp 214–238

Coffin D (2019) Decoding raw digital photos in Linux. https://www.dechifro.org/dcraw/. Accessed 23 Dec 2019

Foster JJ, Temple SE, How MJ, Daly IM, Sharkey CR, Wilby D, Roberts NW (2018) Polarisation vision: overcoming challenges of working with a property of light we barely see. Sci Nat 105:27. https://doi.org/10.1007/s00114-018-1551-3

Grant L, Daughtry CST, Vanderbilt VC (1993) Polarized and specular reflectance variation with leaf surface features. Physiol Plant 88:1–9. https://doi.org/10.1111/j.1399-3054.1993.tb01753.x

Hegedüs R, Horváth G (2004) Polarizational colours could help polarization-dependent colour vision systems to discriminate between shiny and matt surfaces, but cannot unambiguously code surface orientation. Vis Res 44:2337–2348. https://doi.org/10.1016/j.visres.2004.05.004

Heinloth T, Uhlhorn J, Wernet MF (2018) Insect responses to linearly polarized reflections: orphan behaviors without neural circuits. Front Cell Neurosci 12:50. https://doi.org/10.3389/fncel.2018.00050

Horváth G, Gál J, Labhart T, Wehner R (2002) Does reflection polarization by plants influence colour perception in insects? Polarimetric measurements applied to a polarization-sensitive model retina of *Papilio* butterflies. J Exp Biol 205:3281–3298

Horváth G, Hegedüs R (2014) Polarization Characteristics of Forest Canopies with Biological Implications. In: Horváth G (ed) Polarized Light and Polarization Vision in Animal Sciences. Springer Berlin Heidelberg, Berlin, Heidelberg, pp 345–365

Horváth G, Varjú D (1997) Polarization pattern of freshwater habitats recorded by video polarimetry in red, green and blue spectral ranges and its relevance for water detection by aquatic insects. J Exp Biol 200:1155–1163

Horváth G, Varjú D (2004) Polarized Light in Animal Vision: Polarization Patterns in Nature. Springer, New York

Ilić M, Pirih P, Belušič G (2016) Four photoreceptor classes in the open rhabdom eye of the red palm weevil, *Rynchophorus ferrugineus* Olivier. J Comp Physiol A 202:203–213. https://doi.org/10.1007/s00359-015-1065-9

Johnsen S (2011) The Optics of Life. Princeton University Press, New Jersey

Kelber A, Thunell C, Arikawa K (2001) Polarisation-dependent colour vision in *Papilio*. J Exp Biol 204:2469–2480

Kinoshita M, Yamazato K, Arikawa K (2011) Polarization-based brightness discrimination in the foraging butterfly, *Papilio xuthus*. Phil Trans R Soc B 366:688–696. https://doi.org/10.1098/rstb.2010.0200

Koller D (2000) Plants in search of sunlight. In: Advances in Botanical Research. Elsevier, pp 35–131

Können GP (1985) Polarized Light in Nature. Cambridge University Press, New York, NY

Labhart T, Meyer EP (1999) Detectors for polarized skylight in insects: a survey of ommatidial specializations in the dorsal rim area of the compound eye. Microsc. Res. Tech. 47:368–379. https://doi.org/10.1002/(SICI)1097-0029(19991215)47:6<368::AID-JEMT2>3.0.CO;2-Q

Laughlin SB, Menzel R, Snyder AW (1975) Membranes, dichroism and receptor sensitivity. In: Snyder AW, Menzel R (eds) Photoreceptor optics. Springer, Berlin Heidelberg NewYork, pp 237-262. https://doi.org/10.1007/978-3-642-80934-7_15

Maignan F, Bréon F-M, Fédèle E, Bouvier M (2009) Polarized reflectances of natural surfaces: Spaceborne measurements and analytical modeling. Remote Sens Environ 113:2642–2650. https://doi.org/10.1016/j.rse.2009.07.022

Mishra M (2015) An eye ultrastructure investigation of a plant pest *Acyrthosiphon pisum* (Harris) (Insecta: Hemiptera: Aphididae). OAIP 5:41–46. https://doi.org/10.2147/OAIP.S84633

Moody MF, Parriss JR (1960) The discrimination of polarized light by *Octopus*: a behavioural and morphological study. Z Vergl Physiol 44:268-291. https://doi.org/10.1007/BF00298356

Qiu X, Vanhoutte K, Stavenga DG, Arikawa K (2002) Ommatidial heterogeneity in the compound eye of the male small white butterfly, *Pieris rapae crucivora*. Cell Tissue Res 307:371–379. https://doi.org/10.1007/s00441-002-0517-z

Raven PN (2002) Polarized directional reflectance from laurel and mullein leaves. Opt Eng 41:1002–11. https://doi.org/10.1117/1.1467668

Rondeaux G, Herman M (1991) Polarization of light reflected by crop canopies. Remote Sens Environ 38:63–75. https://doi.org/10.1016/0034-4257(91)90072-E

Schindelin J, Arganda-Carreras I, Frise E, et al. (2012) Fiji: an open-source platform for biological-image analysis. Nat Methods 9:676–682. https://doi.org/10.1038/nmeth.2019

Schwind R (1984) The plunge reaction of the backswimmer *Notonecta glauca*. J Comp Physiol A 155:319–321. https://doi.org/10.1007/BF00610585

Stockhammer K (1956) Zur Wahrnehmung der Schwingungsrichtung linear polarisierten Lichtes bei Insekten. Z vergl Physiol 38:30-83. https://doi.org/10.1007/BF00338622

Szaz D, Mihályi D, Farkas A, Egri Á, Barta A, Kriska G, Robertson B, Horváth G (2016) Polarized light pollution of matte solar panels: anti-reflective photovoltaics reduce polarized light pollution but benefit only some aquatic insects. J Insect Conserv 20:1–13. https://doi.org/10.1007/s10841-016-9897-3

Thévenaz P, Ruttimann UE, Unser M (1998) A pyramid approach to subpixel registration based on intensity. IEEE Trans Image Process 7:27–41. https://doi.org/10.1109/83.650848

Vanderbilt V, Grant L (1985) Plant canopy specular reflectance model. IEEE Trans Geosci Remote Sensing GE-23:722–730. https://doi.org/10.1109/TGRS.1985.289390

Wachmann E (1977) Vergleichende Analyse der feinstrukturellen Organisation offener Rhabdome in den Augen der Cucujiformia (Insecta, Coleoptera), unter besonderer Berücksichtigung der Chrysomelidae. Zoomorphologie 88:95–131. https://doi.org/10.1007/BF01880649

Wehner R, Bernard GD (1993) Photoreceptor twist: a solution to the false-color problem. PNAS 90:4132–4135. https://doi.org/10.1073/pnas.90.9.4132

Woolley JT (1971) Reflectance and transmittance of light by leaves. Plant Physiol 47:656–662. https://doi.org/10.1104/pp.47.5.656

2.7. Tables

Table 2.1 Variety and taxonomic information of select host plants (green) and non-host plants (black) of *Pieris rapae*.

common name	latin name	variety	family
onion	Allium cepa L.	Early Yellow Globe	Amaryllidaceae
fall rye	Secale cereale L.	-	Poaceae
pea	Pisum sativum L.	Green Arrow	Fabaceae
radish	Raphanus raphanistrum L. sativus	Cherry Belle	Brassicaceae
rutabaga	Brassica napus L. var. napobrassica	Laurentian Swede	Brassicaceae
canola	Brassica napus L. napus f. annua	Q2	Brassicaceae
collards	Brassica oleracea L. var. acephala	Vates	Brassicaceae
cabbage	Brassica oleracea L. var. capitata f. alba	Early Jersey Wakefield	Brassicaceae
red cabbage	Brassica oleracea L. var. capitata f. rubra	Red Acre	Brassicaceae
white mustard	Sinapis alba L.	AC Pennant	Brassicaceae
spinach	Spinacia oleracea L.	King of Denmark	Amaranthaceae
lettuce	Lactuca sativa L.	Grand Rapids	Asteraceae
carrot	Daucus carota L. sativus	Nantes Coreless	Apiaceae
basil	Ocimum basilicum L.	Genovese	Lamiaceae
oregano	Origanum vulgare L.	-	Lamiaceae
eggplant	Solanum melongena L.	Black Beauty	Solanaceae
pepper	Capsicum annuum L.	Keystone Resistant	Solanaceae
tomato	Solanum lycopersicum L.	Celebrity	Solanaceae
potato	Solanum tuberosum L.	Russett Burbank	Solanaceae

Table 2.2 **Model statements, test statistics, and p-values for statistical models of photo polarimetry determined measurements of intensity (*I*), degree of linear polarization (*DoLP*), and axis of polarization (*AoP*) for the red (R), green (G), blue (B), ultraviolet (UV, Exp. 1 only) color bands in experiments 1-3.**

experiment 1

model statement	*F*	df	*P* value
$I_R \sim species$	14.95	18,192	< 0.0001
$I_G \sim species$	15.67	18,192	< 0.0001
$I_B \sim species$	19.35	18,192	< 0.0001
$I_{UV} \sim species$	16.34	18,192	< 0.0001
$DoLP_R \sim species$	21.87	18.191	< 0.0001
$DoLP_G \sim species$	21.43	18,192	< 0.0001
$DoLP_B \sim species$	97.93	18,192	< 0.0001
$DoLP_{UV} \sim species$	72.79	18,181	< 0.0001
$AoP_R \sim species$	1.76	18,186	0.0334
$AoP_G \sim species$	0.83	18,188	0.6625
$AoP_B \sim species$	1.89	18,191	0.0186
$AoP_{UV} \sim species$	1.02	18,176	0.4454

experiment 2

model statement	χ^2	df	*P* value
$DoLP_R \sim p(\omega) + species + p(\omega) : species + \mathrm{p}(\omega) : \cos\psi^2 + p(\omega) : species : \cos\psi^2 + (1 \mid plant)$	1049	14	< 0.0001
$DoLP_G \sim p(\omega) + species + p(\omega) : species + \mathrm{p}(\omega) : \cos\psi^2 + p(\omega) : species : \cos\psi^2 + (1 \mid plant)$	1059	14	< 0.0001
$DoLP_B \sim p(\omega) + species + p(\omega) : species + \mathrm{p}(\omega) : \cos\psi^2 + p(\omega) : species : \cos\psi^2 + (1 \mid plant)$	1073	14	< 0.0001
$AoP_R \sim \psi + \psi : \phi + \psi : species + (1 \mid plant)$	912	5	< 0.0001
$AoP_G \sim \psi + \psi : \phi + \psi : species + (1 \mid plant)$	801	5	< 0.0001
$AoP_B \sim \psi + \psi : \phi + \psi : species + (1 \mid plant)$	1267	6	< 0.0001

experiment 3

model statement	χ^2	df	*P* value
$DoLP_R \sim p(\omega) + species + atan(16 \cdot \zeta) + p(\omega) : species + p(\omega) : \cos\psi^2 + species : atan(16 \cdot \zeta) + p(\omega) : species : \cos\psi^2 + p(\omega) : atan(16 \cdot \zeta) : \cos\psi^2 + (1 \mid plant)$	342	8	< 0.0001
$DoLP_G \sim p(\omega) + species + atan(16 \cdot \zeta) + p(\omega) : species + p(\omega) : \cos\psi^2 + species : atan(16 \cdot \zeta) + p(\omega) : species : \cos\psi^2 + p(\omega) : atan(16 \cdot \zeta) : \cos\psi^2 + (1 \mid plant)$	386	8	< 0.0001
$DoLP_B \sim p(\omega) + species + atan(16 \cdot \zeta) + p(\omega) : species + p(\omega) : \cos\psi^2 + species : atan(16 \cdot \zeta) + p(\omega) : species : \cos\psi^2 + p(\omega) : atan(16 \cdot \zeta) : \cos\psi^2 + (1 \mid plant)$	284	8	< 0.0001
$AoP_R \sim \psi + \psi : \phi + \psi : atan(16 \cdot \zeta) + \psi : species + \psi : \phi : atan(16 \cdot \zeta) + \psi : species : atan(16 \cdot \zeta) + (1 \mid plant)$	419	6	< 0.0001

The angles (ϕ, θ, ω, ψ, ζ) in the model statements are described in Fig. 2.1. The $p(\omega)$ relationship is defined in equations 1-3. The fixed effect of different plant species in the model is represented by *species*, whereas the random effect of individual plants was fit as an intercept and is represented by (1 | plant). The full R code used for statistical analysis is presented in an associated Dryad dataset (Blake et al., 2020a).

2.8. Figures

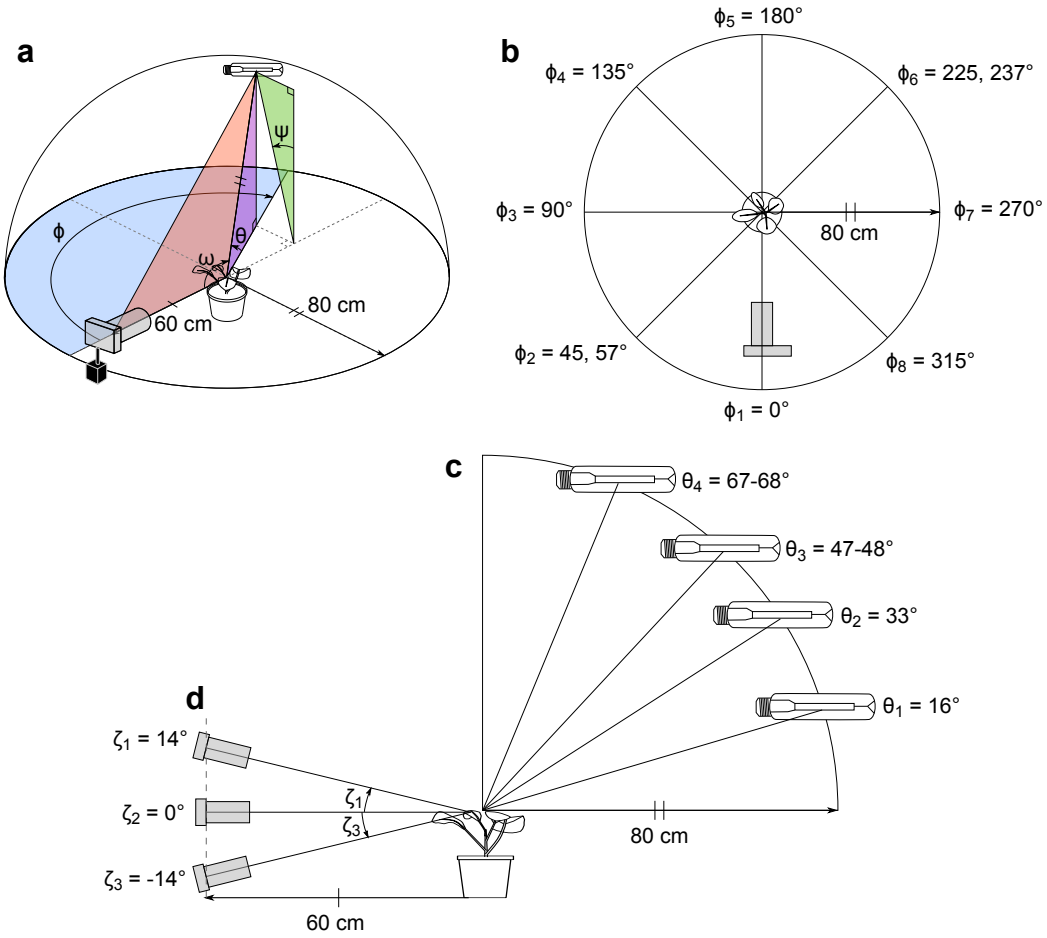

e

θ angles	ϕ angles														
	[1]exp. 2, 0-180°					[1]exp. 2, 180-360°					exp. 3				
16°	0°	45°	90°	135°			237°	270°	315°	0°					
33°	0°	45°	90°	135°	180°						0°	45°	90°	135°	
47-48°	0°	45°	90°	135°	180°	180°	225°	270°	315°	0°	0°	45°	90°	135°	180°
67-68°	[2]0°	57°	90°	135°	[2]180°	[2]180°	225°	270°		[2]0°					

Figure 2.1 **(a) Diagram showing the relative position of the camera, experimental plant and light source as well as the angles between them. The differences in azimuth between the camera and the light source (ϕ), and the elevation of the light source (θ), were manipulated to produce a range of values in the angles ω & ψ. — (b) The range of values for the angle ϕ. — (c) The range of values for the angle θ. — (d) The range of values of camera inclination (ζ). — (e) The degree of linear polarization (*DoLP*) and axis of polarization (*AoP*) were measured using photo polarimetry at each combination of ϕ and θ angles listed in the table for experiments 2 and 3. Due to restrictions of the scaffolding for mounting the metal halide lamp, certain combinations of ϕ and θ were impractical for polarimetry (shown in dark grey). For similar reasons, measurements in experiment 3 were limited to a subset of θ angles, but for each of the ϕ and θ combinations listed in the table, measurements were taken at each ζ value. [1]In experiment 2, plants were either photographed at a ϕ between 0-180° or 180-360°. [2]Due to low *DoLP*, these combinations were excluded from *AoP* analyses.**

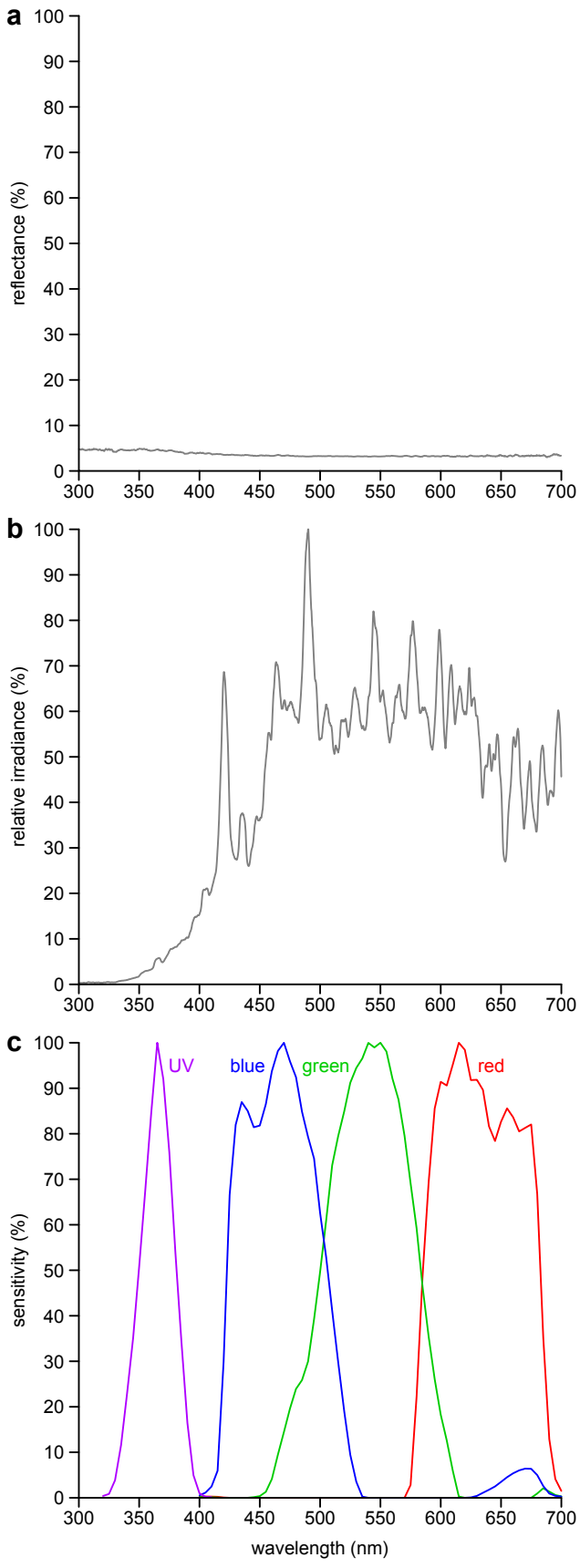
a
reflectance (%)
b
relative irradiance (%)
c
sensitivity (%)
UV
blue
green
red
wavelength (nm)

Figure 2.2 **Spectra of background, illumination sources, and camera sensitivity. (a) Reflection spectrum of the black velvet background. (b) Relative irradiance of the metal halide lamp. (c) Spectral sensitivity of the modified Olympus E-PM1 camera in the ultraviolet (UV), blue, green and red bands of the electromagnetic spectrum. Reflectance spectra were measured with a JAZ spectrometer (Ocean Optics Inc., Dunedin, FL, USA) calibrated with a 99% Spectralon reflectance standard (SRS-99-010, Labsphere, NH, USA). Irradiance spectra were measured with a calibrated HR-4000 spectrophotometer (Ocean Optics Inc.). Isoquantal monochromatic light for spectral sensitivity determination was generated with the same HR-4000 spectrophotometer and a scanning monochromator (MonoScan 2000, Mikropak GmbH, Ostfildern, Germany).**

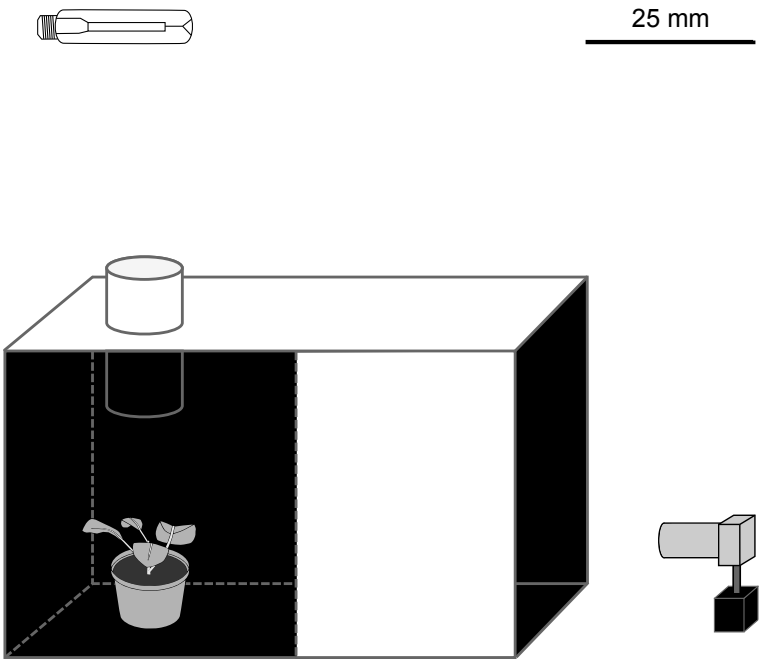

Figure 2.3 **Design for photo polarimetry deployed to characterize the intensity, degree, and axis of linear polarization of various host and non-host plants of *Pieris rapae* in the red, green, blue, and ultraviolet color bands. The camera was positioned so that its optical axis was level with the plant canopy. The plant was positioned underneath the spotlight to avoid illumination of box walls. The angle between the camera and the light source was approximately 90°.**

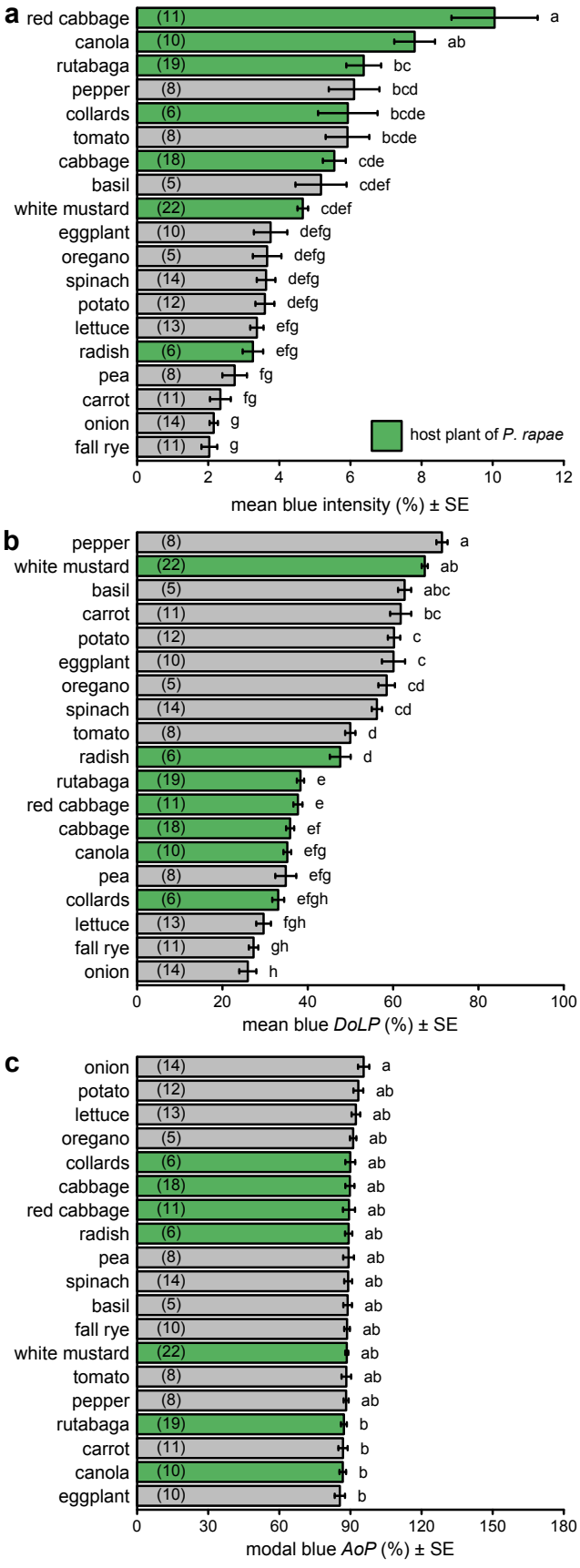
a
red cabbage (11) a
canola (10) ab
rutabaga (19) bc
pepper (8) bcd
collards (6) bcde
tomato (8) bcde
cabbage (18) cde
basil (5) cdef
white mustard (22) cdef
eggplant (10) defg
oregano (5) defg
spinach (14) defg
potato (12) defg
lettuce (13) efg
radish (6) efg
pea (8) fg
carrot (11) fg
onion (14) g
fall rye (11) g
host plant of P. rapae
0 2 4 6 8 10 12
mean blue intensity (%) ± SE
b
pepper (8) a
white mustard (22) ab
basil (5) abc
carrot (11) bc
potato (12) c
eggplant (10) c
oregano (5) cd
spinach (14) cd
tomato (8) d
radish (6) d
rutabaga (19) e
red cabbage (11) e
cabbage (18) ef
canola (10) efg
pea (8) efg
collards (6) efgh
lettuce (13) fgh
fall rye (11) gh
onion (14) h
0 20 40 60 80 100
mean blue DoLP (%) ± SE
c
onion (14) a
potato (12) ab
lettuce (13) ab
oregano (5) ab
collards (6) ab
cabbage (18) ab
red cabbage (11) ab
radish (6) ab
pea (8) ab
spinach (14) ab
basil (5) ab
fall rye (10) ab
white mustard (22) ab
tomato (8) ab
pepper (8) ab
rutabaga (19) b
carrot (11) b
canola (10) b
eggplant (10) b
0 30 60 90 120 150 180
modal blue AoP (%) ± SE

Figure 2.4 **Comparison of intensity (a), degree of linear polarization (*DoLP*) (b), and axis of polarization (*AoP*) (c) among host plants (green bars) and non-host plants (grey bars) of *Pieris rapae*. These measurements used the blue color band. Bars show mean or modal values with the number of plants measured noted in parentheses in each bar. In each subpanel, bars with different letters differ statistically ($p<0.05$), as determined by a post-hoc Tukey test.**

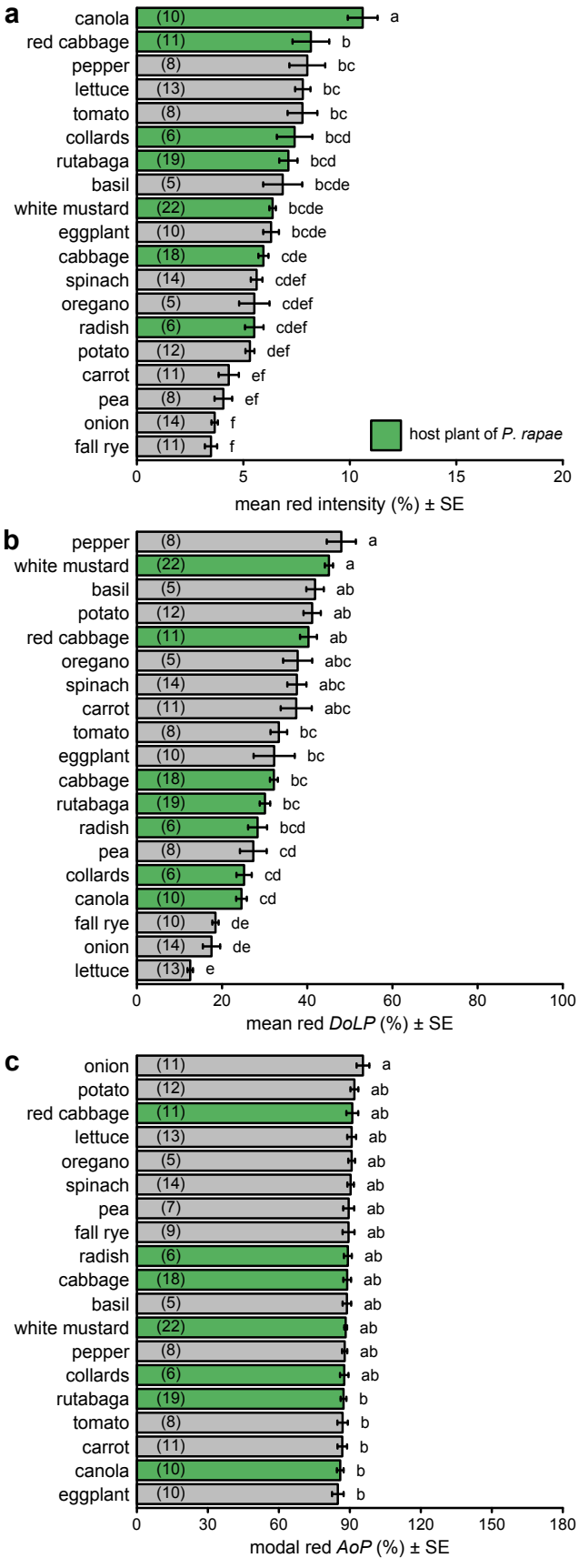
a
canola (10) a
red cabbage (11) b
pepper (8) bc
lettuce (13) bc
tomato (8) bc
collards (6) bcd
rutabaga (19) bcd
basil (5) bcde
white mustard (22) bcde
eggplant (10) bcde
cabbage (18) cde
spinach (14) cdef
oregano (5) cdef
radish (6) cdef
potato (12) def
carrot (11) ef
pea (8) ef
onion (14) f
fall rye (11) f
host plant of P. rapae
0 5 10 15 20
mean red intensity (%) ± SE
b
pepper (8) a
white mustard (22) a
basil (5) ab
potato (12) ab
red cabbage (11) ab
oregano (5) abc
spinach (14) abc
carrot (11) abc
tomato (8) bc
eggplant (10) bc
cabbage (18) bc
rutabaga (19) bc
radish (6) bcd
pea (8) cd
collards (6) cd
canola (10) cd
fall rye (10) de
onion (14) de
lettuce (13) e
0 20 40 60 80 100
mean red DoLP (%) ± SE
c
onion (11) a
potato (12) ab
red cabbage (11) ab
lettuce (13) ab
oregano (5) ab
spinach (14) ab
pea (7) ab
fall rye (9) ab
radish (6) ab
cabbage (18) ab
basil (5) ab
white mustard (22) ab
pepper (8) ab
collards (6) ab
rutabaga (19) b
tomato (8) b
carrot (11) b
canola (10) b
eggplant (10) b
0 30 60 90 120 150 180
modal red AoP (%) ± SE

Figure 2.5 **Comparison of intensity (a), degree of linear polarization (*DoLP*) (b), and axis of polarization (*AoP*) (c) among host plants (green bars) and non-host plants (grey bars) of *Pieris rapae*. These measurements used the red color band. Bars show mean or modal values with number of plants measured noted in parentheses in each bar. Bars with different letters differ statistically ($p<0.05$), as determined by a post-hoc Tukey test.**

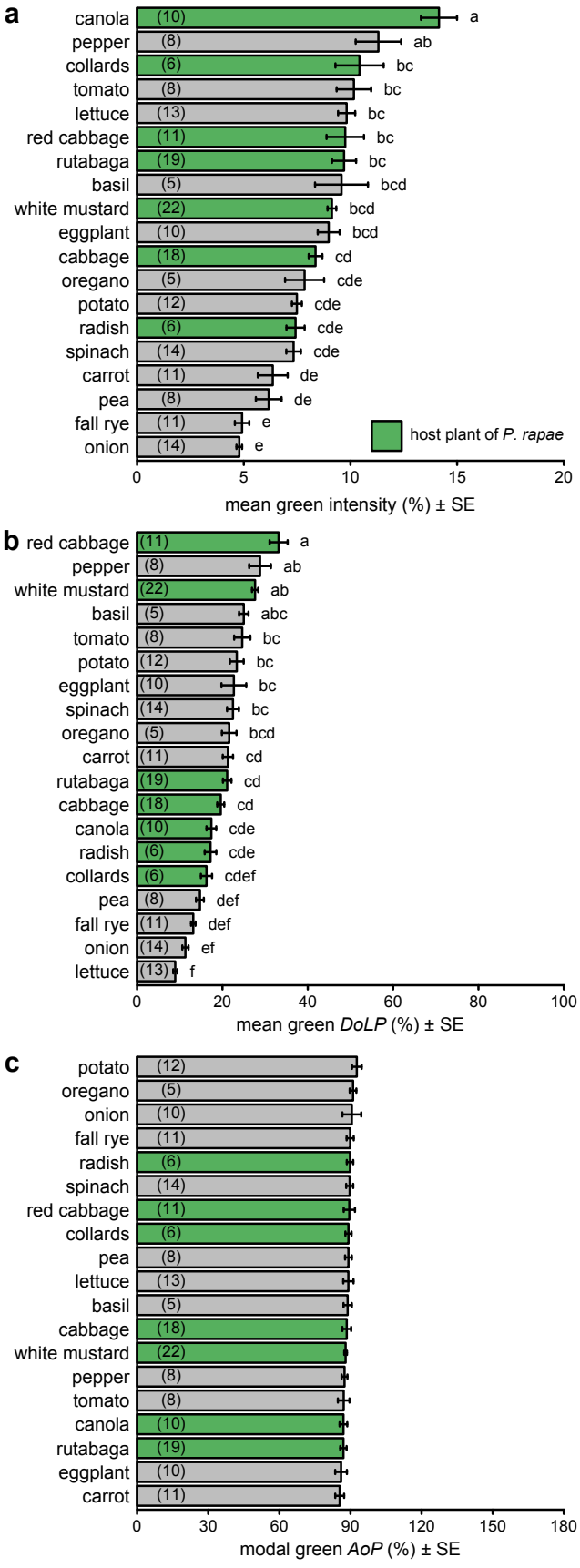
a
canola (10) a
pepper (8) ab
collards (6) bc
tomato (8) bc
lettuce (13) bc
red cabbage (11) bc
rutabaga (19) bc
basil (5) bcd
white mustard (22) bcd
eggplant (10) bcd
cabbage (18) cd
oregano (5) cde
potato (12) cde
radish (6) cde
spinach (14) cde
carrot (11) de
pea (8) de
fall rye (11) e
onion (14) e
host plant of P. rapae
0 5 10 15 20
mean green intensity (%) ± SE
b
red cabbage (11) a
pepper (8) ab
white mustard (22) ab
basil (5) abc
tomato (8) bc
potato (12) bc
eggplant (10) bc
spinach (14) bc
oregano (5) bcd
carrot (11) cd
rutabaga (19) cd
cabbage (18) cd
canola (10) cde
radish (6) cde
collards (6) cdef
pea (8) def
fall rye (11) def
onion (14) ef
lettuce (13) f
0 20 40 60 80 100
mean green DoLP (%) ± SE
c
potato (12)
oregano (5)
onion (10)
fall rye (11)
radish (6)
spinach (14)
red cabbage (11)
collards (6)
pea (8)
lettuce (13)
basil (5)
cabbage (18)
white mustard (22)
pepper (8)
tomato (8)
canola (10)
rutabaga (19)
eggplant (10)
carrot (11)
0 30 60 90 120 150 180
modal green AoP (%) ± SE

Figure 2.6 **Comparison of intensity (a), degree of linear polarization (*DoLP*) (b), and axis of polarization (*AoP*) (c) among host plants (green bars) and non-host plants (grey bars) of *Pieris rapae*. These measurements used the green color band. Bars show mean or modal values with number of plants measured noted in parentheses in each bar. Bars with different letters differ statistically ($p<0.05$), as determined by a post-hoc Tukey test.**

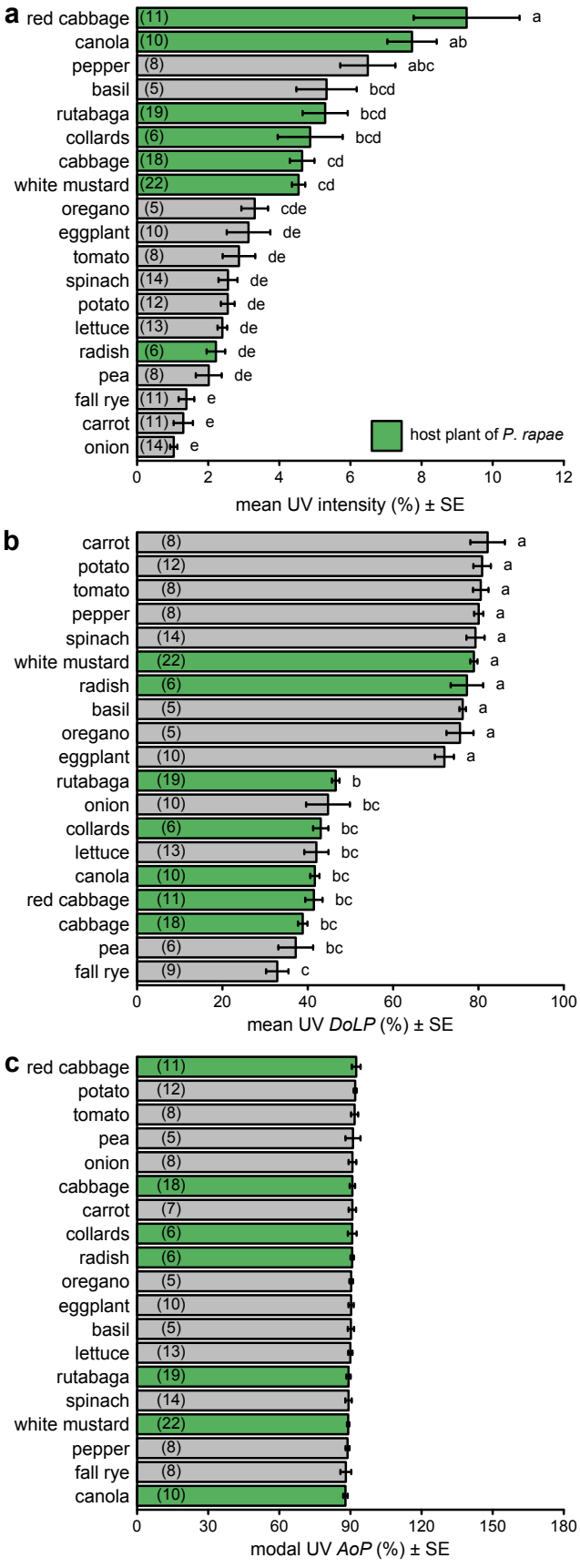
a
red cabbage (11) a
canola (10) ab
pepper (8) abc
basil (5) bcd
rutabaga (19) bcd
collards (6) bcd
cabbage (18) cd
white mustard (22) cd
oregano (5) cde
eggplant (10) de
tomato (8) de
spinach (14) de
potato (12) de
lettuce (13) de
radish (6) de
pea (8) de
fall rye (11) e
carrot (11) e
onion (14) e
host plant of P. rapae
0 2 4 6 8 10 12
mean UV intensity (%) ± SE
b
carrot (8) a
potato (12) a
tomato (8) a
pepper (8) a
spinach (14) a
white mustard (22) a
radish (6) a
basil (5) a
oregano (5) a
eggplant (10) a
rutabaga (19) b
onion (10) bc
collards (6) bc
lettuce (13) bc
canola (10) bc
red cabbage (11) bc
cabbage (18) bc
pea (6) bc
fall rye (9) c
0 20 40 60 80 100
mean UV DoLP (%) ± SE
c
red cabbage (11)
potato (12)
tomato (8)
pea (5)
onion (8)
cabbage (18)
carrot (7)
collards (6)
radish (6)
oregano (5)
eggplant (10)
basil (5)
lettuce (13)
rutabaga (19)
spinach (14)
white mustard (22)
pepper (8)
fall rye (8)
canola (10)
0 30 60 90 120 150 180
modal UV AoP (%) ± SE

Figure 2.7 **Comparison of intensity (a), degree of linear polarization (*DoLP*) (b), and axis of polarization (*AoP*) (c) among host plants (green bars) and non-host plants (grey bars) of *Pieris rapae*. These measurements used the UV color band. Bars show mean or modal values with number of plants measured noted in parentheses in each bar. Bars with different letters differ statistically ($p<0.05$), as determined by a post-hoc Tukey test.**

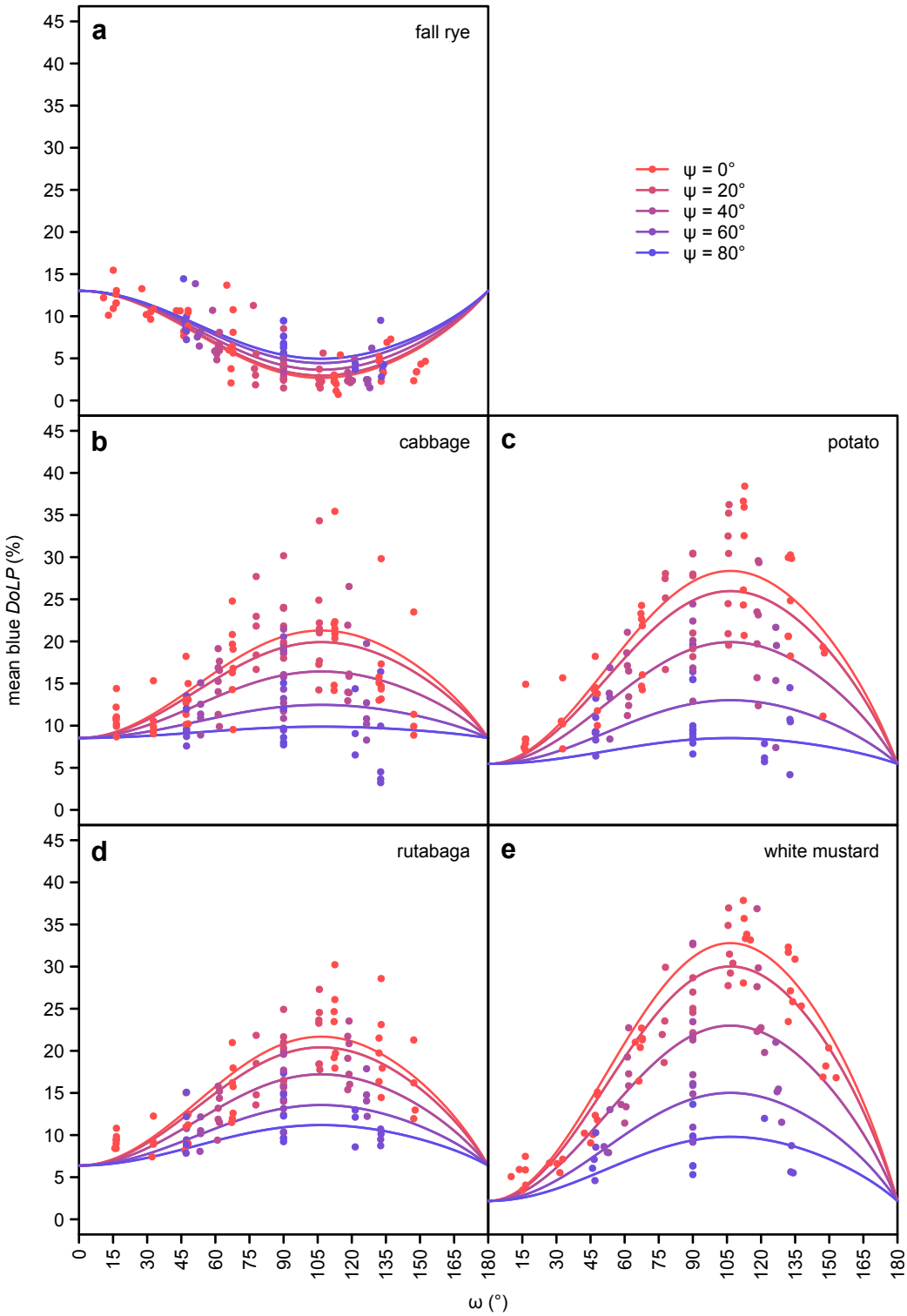
a
fall rye
b
cabbage
c
potato
d
rutabaga
e
white mustard
ψ = 0°
ψ = 20°
ψ = 40°
ψ = 60°
ψ = 80°
mean blue DoLP (%)
ω (°)
0
5
10
15
20
25
30
35
40
45
0
15
30
45
60
75
90
105
120
135
150
165
180

Figure 2.8 **The effect of ω (angle between observer and light source with the plant at its vertex; see Fig. 2.1) and ψ (2-dimensional component of ω perpendicular to the plane passing through both the observer and the plant; see Fig. 2.1) on the mean degree of linear polarization (*DoLP*) of the blue color band, as measured in five select plant species using photo polarimetry. Cabbage, rutabaga and white mustard are host plants of *Pieris rapae*.**

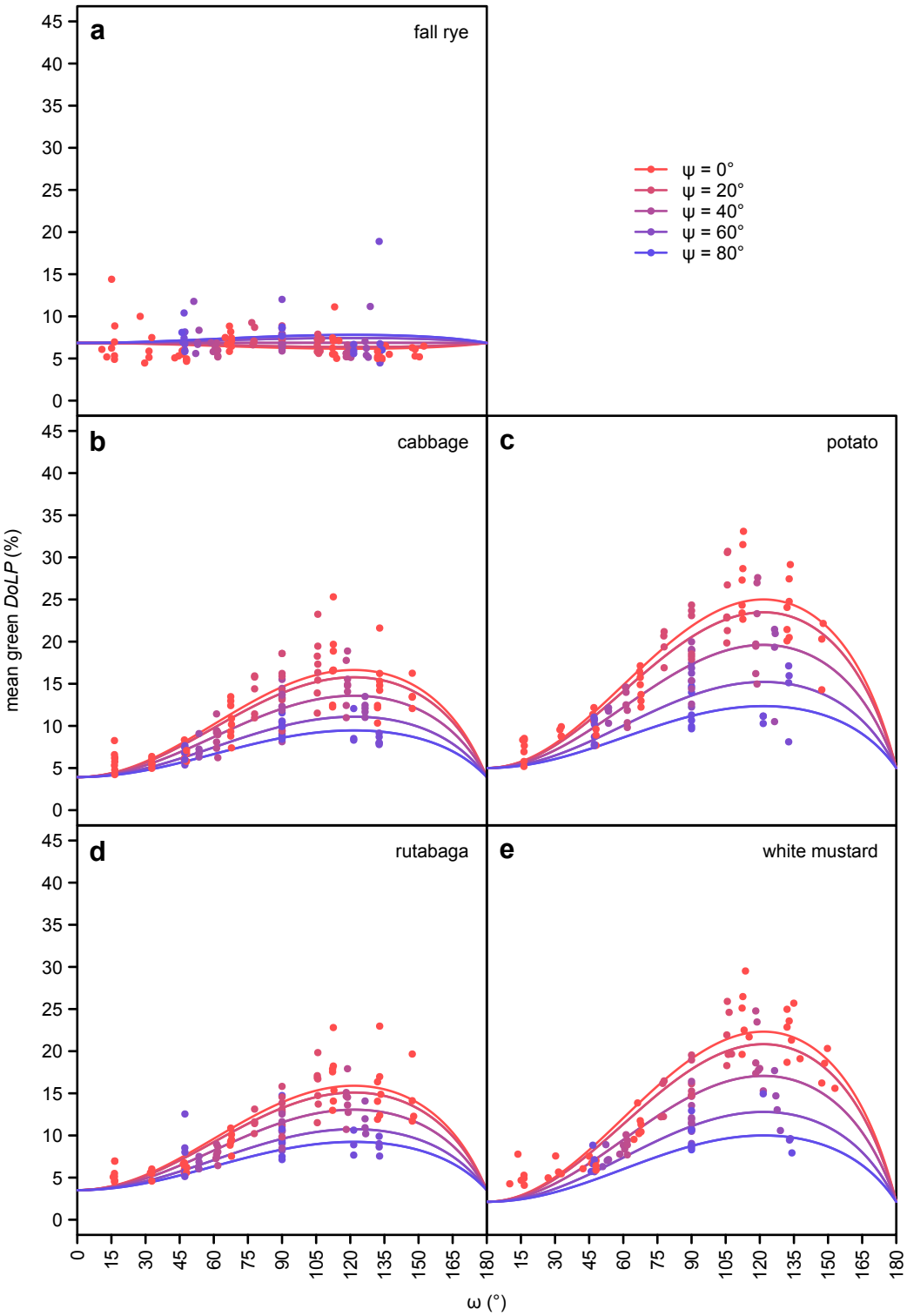
a
fall rye
b
cabbage
c
potato
d
rutabaga
e
white mustard
ψ = 0°
ψ = 20°
ψ = 40°
ψ = 60°
ψ = 80°
mean green DoLP (%)
ω (°)
0
5
10
15
20
25
30
35
40
45
0
15
30
45
60
75
90
105
120
135
150
165
180

Figure 2.9 **The effect of ω (angle between observer and light source with the plant at its vertex; see Fig. 2.1) and ψ (2-dimensional component of ω perpendicular to the plane passing through both the observer and the plant; see Fig. 2.1) on the mean degree of linear polarization (*DoLP*) of the green color band, as measured in five select plant species using photo polarimetry. Cabbage, rutabaga and white mustard are host plants of *Pieris rapae*.**

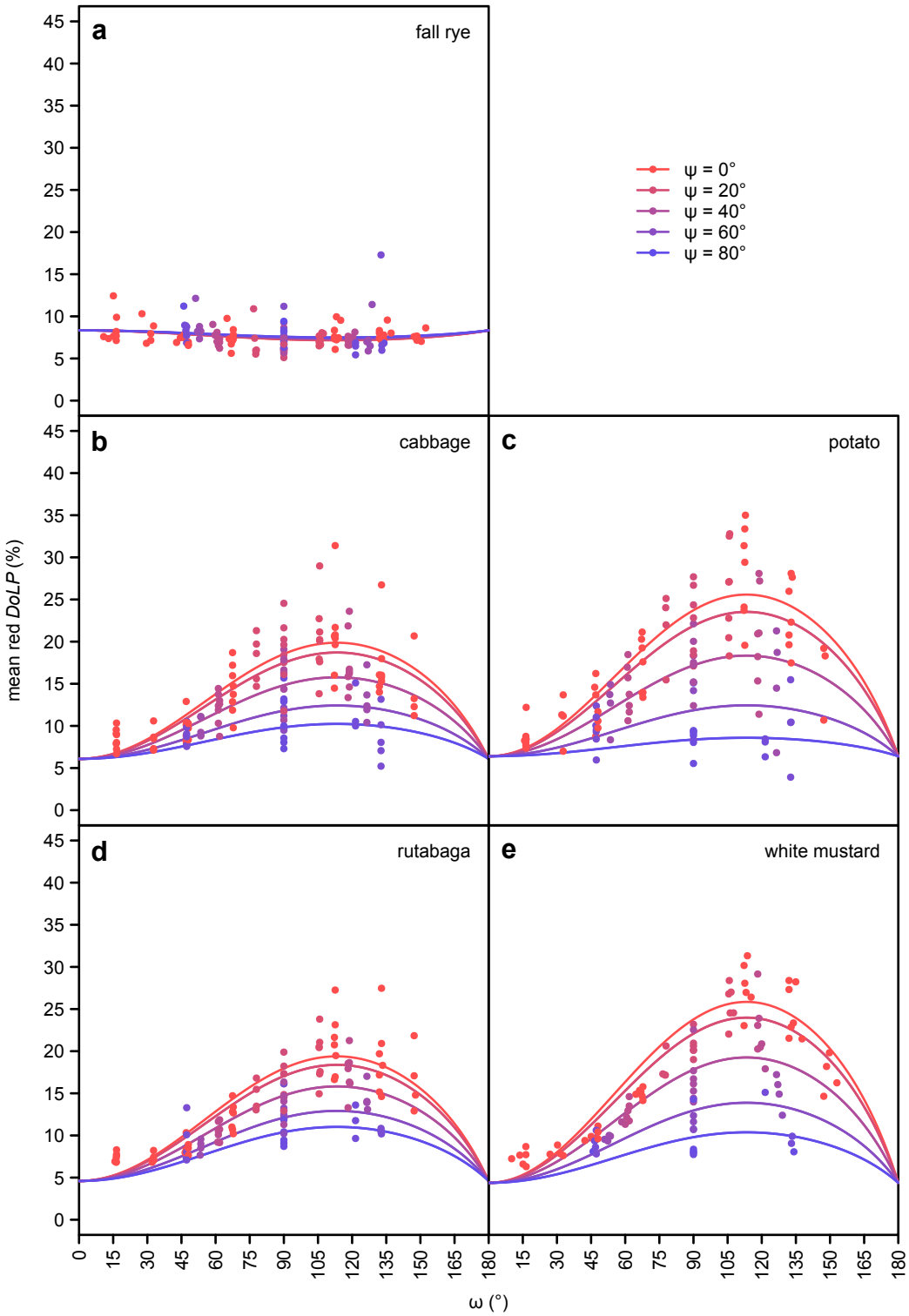
a
fall rye
b
cabbage
c
potato
d
rutabaga
e
white mustard
ψ = 0°
ψ = 20°
ψ = 40°
ψ = 60°
ψ = 80°
mean red DoLP (%)
ω (°)

Figure 2.10 **The effect of ω (angle between observer and light source with the plant at its vertex; see Fig. 2.1) and ψ (2-dimensional component of ω perpendicular to the plane passing through both the observer and the plant; see Fig. 2.1) on the mean degree of linear polarization (*DoLP*) of the blue color band, as measured in five select plant species using photo polarimetry. Cabbage, rutabaga and white mustard are host plants of *Pieris rapae*.**

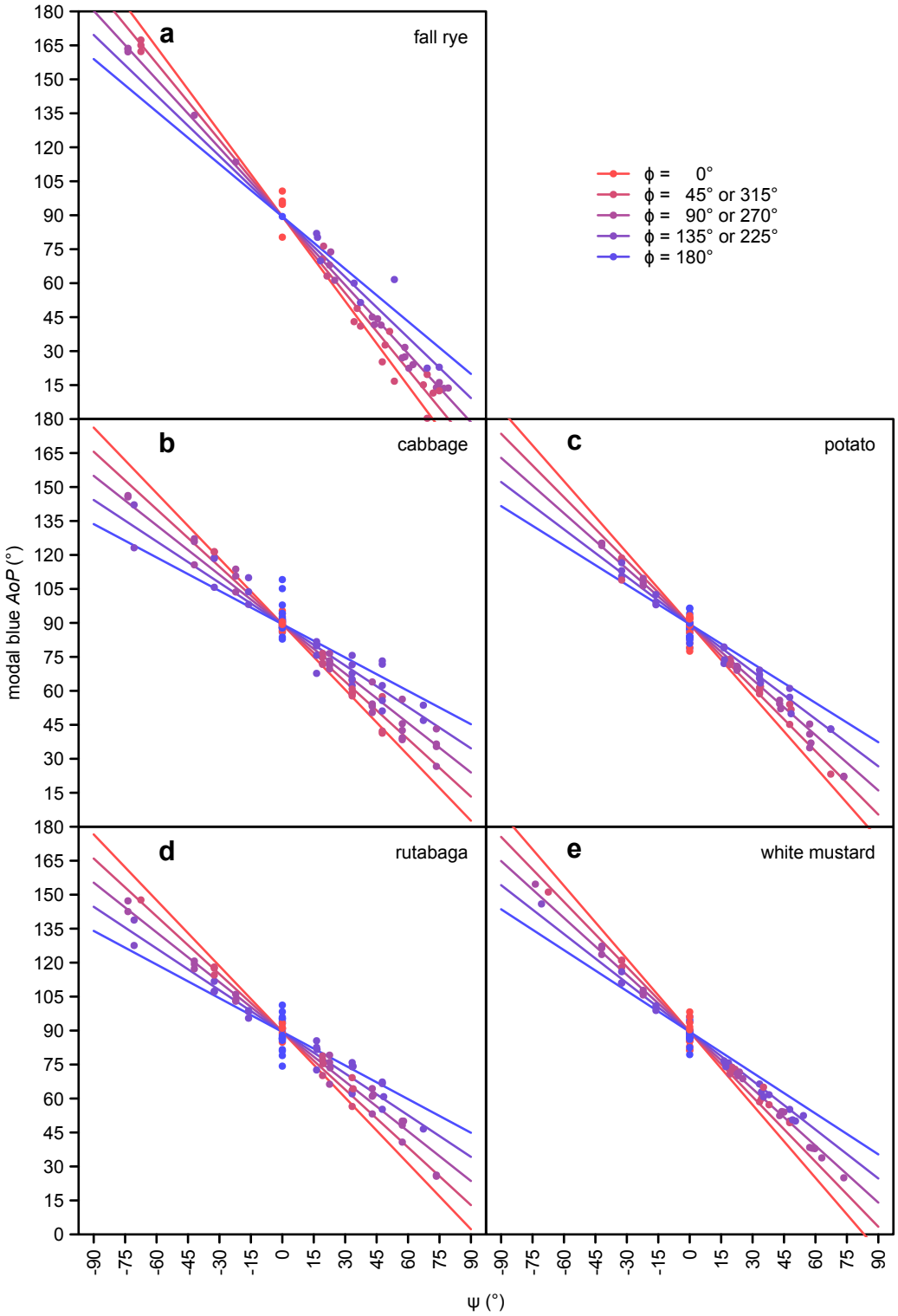
a
fall rye
b
cabbage
c
potato
d
rutabaga
e
white mustard
ϕ = 0°
ϕ = 45° or 315°
ϕ = 90° or 270°
ϕ = 135° or 225°
ϕ = 180°
modal blue AoP (°)
ψ (°)

Figure 2.11 **The effect of ψ (2-dimensional component of ω perpendicular to the plane passing through both the observer and the plant; see Fig. 2.1) and ϕ (angle between the azimuth of the observer and the light source; see Fig. 2.1) on the modal axis of polarization (*AoP*) of the blue color band, as measured in five select plant species using photo polarimetry. Cabbage, rutabaga and white mustard are host plants of *Pieris rapae*.**

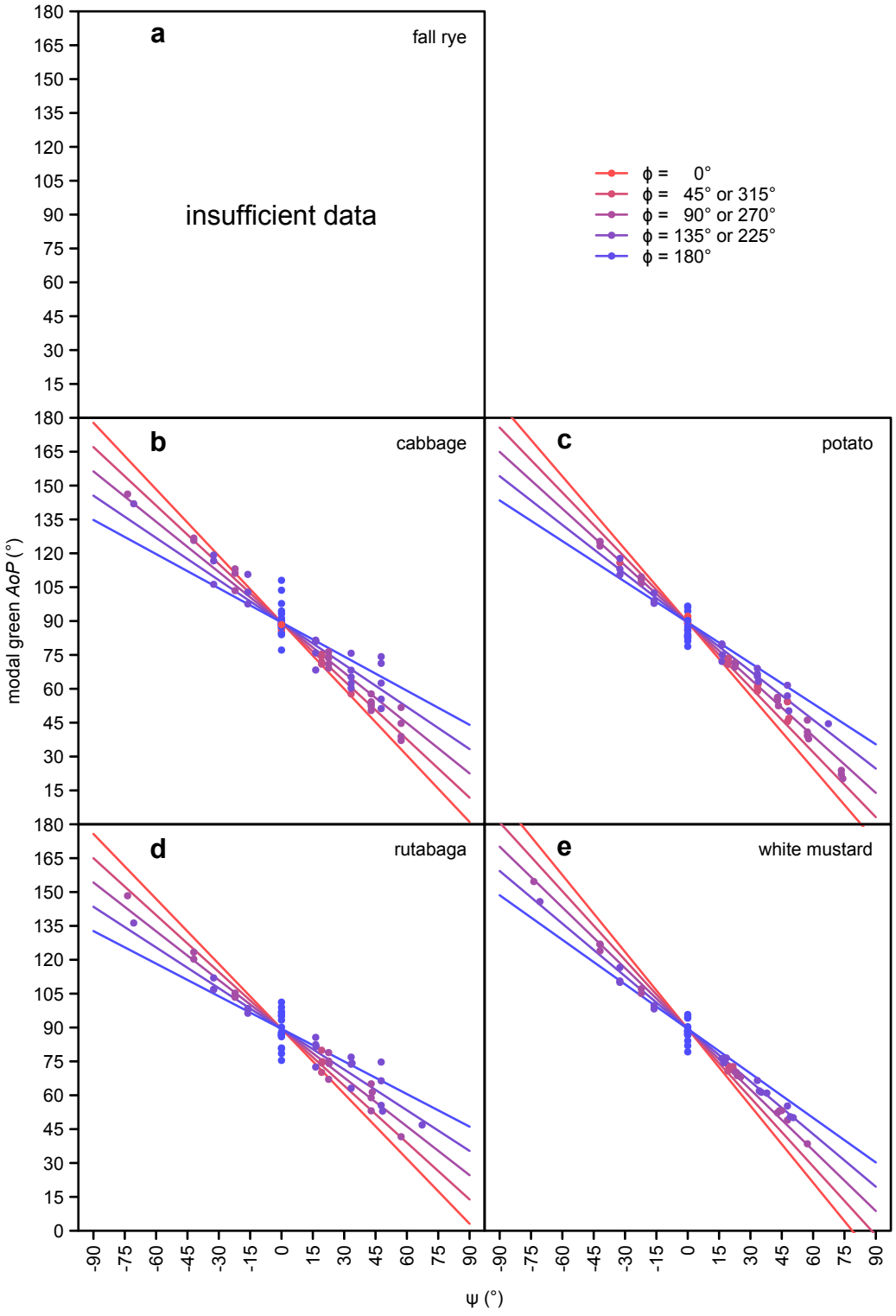
a
fall rye
insufficient data
ϕ = 0°
ϕ = 45° or 315°
ϕ = 90° or 270°
ϕ = 135° or 225°
ϕ = 180°
b
cabbage
c
potato
d
rutabaga
e
white mustard
modal green AoP (°)
Ψ (°)

Figure 2.12 **The effect of ψ (2-dimensional component of ω perpendicular to the plane passing through both the observer and plant; see Fig. 2.1) and ϕ (angle between the azimuth of the observer and the light source; see Fig. 2.1) on the modal axis of polarization (*AoP*) of the green color band, as measured in five select plant species using photo polarimetry. Cabbage, rutabaga and white mustard are host plants of *Pieris rapae*. Fall rye data were excluded from analyses due to an insufficient number of measurements meeting the inclusion criterion (>10% of pixels with a degree of linear polarization above 15%).**

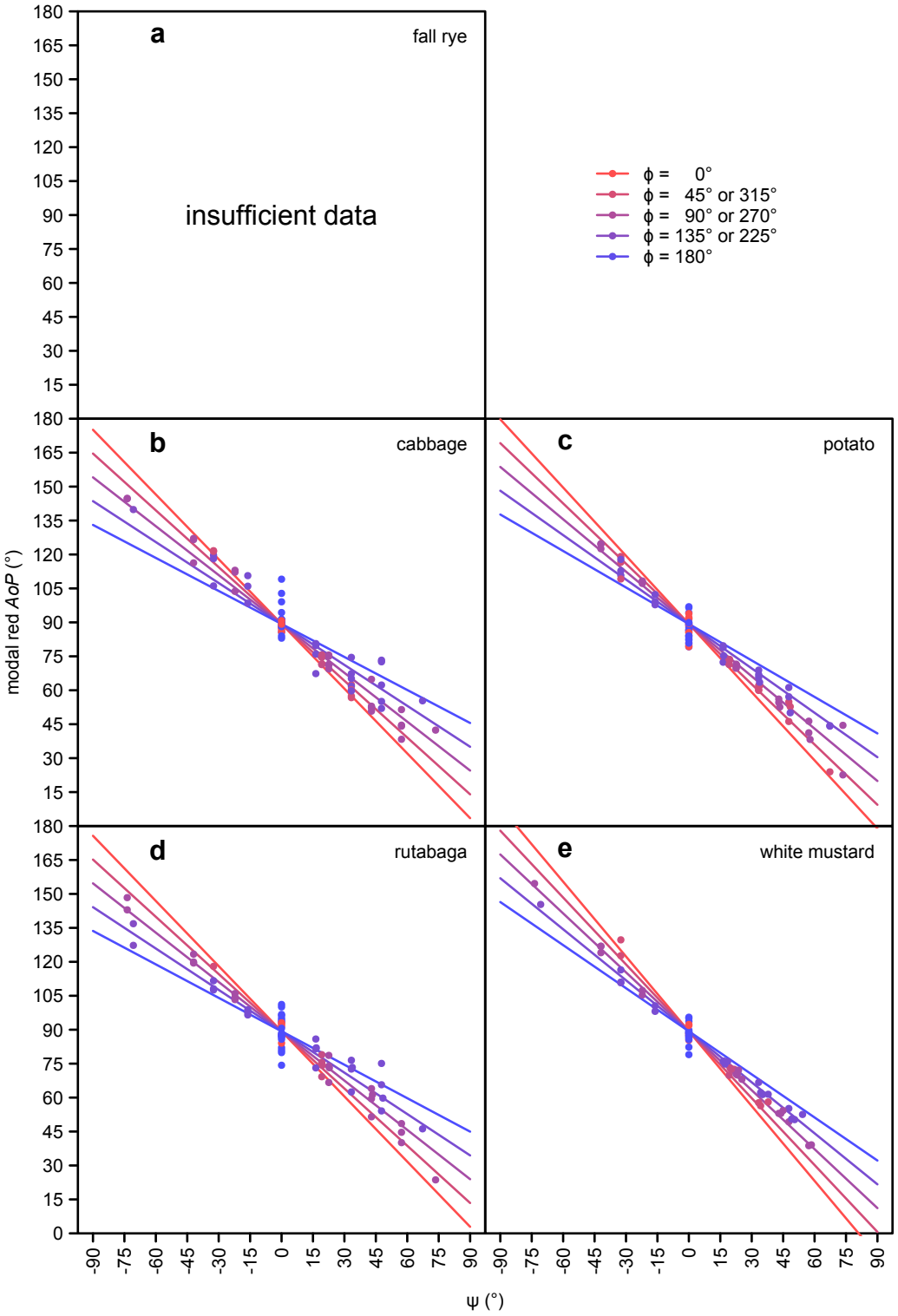
a
fall rye
insufficient data
ϕ = 0°
ϕ = 45° or 315°
ϕ = 90° or 270°
ϕ = 135° or 225°
ϕ = 180°
b
cabbage
c
potato
d
rutabaga
e
white mustard
modal red AoP (°)
Ψ (°)

Figure 2.13 **The effect of ψ (2-dimensional component of ω perpendicular to the plane passing through both the observer and plant; see Fig. 2.1) and ϕ (angle between the azimuth of the observer and the light source; see Fig. 2.1) on the modal axis of polarization (*AoP*) of the red color band, as measured in four select plant species using photo polarimetry. Cabbage, rutabaga and white mustard are host plants of *Pieris rapae*. Fall rye data were excluded from analyses due to an insufficient number of measurements meeting the inclusion criterion (>10% of pixels with a degree of linear polarization above 15%).**

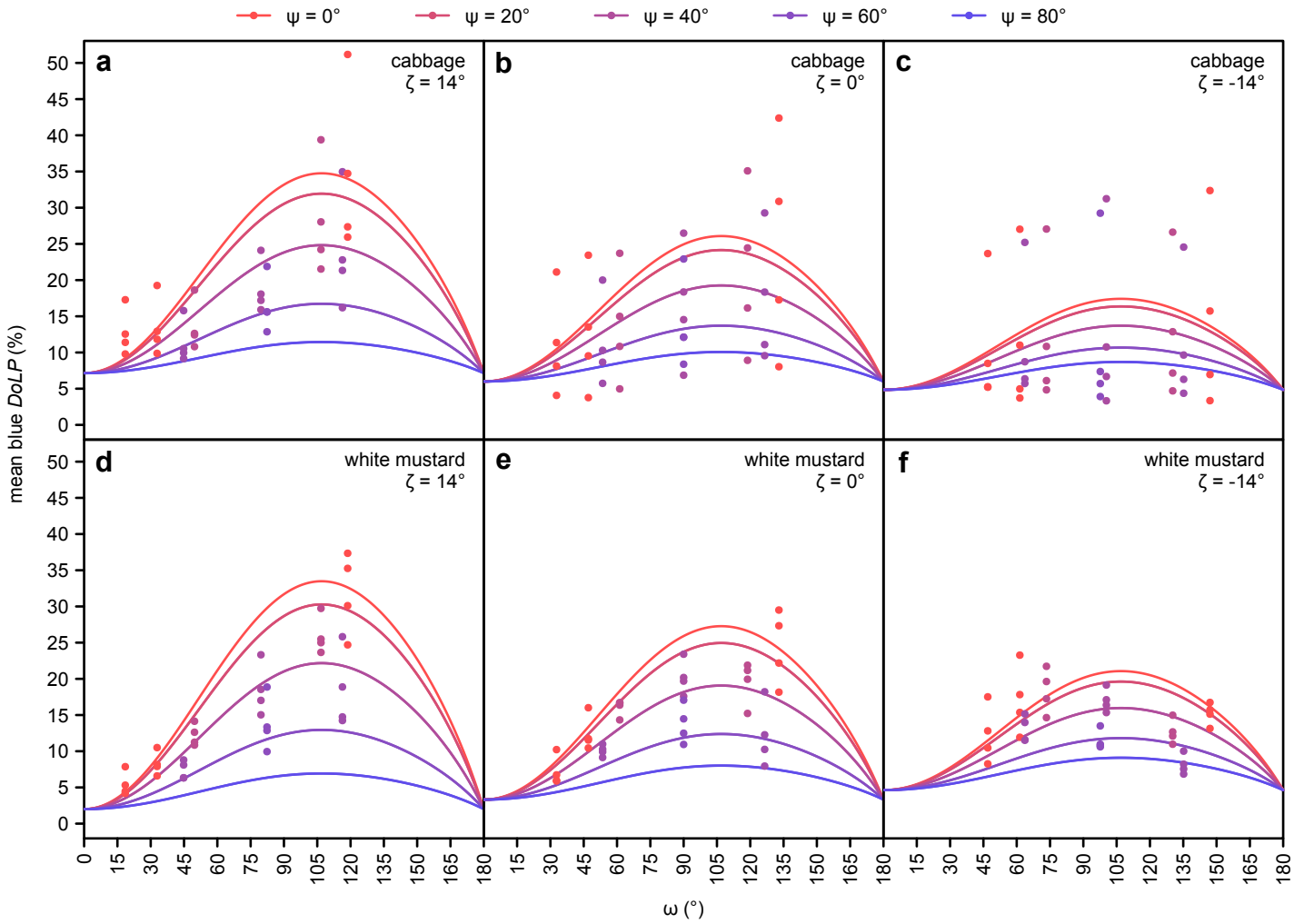

Figure 2.14 **The additional effect of observer elevation (ζ; see Fig. 2.1) on the mean degree of linear polarization (*DoLP*) of the blue color band, as measured in cabbage and white mustard (host plants of *Pieris rapae*) using photo polarimetry.**

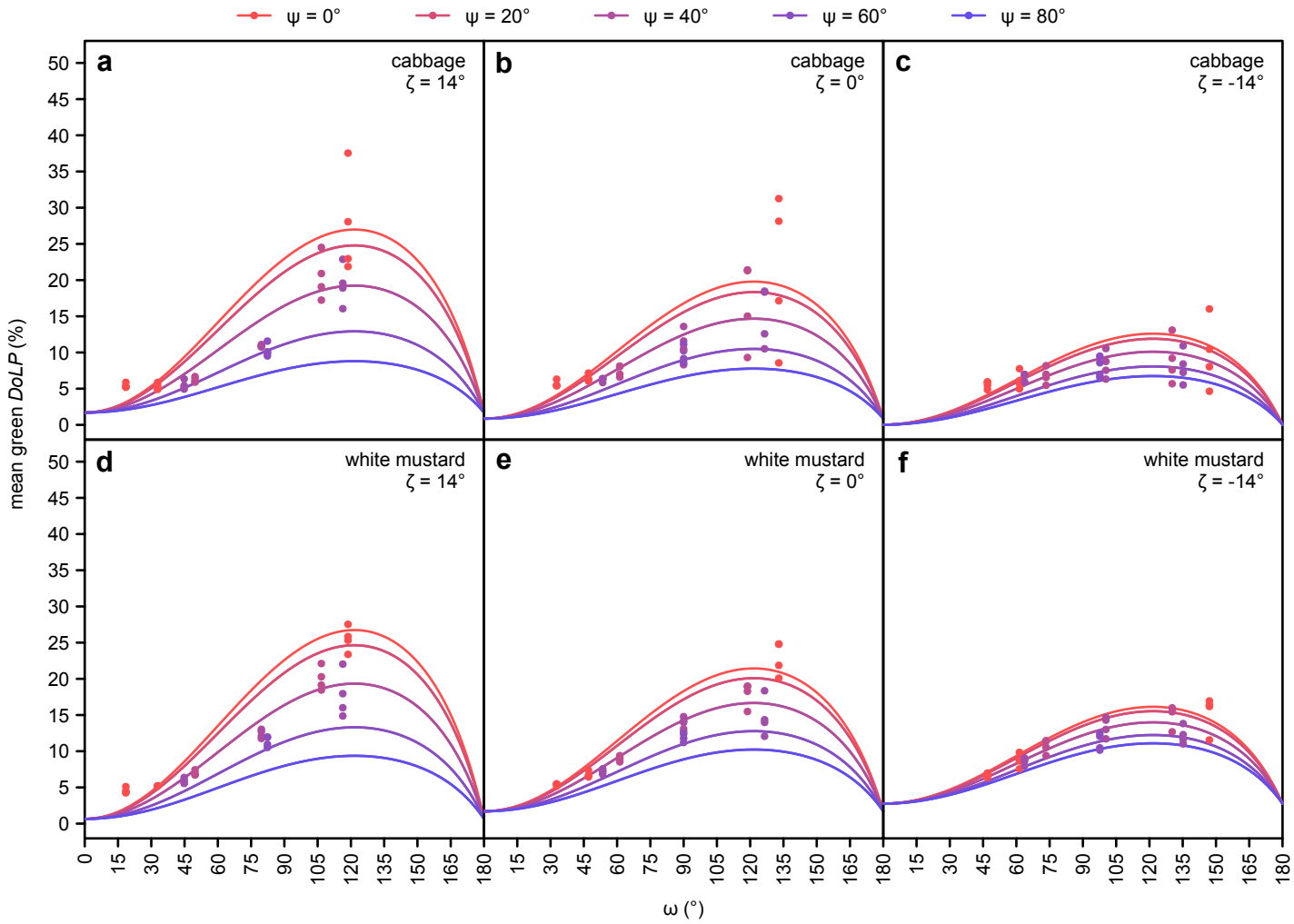

Figure 2.15 **Additional effect of ζ (elevation of the observer; see Fig. 2.1) on the mean degree of linear polarization (*DoLP*) of the green color band, as measured in cabbage and white mustard (host plants of *Pieris rapae*) using photo polarimetry.**

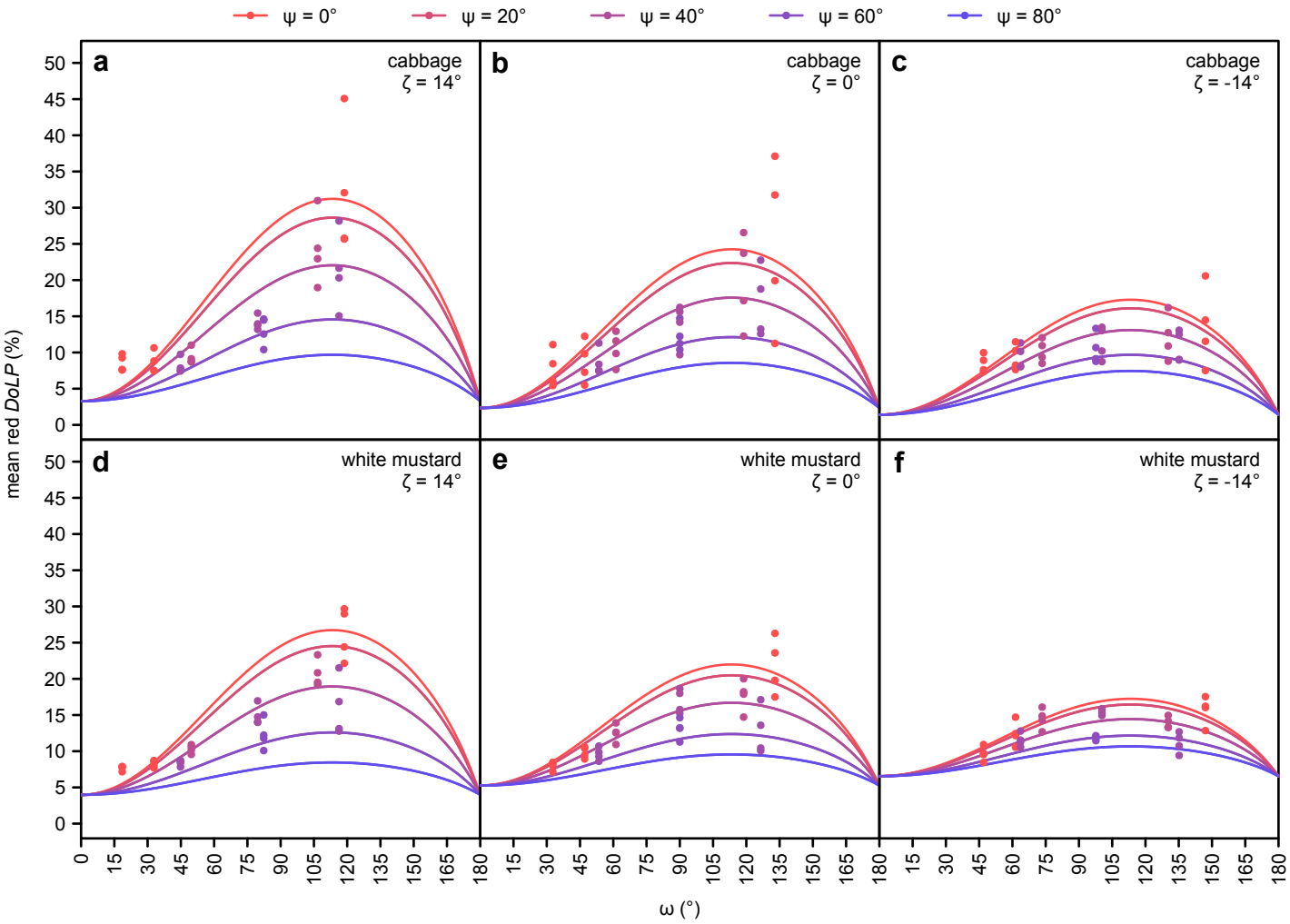

Figure 2.16 **Additional effect of ζ (elevation of the observer; see Fig. 2.1) on the mean degree of linear polarization (*DoLP*) of the red color band, as measured in cabbage and white mustard (host plants of *Pieris rapae)* using photo polarimetry.**

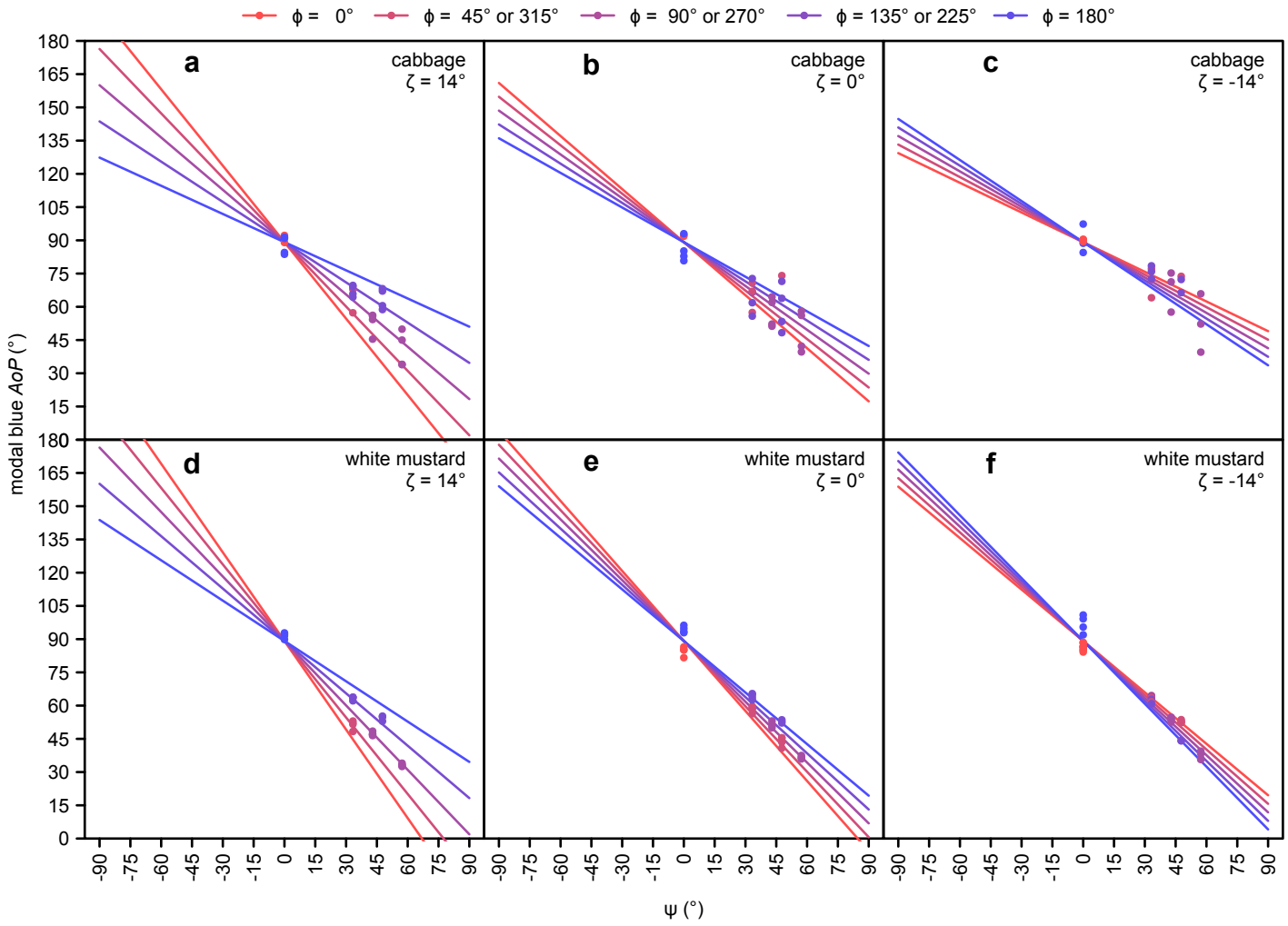
ϕ = 0°
ϕ = 45° or 315°
ϕ = 90° or 270°
ϕ = 135° or 225°
ϕ = 180°
a
cabbage
ζ = 14°
b
cabbage
ζ = 0°
c
cabbage
ζ = -14°
d
white mustard
ζ = 14°
e
white mustard
ζ = 0°
f
white mustard
ζ = -14°
modal blue AoP (°)
ψ (°)

Figure 2.17 **Additional effect of ζ (elevation of the observer; see Fig. 2.1) on the modal axis of polarization (*AoP*) of the blue color band, as measured in cabbage and white mustard (hosts of *Pieris rapae*) using photo polarimetry. Red and green color band data were excluded from analyses due to an insufficient number of measurements meeting the inclusion criterion (<10% of pixels with a degree of linear polarization above 15%).**

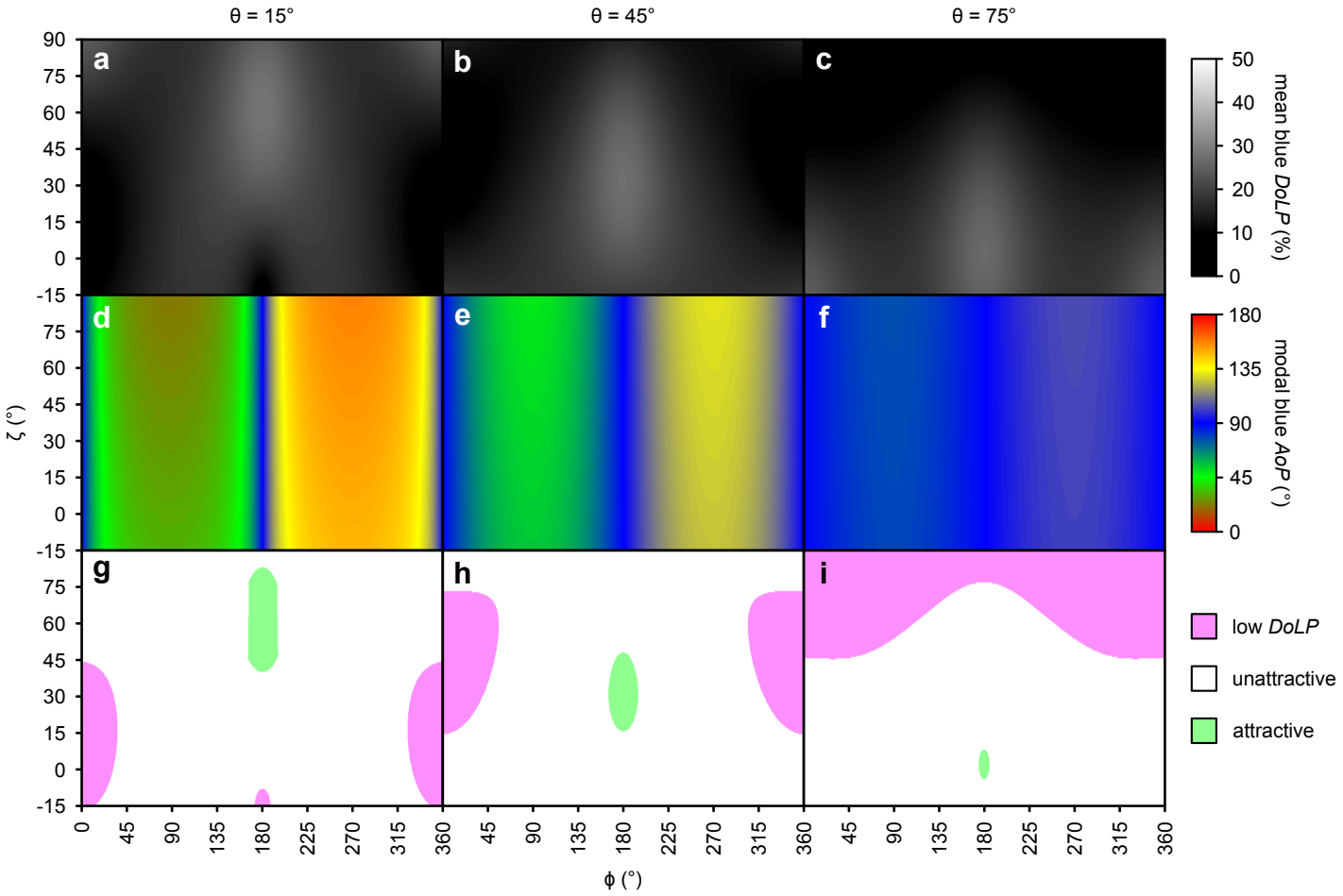
θ = 15°
θ = 45°
θ = 75°
a
b
c
d
e
f
g
h
i
ζ (°)
ϕ (°)
mean blue DoLP (%)
modal blue AoP (°)
low DoLP
unattractive
attractive

Figure 2.18 **Effects of approach direction (angle between the azimuth of the observer and the light source (ϕ; see Fig. 1) and elevation of the observer (ζ; see Fig. 2.1) on the mean degree of linear polarization (*DoLP*) (a-c) and the modal axis of polarization (*AoP*) (d-f) of the blue color band of cabbage plants (host of *Pieris rapae*). Attractiveness of resulting polarization characteristics to *P. rapae* (g-i), based on a previous behavioral study (Blake et al. 2019). Approach trajectories resulting in attractive characteristics (*DoLP* = 26-36% and *AoP* = 0-38, 53-128 or 143-180°) and unattractive characteristics (*DoLP* = 10-26% or *AoP* = 38-53°, 128-143°) are shown in green and white, respectively, with pink indicating trajectories resulting in a moderately-attractive low *DoLP* (<10%). Higher *DoLP* (36-60%) would also be unattractive but were not predicted by these models. These effects changed with light source elevation (θ; see Fig. 2.1) which is shown at 15° (a, d, g), 45° (b, e, h) and 75° (c, f, i).**

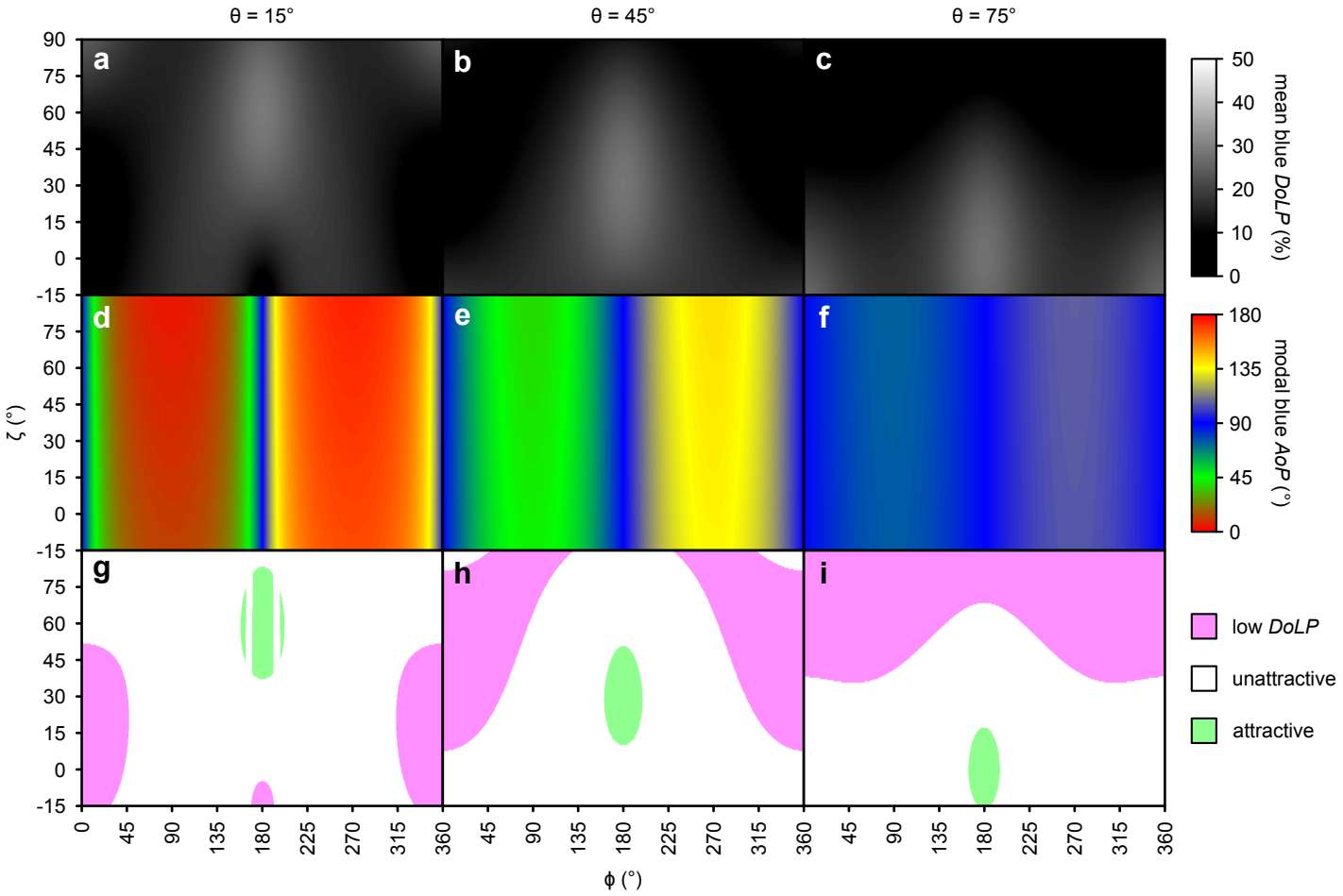
θ = 15°
θ = 45°
θ = 75°
a
b
c
d
e
f
g
h
i
ζ (°)
ϕ (°)
mean blue DoLP (%)
modal blue AoP (°)
low DoLP
unattractive
attractive

Figure 2.19 **Effects of approach direction (angle between the azimuth of the observer and the light source (ϕ, see Fig. 1) and elevation of the observer (ζ; see Fig. 2.1) on the mean degree of linear polarization (*DoLP*) (a-c) and the modal axis of polarization (*AoP*) (d-f) of the blue color band of white mustard plants (host of *Pieris rapae*). Attractiveness of resulting polarization characteristics to *Pieris rapae* (g-i), based on a previous behavioral study (Blake et al. 2019). Approach trajectories resulting in attractive characteristics (*DoLP* = 26-36% and *AoP* = 0-38, 53-128 or 143-180°) and unattractive characteristics (*DoLP* = 10-26% or *AoP* = 38-53°, 128-143°) are shown in green and white, respectively, with pink indicating trajectories resulting in a moderately-attractive low *DoLP* (<10%). Higher *DoLP* (36-60%) would also be unattractive but were not predicted by these models. These effects changed with light source elevation (θ; see Fig. 2.1) which is shown at 15° (a, d, g), 45° (b, e, h) and 75° (c, f, i).**

Chapter 3.

Compound eyes of the small white butterfly *Pieris rapae*, have three distinct classes of red photoreceptors[1]

[1]The corresponding manuscript is published in *Journal of Comparative Physiology A* (2019, doi.org/10.1007/s00359-019-01330-8) with the following authors: Blake AJ, Pirih P, Qiu X, Stavenga DG, Arikawa K, Gries G

3.1. Abstract

The two subspecies of the Small White butterfly, the European *Pieris rapae rapae* and the Asian *P. r. crucivora*, differ in wing colouration. Under ultraviolet light, the wings of both male and female *P. r. rapae* appear dark, whereas the wings of male *P. r. crucivora* are dark and those of females are bright. It has been hypothesized that these sexually dimorphic wing reflections in *P. r. crucivora* may have induced the evolution of a fluorescing-screening pigment in the violet-opsin-expressing photoreceptors of males, thus facilitating greater wavelength discrimination near 400 nm. Comparing the compound eyes of the two subspecies using genetic, microscopical, spectrographic and histological methods revealed no differences that would meaningfully affect photoreceptor sensitivity, suggesting that the fluorescing-screening pigment did not evolve in response to sexually dimorphic wing reflections. Our investigation further revealed that (*i*) the peri-rhabdomal reddish-screening pigments differ among the three ommatidial types; (*ii*) each of the ommatidial types exhibits a unique class of red photoreceptor with a distinct spectral peak; and (*iii*) the blue, green, and red photoreceptors of *P. rapae* exhibit a polarization sensitivity > 2, with red photoreceptors allowing for a two-channel opponency form of polarization sensitivity.

3.2. Introduction

The compound eyes of many insects are composed of thousands of ommatidia. These ommatidia are often not uniform across the eye and differ in the expression of visual pigments in a stochastic mosaic governed by a single transcription factor (Perry et al. 2016). The ventral compound eye of the Asian subspecies of the Small White butterfly, *Pieris rapae crucivora* Boisduval 1836 (Pieridae), exhibits a mosaic of three ommatidial types (Qiu et al. 2002) which are most readily distinguished by the trapezoidal (I), square (II), or rectangular (III) arrangement of pigment clusters surrounding the rhabdom. As is typical of pierid and papilionid butterflies, the distal, proximal and basal parts of the fused rhabdom are composed of the photoreceptors R1-4, R5-8, and R9, respectively (Fig. 3.1; Shimohigashi and Tominaga 1991). The R1-4 photoreceptors express four different rhodopsins (PrUV, PrV, PrB, PrL) which absorb maximally in the ultraviolet (UV), violet, blue, and green-yellow wavelength ranges, respectively; all R5-8 photoreceptors (and presumably also R9) express PrL (Table 3.1; Wakakuwa et al. 2004; Arikawa et al. 2005). Remarkably, however, intracellular recordings have revealed at least eight spectral classes of photoreceptors (Qiu and Arikawa 2003a,b; Arikawa et al. 2005).

As the rhodopsin molecules of a photoreceptor reside in its rhabdomere, the spectral sensitivity of the photoreceptor is determined by how much of the light flux propagating in the rhabdom its rhodopsin molecules absorb at each wavelength (Snyder 1979; Stavenga 2006). The rhabdom acts as an optical waveguide, and therefore the light flux does not fully propagate inside the rhabdom boundary. The part outside the boundary encounters the rhabdom-surrounding pigment clusters that thus act as spectral filters and consequently affect the spectral sensitivity of the photoreceptors. This holds specifically for those photoreceptors (R5-9) that contribute microvilli in the proximal and basal parts of the rhabdom (Qiu et al. 2002; Arikawa et al. 2005; Stavenga and Arikawa 2011).

Microspectrophotometry on histological sections identified two peri-rhabdomal pigment types. Pale-red pigment clusters were found in ommatidial types I and III, and deep-red pigment in ommatidial type II (Stavenga and Arikawa 2011). This finding agreed with observations of the eyeshine observable in live butterflies studied under epi-illumination light microscopy (Qiu et al. 2002). Eyeshine in butterfly eyes is created by a strongly folded tracheole, the tapetum, that exists below each rhabdom and that acts as

an interference reflector. Incident light that has propagated down to the basal end of the rhabdom, without having been absorbed by either the rhodopsins in the rhabdom or the surrounding pigment clusters, is reflected by the tapetum and then travels back through the rhabdom, eventually exiting the ommatidium through its facet lens. The eyeshine colour has been characterized as either pale-red or deep-red, corresponding well to the colour of the pigment clusters that surrounds the rhabdoms (Qiu et al. 2002; Stavenga and Arikawa 2011).

Fluorescence microscopy with a blue-violet excitation light revealed the presence, exclusively in males, of a distinctly fluorescing pigment in type II ommatidia. This pigment was shown to act as a violet-absorbing pigment on the R1 and R2 photoreceptors. These photoreceptors express the PrV rhodopsin, so that in females they are violet-sensitive photoreceptors, but the filtering effect of the pigment results in the double-peaked blue photoreceptors of males (Fig. 3.2b; Table 3.1; Arikawa et al. 2005). Similarly, in *Papilio* a fluorescing pigment, presumably 3-hydroxyretinol, narrows the sensitivity of a UV opsin-expressing photoreceptor to create a narrow-band violet receptor (Arikawa et al. 1999a). However, the identity of the pigment in *P. rapae* remains elusive as its peak absorbance of ~420 nm contrasts that of 3-hydroxyretinol (~320 nm) (Arikawa et al. 2005).

The sexual differences in the eye pigmentation of *P. r. crucivora* might be related to the marked sexual dimorphism in UV reflections from their wings (Fig. 3.2a). The reflectance of male and female wings in the UV wavelength range is low and high, respectively. In contrast, in the European subspecies of *P. rapae* (Linnaeus, 1758), *P. r. rapae* (Linnaeus, 1758), the UV reflectance of both male and female wings is low (Obara 1970; Obara and Majerus 2000; Giraldo and Stavenga 2007). As a behavioural “flutter response”, used by resting males to deter approaching males, is present in both subspecies, the UV reflectance of *P. r. rapae* wings is likely the ancestral state (Obara and Majerus 2000). It therefore has been hypothesized that the divergent spectral sensitivity of the double-peaked blue photoreceptors of *P. r. crucivora* males (Fig. 3.2b) is an adaptation that enables greater wavelength discrimination near 400 nm, thereby improving the males’ ability to discriminate females from males based on differential UV reflectance of their wings (Arikawa et al. 2005).

To test this hypothesis, we performed a comparative study of the compound eyes of *P. r. rapae* and *P. r. crucivora*, using a combination of genetics, spectrophotometry, electron microscopy, and *in vivo* eyeshine observations coupled with histological localization. Most of these data were available for *P. r. crucivora* but additional spectrophotometry, histology and microscopy measurements were necessary for *P. r. rapae*. Our findings also prompted a re-examination of previously obtained electrophysiological recordings of *P. r. crucivora* photoreceptors that yielded spectral and polarization sensitivities.

3.3. Materials and Methods

3.3.1. Experimental insects

Males and females of *P. r. crucivora* were taken from a laboratory colony started from eggs laid by females collected around the campus of Yokohama City University. Larvae were reared on fresh kale leaves at 19 °C under a photoperiod of 8:16 h (L:D). Pupae were stored at 4 °C for at least 3 months before adults were allowed to eclose at 25 °C. Adults were used in experiments within 4 d of eclosion.

Males and females of *P. r. rapae* were taken from a laboratory colony started from eggs procured from Carolina Biological Supply Company (Item # 144102; NC, USA). Larvae were reared on a wheat-germ casein diet. Adults were allowed to eclose from pupae that were kept at room temperature or held at 4 °C for up to two weeks (Webb and Shelton 1988). Both larvae and adults were held in a rearing room with a temperature and light regime of 18-24 °C and 8:16 h L:D.

3.3.2. *P. r. rapae* opsin sequences

The complete genome of *P. r. rapae* was recently sequenced and annotated (Shen et al. 2016). MEGA7 (Kumar et al. 2016) was deployed to generate a maximum likelihood phylogenetic tree of opsins from an alignment of the *P. r. rapae* sequences and all available full opsin protein sequences from the Pieridae.

3.3.3. Histology

To examine ommatidial heterogeneity in pigment clusters, isolated eyes were fixed at room temperature for 30 min in 4% paraformaldehyde (PA) in a 0.1 M sodium cacodylate buffer (CB) with a pH of 7.4. Eyes were then dehydrated in a graded series of acetone, infiltrated with propylene oxide, and embedded in Epon. Unstained transverse sections of 5-10 µm thickness were observed and photographed with a regular transmission light microscope.

Eyes prepared for electron microscopy were fixed with 2.5% glutaraldehyde and 2% PA in 0.1 M CB at 4 °C overnight, post-fixed in 2% OsO_4 in 0.1 M CB for 2 h at room temperature, and embedded as described above. Ultra-thin sections were prepared and stained with 1% uranyl acetate prior to observations with a transmission electron microscope (H7600 or H7650, Hitachi, Tokyo).

3.3.4. Eyeshine and ommatidial fluorescence

The spatial arrangement of ommatidial types, both in the ventral and dorsal eye regions, was investigated in the eyes of living butterflies, using epi-illumination with a modified telemicroscopic optical assembly (Stavenga 2002) equipped with a 50% beam splitter, a long working distance air objective (LUCplanFLN20X, NA 0.45, WD 6.4–7.6 mm, Olympus, Tokyo, JP) and a monochrome digital camera (Chameleon3, CM3-U3-31S4M-CS, Point Grey/FLIR BC, CA). The light source, a 500 W Xenon lamp, was bandpass-filtered between 500 and 710 nm (20 nm bandwidth; Asahi Spectra, Tokyo, JP). Ommatidial fluorescence was recorded by replacing the beam splitter with standard fluorescence cubes (U-MWU, U-MWBV; Olympus).

Reflectance and fluorescence measurements from four eyes of three females and five eyes of three males, with 100-450 ommatidial measurements per eye, were used to classify the ommatidia into groups using *k*-means clustering (Hartigan and Wong 1979). After the *in vivo* measurements, the eyes were fixed, sectioned and observed under a light microscope. The histology indicated four distinct ommatidial types (dorsal; ventral types I-III), which mapped well with the ommatidial groups derived by *k*-means clustering.

3.3.5. Absorbance spectra of the reddish screening pigments

Absorbance spectra of the reddish peri-rhabdomal screening pigments were obtained from unstained transverse eye sections of both male and female *P. r. rapae*. Hyperspectral imaging was performed using (*i*) a modified Zeiss Axioskop 2 FS microscope with a fixed tube lens (f165 mm), (*ii*) a motorized z-stage and either a Zeiss Neofluar 40×0.85 dry objective or a Zeiss Ultrafluar 40×0.60 immersion objective, and (*iii*) a monochrome camera (Blackfly 23S6M; IMX249, pixel size 5.86 µm or Flea 32S2M; IMX036, pixel size 2.5 µm; FLIR/PointGrey). The light source was a PTI Deltascan 4000 system with a 75 W XBO lamp and a motorized monochromator. A quartz fiber (800 µm, NA 0.22) connected the light source to an achromatic condensor (NA 0.9). Hyperspectral image stacks of the sections were taken in the range of 360 to 730 nm. Prior to taking the stacks, the best focus position at each wavelength was determined by maximizing the variance of subimage blocks of a calibration slide. Using Fiji (Schinderlin et al. 2012), the measured stack was divided with a reference stack taken in the same microscope slide, yielding a transmittance stack and was then registered using the StackReg plugin (Thévenaz et al. 1998). In each section, the transmission of the reddish screening pigments of 10-64 ommatidia of each type were taken and used to calculate non-normalized and normalized absorbance spectra.

3.3.6. Electrophysiology

Intracellular recordings of the spectral sensitivities of *P. r. crucivora* photoreceptors reported by Qiu and Arikawa (2003a,b) and Arikawa et al. (2005), together with unpublished recordings lacking histological identification, were all re-analyzed using the originally recorded response voltages. Previous electrophysiological analyses were constrained to recordings with histological localization. All available recordings with maximal response amplitude > 30 mV were included, and the spectral class and (in most cases) ommatidial type of these recordings were inferred by comparing their spectral sensitivity with that of marked photoreceptors. In our analyses, red photoreceptors were assigned to three rather than two classes (Qiu et al. 2002), based on ommatidial type. The procedure for intracellular recordings has been described in detail (Qiu and Arikawa 2003ab; Arikawa et al. 2005) and is only outlined below. Isoquantal monochromatic 30 ms stimuli were generated by a 500 W Xenon arc lamp directed through a series of narrow-band interference filters and a neutral density wedge. The light beam was

focused on the tip of an optical fiber that was attached to the perimeter device, where it provided a point source of light (diameter 0.6°). The spectral sensitivity of the recorded photoreceptor was determined by stimulating the cell with a series of monochromatic flashes (300-700 nm). The stimulus intensity–response function was measured at the peak wavelength (λ_{max}) over an intensity range of 5 log units. For most cells, the polarization sensitivity ratio (*PS*: maximal sensitivity/minimal sensitivity) at the λ_{max} was also measured. An ultraviolet-capable polarizer was inserted in front of the eye and rotated through 360° to produce flashes varying in axis of polarization from 0-180°. A sinusoidal curve was fitted to the data, yielding the *PS* and the axis of peak sensitivity to linearly polarized light, ϕ_{max}. The presented *PS* measurements for all receptor classes, except for the female violet class, are from male *P. r. crucivora*.

3.4. Results

3.4.1. Opsin sequences of P. r. rapae and P. r. crucivora

The amino acid sequences of *P. r. rapae* opsins deduced from genomic sequences (Shen et al. 2016) closely resembled those of *P. r. crucivora,* deviating by zero to three amino acids, and grouped tightly when the phylogeny of these sequences was reconstructed (Fig. 3.3). None of the amino acid differences occurred in regions identified as important for spectral tuning (Salcedo et al. 2003; Wakakuwa et al. 2010). Based on the similarity in opsin sequences between *P. r. rapae* and *P. r. crucivora,* the absorbance of their opsins can be inferred to be nearly identical.

3.4.2. Ommatidial heterogeneity in *P. r. rapae*

Light- and electron-microscopic examination of the ommatidial structures of *P. r. rapae* and *P. r. crucivora* did not reveal any differences between the subspecies in the arrangement of microvilli or pigment clusters that would significantly affect photoreceptor sensitivity (Figs. 3.1, 3.4; Qiu et al. 2002). As in *P. r. crucivora* (Arikawa et al. 2005), ommatidial structures of *P. r. rapae* were found not to be sexually dimorphic (Fig. 3.4, female ommatidia; Fig. 3.5, male ommatidia).

The clusters of pigment surrounding the rhabdoms of *P. r. crucivora* have previously been divided into two pigment classes: pale-red and deep-red (Qiu et al.

2002). However, careful observation of unstained light microscopic sections of *P. r. rapae* and *P. r. crucivora* compound eyes revealed that both subspecies appear to have three pigment classes, pale-orange, deep-pinkish-red, and pale-red, located in ommatidial types I, II, and III, respectively (Fig. 3.1).

3.4.3. Eyeshine in *P. r. rapae*

The spectral composition of the light reflected from the ommatidia is affected both by the perirhabdomal screening pigments and by the tuning of the tapetum. In both males (Fig. 3.6) and females (Fig. 3.7), there were distinct differences in the eyeshine of the three ventral ommatidial types. Under monochromatic illumination, type I ommatidia appeared bright under 620 nm light, type II ommatidia under 670 nm light, and type III ommatidia appeared bright both under 670 nm and 690 nm light. The reflectance λ_{max} of ommatidial types I, II and III was ~640 nm, 680 nm and 660 nm, respectively (Fig. 3.8). Variation in peak ommatidial reflectance among eyes was small relative to variation among ommatidia in a single eye. However, these measurements were taken from a single laboratory colony and greater variation among or within wild populations is possible. We did not compare the reflectance between the two subspecies or between the reared and wild animals.

The dorsal area of *P. rapae* eyes also has a prominent eyeshine but its colour varies between green and red (see Fig. 2c in Stavenga 2002). The mean reflectance spectrum of the dorsal eye area peaks at ~610 nm (Fig. 3.8). It is likely that the low reflectance below 610 nm is chiefly determined by the absorption of visual pigments, as the dorsal ommatidia are devoid of the red screening pigments (Qiu and Arikawa 2003a).

3.4.4. Absorbance spectra of reddish screening pigments

The absorbance spectra of reddish screening pigments of male and female *P. r. rapae* differed among ommatidial types, with type II ommatidia having the greatest absorbance followed by type III and I (Fig. 3.9a,b). Additionally, type II pigments had greater absorbance in the red wavelength range of the spectrum (Fig. 3.9c,d), with only minor differences between the normalized spectra of type I and III ommatidia.

3.4.5. Ommatidial fluorescence

Like eyeshine observations, fluorescence microscopy offers a powerful means to distinguish ommatidial types. Type II ommatidia of both male *P. r. rapae* and *P. r. crucivora* exhibited a strong blue-violet and ultraviolet light-induced fluorescence (Fig. 3.6). The fluorescence in ommatidial types I and III of males was weak, resembling that of all ommatidial types of females (Figs. 3.6d,e, 3.7d,e).

3.4.6. Re-examination of spectral sensitivity in *P. r. crucivora*

Our adjusted view that the three ommatidial types differ in fluorescence characteristics and the composition of screening pigments prompted us to re-analyze the previously reported photoreceptor spectral sensitivities (Qiu and Arikawa 2003ab; Arikawa et al. 2005). We concluded that the spectral sensitivities of the red photoreceptors were distinct in each of the ommatidial types (Fig. 3.10), in line with the eyeshine and pigment absorption measurements (Fig. 3.8, 3.9). The red photoreceptors in the three ommatidial types were determined to have sensitivity peaks (λ_{max}) at around 610 nm (Ri; type I), 640 nm (Rii; type II), and 630 nm (Riii; type III). Furthermore, compared to Ri, the Riii photoreceptors have a greater sensitivity in the 400-500 nm range, and the Rii photoreceptors of males have a sensitivity trough near 420 nm, due to the distally-located, fluorescing and violet-absorbing pigment, which acts as a violet spectral filter (Qiu et al. 2002; Stavenga and Arikawa 2011).

3.4.7. Polarization sensitivity in *P. r. crucivora*

The photoreceptors of *P. r. crucivora* have different spectral and polarization sensitivities, as summarized in Fig. 3.11 and Table 3.1. The UV-sensitive photoreceptors (R1,2) in ommatidial types I and III have a similar (t = 2.19, df = 6.95, p = 0.07) but very low *PS* of ~1. In contrast, the blue-sensitive photoreceptors (R1,2) in type I ommatidia have a high *PS* of ~3, with an approximately vertical axis of maximal polarisation sensitivity (ϕ_{max} ~ 0º), i.e., about parallel to the body's dorso-ventral plane. The green-sensitive photoreceptors (R3,4) in type I and III ommatidia have a similar *PS* (t = 1.87, df = 3.34, p = 0.15) of ~2 with mostly a horizontal ϕ_{max} (~ 90º). The blue-suppressed green photoreceptors (R3,4) in type II ommatidia have a *PS* of ~1.3 which is lower than that of green photoreceptors (R3,4) in ommatidial type I and III. Red-sensitive photoreceptors

(R5-8) show a *PS* of ~2 in all three ommatidial types, but the mostly oblique ϕ_{max} differs between type II and types I and III, with the axes of polarization shifted towards vertical in types I and III (Fig. 3.11, Table 3.1).

3.5. Discussion

3.5.1. Comparison of the compound eyes of *P. r. crucivora* and *P. r. rapae*

Our data support the conclusion that the compound eyes of *P. r. rapae* and *P. r. crucivora* are (nearly) identical. Between the two subspecies, there are only minimal differences in (a) opsin sequences (implying functionally identical visual pigments), (b) eyeshine, (c) distributions of blue-violet fluorescing pigment among ommatidial types and sexes, and (d) microvillar arrangements (implying similar polarization sensitivities). In particular, observations of fluorescence strongly suggest both *P. r. rapae* and *P. r. crucivora* are sexually dimorphic in the spectral sensitivity of their type II R1,2 photoreceptors, implying that this dimorphism is an ancestral trait in both subspecies rather than an adaptation in *P. r. crucivora* to enhance discrimination between males and females. We did not perform intracellular recordings on *P. r. rapae* eyes, but given the similarity in both visual and screening pigments as well as in microvillar arrangement, photoreceptor classes in both subspecies can be expected to have similar spectral and polarization sensitivities.

3.5.2. Ommatidial heterogeneity of red-screening pigments

Spectrophotometry on the photoreceptor screening pigments revealed distinctly different absorbance spectra for the three ommatidial types of *P. r. rapae*. The absorbance of pigments in *P. r. rapae* differs from that previously reported for *P. r. crucivora*. The only subtle differences in pigment appearance and eyeshine reflectance between the two subspecies are likely attributable to diverging methods used to determine absorbance in each subspecies. We used colony-derived *P. r. rapae* adults measuring their eyes with an enhanced imaging microspectrophotometry (MSP) method (Arikawa et al. 2009), whereas previous studies used wild caught *P. r. crucivora,* and non-imaging MSP methods. These measurement also did not distinguish between type I and III ommatidia (Qiu et al. 2002; Stavenga and Arikawa 2011).

The MSP of histological sections from the compound eyes of *Papilio xuthus* and female *Colias erate* demonstrated the presence of two classes of peri-rhabdomal screening pigments (Arikawa et al. 1999b; Ogawa et al. 2013). *Pieris rapae* seems to be the first documented example of a butterfly with differences among screening pigments in all three ommatidial types (at least in terms of pigment density), although imaging MSP of male *C. erate* ommatidia have shown some small differences in pigment density among ommatidial types. Females of *C. erate* possess three classes of red photoreceptors with different λ_{max} but optical models suggest only two screening pigments (Ogawa et al. 2013). Possible differences in pigment density between ommatidial types may play a role in spectral tuning not only in *P. rapae* but also in *C. erate*.

Butterflies use red photoreceptors to help discern green and yellow leaves, the latter often senescing and suboptimal for oviposition and larval development (Kelber 1999, 2001). As optimal wavelength discrimination is achieved by overlapping sensitivity between photoreceptor classes (Kelber et al. 2003), the additional overlap in sensitivity between three, rather than two, classes of red photoreceptors could further enhance wavelength discrimination in the > 600 nm range, thereby improving perception of subtle differences in leaf colour. Wavelength discrimination has been predicted for *P. rapae* and *C. erate* with receptor noise-limited color opponent models (Vorobyev and Osorio, 1998) that assumed all photoreceptor classes contribute to discrimination (Ogawa et al. 2013). The selection pressure for discerning wavelengths > 600 nm should be greatest for gravid females seeking host plants. Yet, only females of *C. erate,* but not *P. rapae,* possess more red photoreceptor classes than males and thus are likely to have a greater discriminatory ability than their male counterparts for wavelengths > 600 nm. The selective forces that led to multiple classes of red photoreceptor in male *P. rapae* but not in male *C. erate* are not yet known.

3.5.3. Polarization sensitivities of photoreceptors

Visual pigments in insect photoreceptors are bound to membranes of the microvilli composing the rhabdom (Horváth and Varjú 2004). Consequently, light polarized in a direction parallel to the microvilli is more easily absorbed by these pigments resulting in polarization sensitivity. The alignment of a photoreceptor's microvilli affects its sensitivity to polarized light, with curving of the microvilli serving to degrade this sensitivity.

Electron micrographs of the upper part of the rhabdom of *P. r. rapae* and *P. r. crucivora* ommatidia seem to reveal a greater degree of curving in the microvilli of R3,4 photoreceptors in type II ommatidia than in type I and III ommatidia. This microvillar arrangement would explain the high *PS* of the green photoreceptors (R3,4) in type I and III ommatidia relative to type II ommatidia. The *PS* remains high in type I and III green photoreceptors despite the curving of microvilli in the middle part of the rhabdom.

The higher *PS* (~2) of the red photoreceptors (R5-8) is expected given their parallel microvilli (Qiu et al. 2002), however the difference in ϕ_{max} of red photoreceptors among ommatidial types was surprising considering the ommatidial heterogeneity in the microvillar arrangement of photoreceptors R5-8. Type II and III red photoreceptors have ϕ_{max} values in line with microvillar orientations, near 45/135° for the square type II and closer to vertical for the rectangular type III. In contrast, the type I red photoreceptors despite their trapezoidal arrangement also have ϕ_{max} values shifted to the vertical. While the arrangement in all ommatidial types is similar below a depth of 420 µm, one would expect a substantial portion of light to be absorbed by the photoreceptor above this point in the rhabdom (Stavenga and Arikawa 2011) where microvillar arrangement differs.

Further optical modeling of the *P. rapae* compound eye is necessary to discover possible polarizing filter effects of the microvilli of the distal photoreceptors (Snyder 1973). The near-orthogonal arrangement of red photoreceptors within a single class should allow for bipolat (vision system receiving input from two polarization-sensitive analyzer channels with different e-vector tuning axes) polarization opponency (How and Marshall 2014) in *P. rapae*. This opponency mechanism could allow for the discrimination, although with considerable ambiguity, among objects differing in polarization. If receptor input from type II ommatidia is combined with the input from type I+III ommatidia to a full tripolat mechanism, the polarization ambiguities might be reduced at the expense of introducing some colour ambiguity. Clearly, further studies are needed to determine whether and how *P. rapae* senses, processes and uses the combined information conveyed in colour and polarization of light.

3.6. References

Arikawa K, Mizuno S, Scholten DGW, Kinoshita M, Seki T, Kitamoto J, Stavenga DG (1999a) An ultraviolet absorbing pigment causes a narrow-band violet receptor and a single-peaked green receptor in the eye of the butterfly *Papilio*. Vis Res 39:1–8. https://doi.org/10.1016/S0042-6989(98)00070-4

Arikawa K, Scholten DGW, Kinoshita M, Stavenga DG (1999b) Tuning of photoreceptor spectral sensitivities by red and yellow pigments in the butterfly *Papilio xuthus*. Zool Sci 16:17–24. https://doi.org/10.2108/zsj.16.17

Arikawa K, Wakakuwa M, Qiu X, Kurasawa M, Stavenga DG (2005) Sexual dimorphism of short-wavelength photoreceptors in the small white butterfly, *Pieris rapae crucivora*. J Neurosci 25:5935–5942. https://doi.org/10.1523/JNEUROSCI.1364-05.2005

Arikawa K, Pirih P, Stavenga DG. (2009) Rhabdom constriction enhances filtering by the red screening pigment in the eye of the eastern pale clouded yellow butterfly, *Colias erate* (Pieridae). J Exp Biol 212:2057-64. http://doi.org/10.1242/jeb.030692

Giraldo MA, Stavenga DG (2007) Sexual dichroism and pigment localization in the wing scales of *Pieris rapae* butterflies. Proc R Biol Sci B 274:97–102. https://doi.org/10.1098/rspb.2006.3708

Hartigan JA, Wong, MA (1979) Algorithm AS 136: A K-means clustering algorithm. J R Stat Soc Ser C Appl Stat., 28:100–108. http://doi.org/10.2307/2346830

Horváth G, Varjú D (2004) Polarized Light in Animal Vision. Springer, New York

How MJ, Marshall NJ (2014) Polarization distance: a framework for modelling object detection by polarization vision systems. Proc R Soc B 281:20131632. http://doi.org/10.1098/rspb.2013.1632

Kelber A (1999). Ovipositing butterflies use a red receptor to see green. J Exp Biol 202:2619–2630.

Kelber A (2001). Receptor based models for spontaneous colour choices in flies and butterflies. Entomol Exp Appl 99:231–244. https://doi.org/10.1046/j.1570-7458.2001.00822.x

Kelber A, Vorobyev M, Osorio D. (2003). Animal colour vision—behavioural tests and physiological concepts. Biol Rev 78:81–118.

Kumar S, Stecher G, Tamura K (2016) MEGA7: Molecular evolutionary genetics analysis version 7.0 for bigger datasets. Mol Biol Evol 33:1870–1874. https://doi.org/10.1093/molbev/msw054

Obara Y (1970) Studies on the mating behavior of the white cabbage butterfly, *Pieris rapae crucivora* Boisduval. J Comp Physiol A 69:99–116. https://doi.org/10.1007/BF00340912

Obara Y, Majerus MEN (2000) Initial mate recognition in the British cabbage butterfly, *Pieris rapae rapae*. Zool Sci 17:725–730. https://doi.org/10.2108/zsj.17.725

Ogawa Y, Kinoshita M, Stavenga DG, Arikawa K (2013) Sex-specific retinal pigmentation results in sexually dimorphic long-wavelength-sensitive photoreceptors in the eastern pale clouded yellow butterfly, *Colias erate*. J Exp Biol 216:1916–1923. https://doi.org/10.1242/jeb.083485

Perry M, Kinoshita M, Saldi G, Huo L, Arikawa K, Desplan C (2016) Molecular logic behind the three-way stochastic choices that expand butterfly colour vision. Nature 535:280–284. https://doi.org/10.1038/nature18616

Qiu X, Arikawa K (2003a) Polymorphism of red receptors: sensitivity spectra of proximal photoreceptors in the small white butterfly *Pieris rapae crucivora*. J Exp Biol 206:2787–2793. https://doi.org/10.1242/jeb.00493

Qiu X, Arikawa K (2003b) The photoreceptor localization confirms the spectral heterogeneity of ommatidia in the male small white butterfly, *Pieris rapae crucivora*. J Comp Physiol A 189:81–88. https://doi.org/10.1007/s00359-002-0380-0

Qiu X, Vanhoutte K, Stavenga DG, Arikawa K (2002) Ommatidial heterogeneity in the compound eye of the male small white butterfly, *Pieris rapae crucivora*. Cell Tissue Res 307:371–379. https://doi.org/10.1007/s00441-002-0517-z

Salcedo E, Zheng L, Phistry M, Bagg EE, Britt SG (2003) Molecular basis for ultraviolet vision in invertebrates. J Neurosci 23:10873–10878. https://doi.org/10.1523/JNEUROSCI.23-34-10873.2003

Schindelin J, Arganda-Carreras I, Frise E, *et al*. (2012) Fiji: an open-source platform for biological-image analysis. Nat Methods 9:676–682. https://doi.org/10.1038/nmeth.2019

Shen J, Cong Q, Kinch LN, Borek D, Otwinowski Z, Grishin NV (2016) Complete genome of *Pieris rapae*, a resilient alien, a cabbage pest, and a source of anti-cancer proteins. F1000Res 5:2631–15. https://doi.org/10.12688/f1000research.9765.1

Shimohigashi M, Tominaga Y (1991) Identificaton of UV, green and red receptors, and their projection to lamina in the cabbage butterfly, *Pieris rapae*. Cell Tissue Res 263:49–59. https://doi.org/10.1007/BF00318399

Snyder AW (1973) Polarization sensitivity of individual retinula cells. J Comp Physiol A 83:331–360. https://doi.org/10.1007/BF00696351

Snyder AW (1979) Physics of vision in compound eyes. In: Autrum HJ (ed) Handbook of sensory physiology, VII/6a. Springer, Berlin, pp 225-313

Stavenga DG (2002) Reflections on colourful ommatidia of butterfly eyes. J Exp Biol 205:1077–1085.

Stavenga DG (2006) Invertebrate photoreceptor optics. In: Nilsson D-E, Warrant EJ (eds) *Invertebrate Vision*. Cambridge University Press, pp 1–42

Stavenga DG, Arikawa K (2011) Photoreceptor spectral sensitivities of the Small White butterfly *Pieris rapae crucivora* interpreted with optical modeling. J Comp Physiol A 197:373–385. https://doi.org/10.1007/s00359-010-0622-5

Thévenaz P, Ruttimann UE, Unser M (1998) A pyramid approach to subpixel registration based on intensity. IEEE Trans Image Process 7:27–41. https://doi.org/10.1109/83.650848

Vorobyev M, Osorio D (1998). Receptor noise as a determinant of colour thresholds. Proc R Soc B 265:351–358. http://doi.org/10.1098/rspb.1998.0302

Wakakuwa M, Stavenga DG, Kurasawa M, Arikawa K (2004) A unique visual pigment expressed in green, red and deep-red receptors in the eye of the small white butterfly, *Pieris rapae crucivora*. J Exp Biol 207:2803–2810. https://doi.org/10.1242/jeb.01078

Wakakuwa M, Terakita A, Koyanagi M, Stavenga DG, Shichida Y, Arikawa K (2010) Evolution and mechanism of spectral tuning of blue-absorbing visual pigments in butterflies. PLoS One 5:e15015–8. https://doi.org/10.1371/journal.pone.0015015

Webb SE, Shelton AM (1988) Laboratory rearing of the Imported Cabbageworm. In: New Yorks Food and Life Sciences Bulletin. New York State Agricultural Experiment Station, Geneva, New York

3.7. Tables

Table 3.1 Summary of the three ommatidial types in *Pieris rapae*.

Ommatidial type	**I**				**IIf**[a]				**IIm**[a]				**III**			
Rhabdom shape	Trapezoid				Square				Square				Rectangular			
Eye shine / reflection λ_{max} (nm)	Pale-red / ~640				Deep-red / ~680				Deep-red / ~680				Pale-red / ~660			
Pigment color[b] / absorption λ_{max} (nm)	Pale-orange / ~487-503				Deep-pinkish-red / ~494				Deep-pinkish-red / ~485				Pale-red / ~472-489			
Fluorescence	Weak (R1 or R2)				None				Strong (R1 and R2)				None			
Photoreceptor	**S(λ) / λ_{max} (nm)**	**Opsin**	**PS**	**ϕ_{max} (º)**	**S(λ) / λ_{max} (nm)**	**Opsin**	**PS**	**ϕ_{max} (º)**	**S(λ) / λ_{max} (nm)**	**Opsin**	**PS**	**ϕ_{max} (º)**	**S(λ) / λ_{max} (nm)**	**Opsin**	**PS**	**ϕ_{max} (º)**
R1	UV[c] / ~350	PrUV	1.1	NA	V / ~400	PrV	1.2	7	dB / ~460	PrV	1.3	9	UV / ~350	PrUV	1.1	NA
R2	B[c] / ~450	PrB	2.9	6	V / ~400	PrV	1.2	7	dB / ~460	PrV	1.3	9	UV / ~350	PrUV	1.1	NA
R3,4	G / ~560	PrL	1.9	95	G / ~560	PrL	1.3[d]	91[d]	dG / ~560	PrL	1.3	91	G / ~560	PrL	1.9	95
R5,7	Ri / ~610	PrL	2.2	155	Rii / ~640	PrL	1.9[d]	131[d]	Rii / ~640	PrL	1.9	131	Riii / ~630	PrL	2.1	156
R6,8	Ri / ~610	PrL	2.2	34	Rii / ~640	PrL	1.9[d]	52[d]	Rii / ~640	PrL	1.9	52	Riii / ~630	PrL	2.1	33
R9	R?	PrL?	?	?	R?	PrL?	?	?	R?	PrL?	?	?	R?	PrL?	?	?

This table compiles published information on *P. r. crucivora* (see Table 1, Stavenga et al. 2011), new observations of *P. r. rapae*, and a re-examination of electrophysiological recordings (some previously unpublished) from *P. r. crucivora* eyes.*S*(*λ*) - photoreceptor class as derived from the wavelength range of its spectral sensitivity: UV - ultraviolet, V - violet, dB - double-peaked blue, B - blue, G - green, dG - blue-suppressed green (Stavenga and Arikawa 2011), Ri - red with peak wavelength λ_{max} ~ 610 nm, Rii - red with λ_{max} ~ 640 nm, Riii - red with λ_{max} ~ 630 nm; *PS* - polarization sensitivity; ϕ_{max} - angle of maximal polarization sensitivity

[a] IIf - type II ommatidia of females, IIm - type II ommatidia of males

[b] The pigments were previously reported for type I and type III ommatidia as pale-red, and for type II ommatidia as deep-red (Qiu et al. 2003b)

[c] The R1 and R2 photoreceptors of type I ommatidia contain either the UV and B rhodopsins (narrow trapezoidal side up) or the B and UV rhodopsins (wide trapezoidal side up), see Fig. 3.1

[d] *PS* and ϕ_{max} (°) values for females were inferred from electrophysiology recordings of males

3.8. Figures

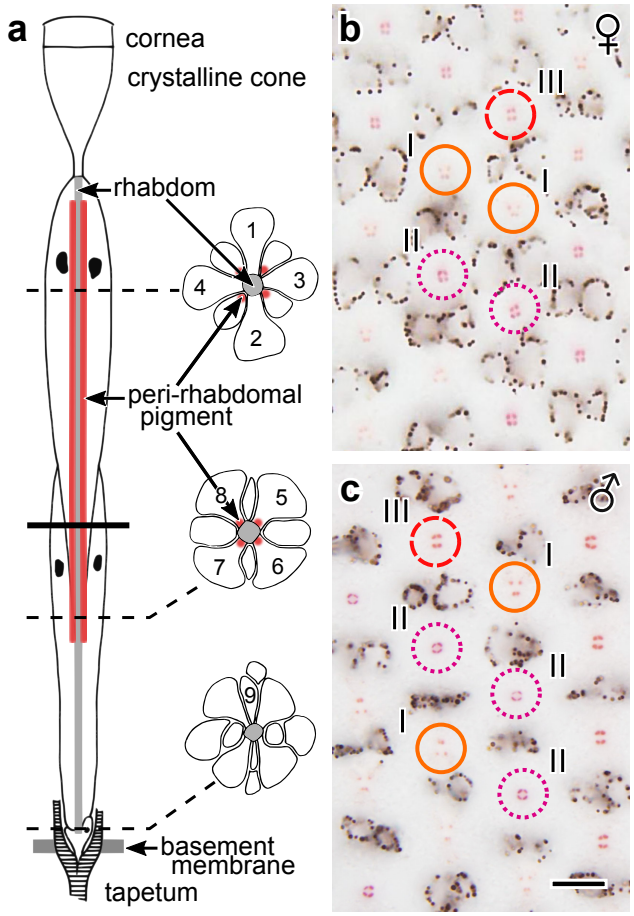

Figure 3.1 **Anatomy of the ommatidia in the compound eye (fronto-ventral part) of *Pieris rapae rapae*. (a) Diagram of the tiered ommatidium showing the position of the nine photoreceptors. The length of the corneal lens and crystalline cones is ~100 µm, with the rhabdom extending between 200-600 µm depending on the specimen's sex and the position in the compound eye. The rhabdom is composed of microvilli from photoreceptors R1-4 in the distal half of the ommatidium and from photoreceptors R5-8 in the proximal half of the ommatidium. Only in the very basal part of the ommatidium does photoreceptor R9 contribute microvilli. Clusters of peri-rhabdomal pigment exist in the somata in the upper two thirds of the proximal photoreceptors R5-8. The horizontal bold line indicates the depth level of the histological sections shown on the right. (b, c) Sections of the compound eyes of a female and a male *P. r. rapae*, respectively. The pigment color and the arrangement of pigment clusters differ among ommatidial types. Pale-orange (solid circle), deep-pinkish (dotted circle), and pale-red pigments (dashed circle) are arranged in trapezoidal, square, and rectangle clusters in type I, II and III ommatidia, respectively. Scale bar: 10 µm**

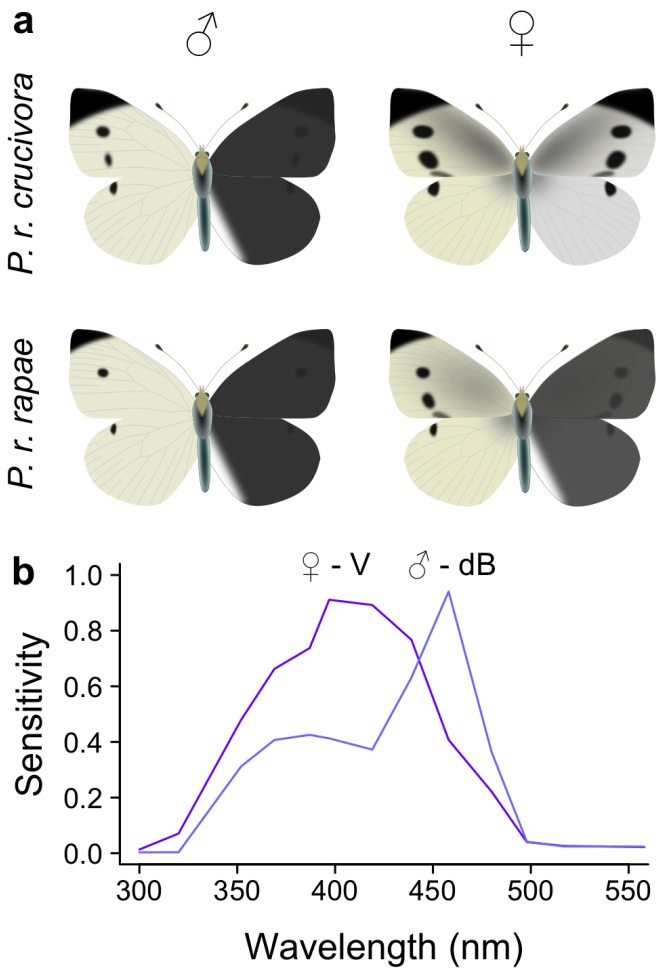

Figure 3.2 **(a) Diagram showing the appearance of the dorsal wing surface of male and female *Pieris rapae crucivora* and *Pieris rapae rapae* in conventional (human visible) photographs (left) and in UV photographs (right), based on photographs from Obara and Majerus (2000). (b) Comparison of the spectral sensitivity of the PrV opsin, expressing double-peaked blue and violet R1,2 photoreceptors in male and female *P. r. crucivora*.**

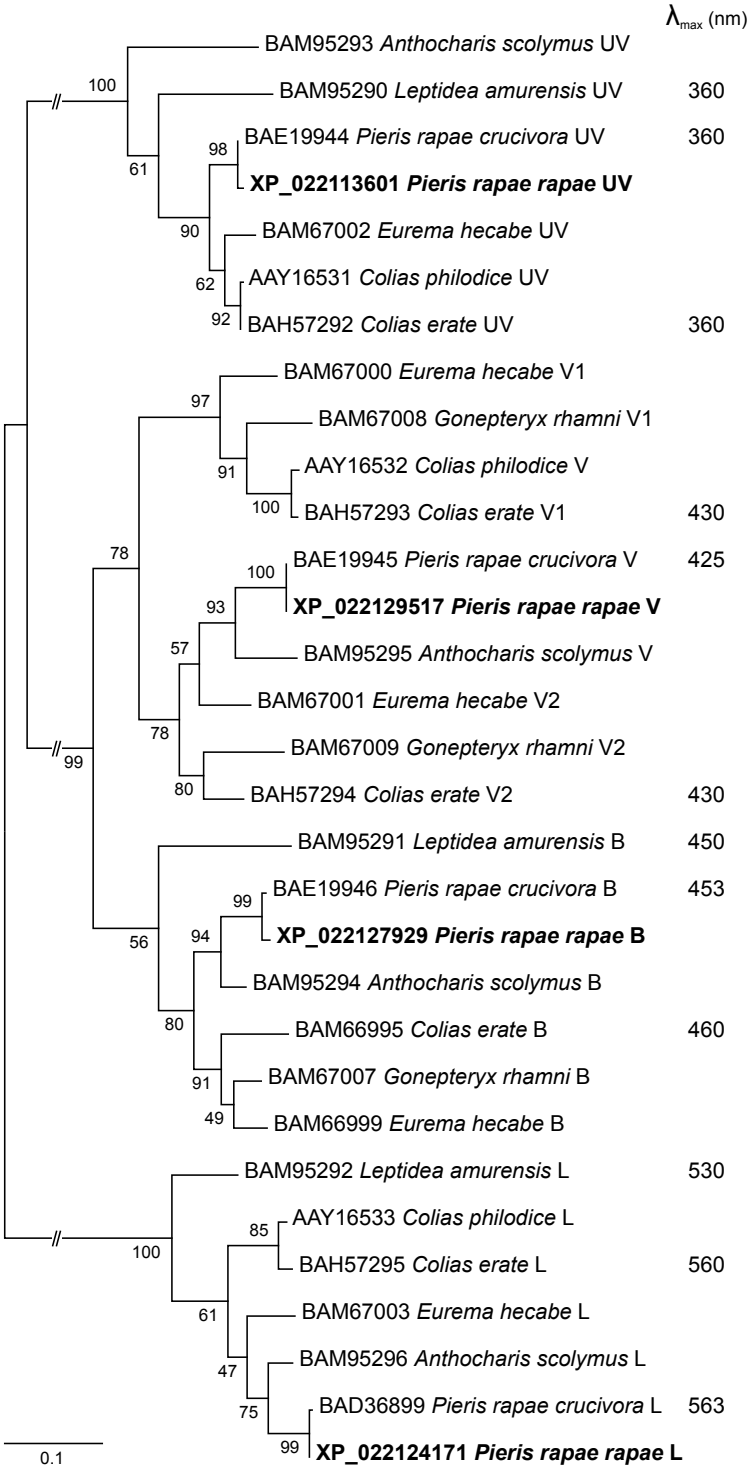
λmax (nm)
BAM95293 Anthocharis scolymus UV
BAM95290 Leptidea amurensis UV 360
BAE19944 Pieris rapae crucivora UV 360
XP_022113601 Pieris rapae rapae UV
BAM67002 Eurema hecabe UV
AAY16531 Colias philodice UV
BAH57292 Colias erate UV 360
BAM67000 Eurema hecabe V1
BAM67008 Gonepteryx rhamni V1
AAY16532 Colias philodice V
BAH57293 Colias erate V1 430
BAE19945 Pieris rapae crucivora V 425
XP_022129517 Pieris rapae rapae V
BAM95295 Anthocharis scolymus V
BAM67001 Eurema hecabe V2
BAM67009 Gonepteryx rhamni V2
BAH57294 Colias erate V2 430
BAM95291 Leptidea amurensis B 450
BAE19946 Pieris rapae crucivora B 453
XP_022127929 Pieris rapae rapae B
BAM95294 Anthocharis scolymus B
BAM66995 Colias erate B 460
BAM67007 Gonepteryx rhamni B
BAM66999 Eurema hecabe B
BAM95292 Leptidea amurensis L 530
AAY16533 Colias philodice L
BAH57295 Colias erate L 560
BAM67003 Eurema hecabe L
BAM95296 Anthocharis scolymus L
BAD36899 Pieris rapae crucivora L 563
XP_022124171 Pieris rapae rapae L
0.1

Figure 3.3 **Phylogeny of opsin amino acid sequences in the Pieridae, as determined by maximum likelihood analysis. The numbers at nodes indicate the maximum likelihood bootstrap values. Accession numbers, opsin type [UV, Violet (V, V1, V2), Blue (B), Long (L)], and absorption peak wavelength, λ_{max} (where available), are listed with species names**

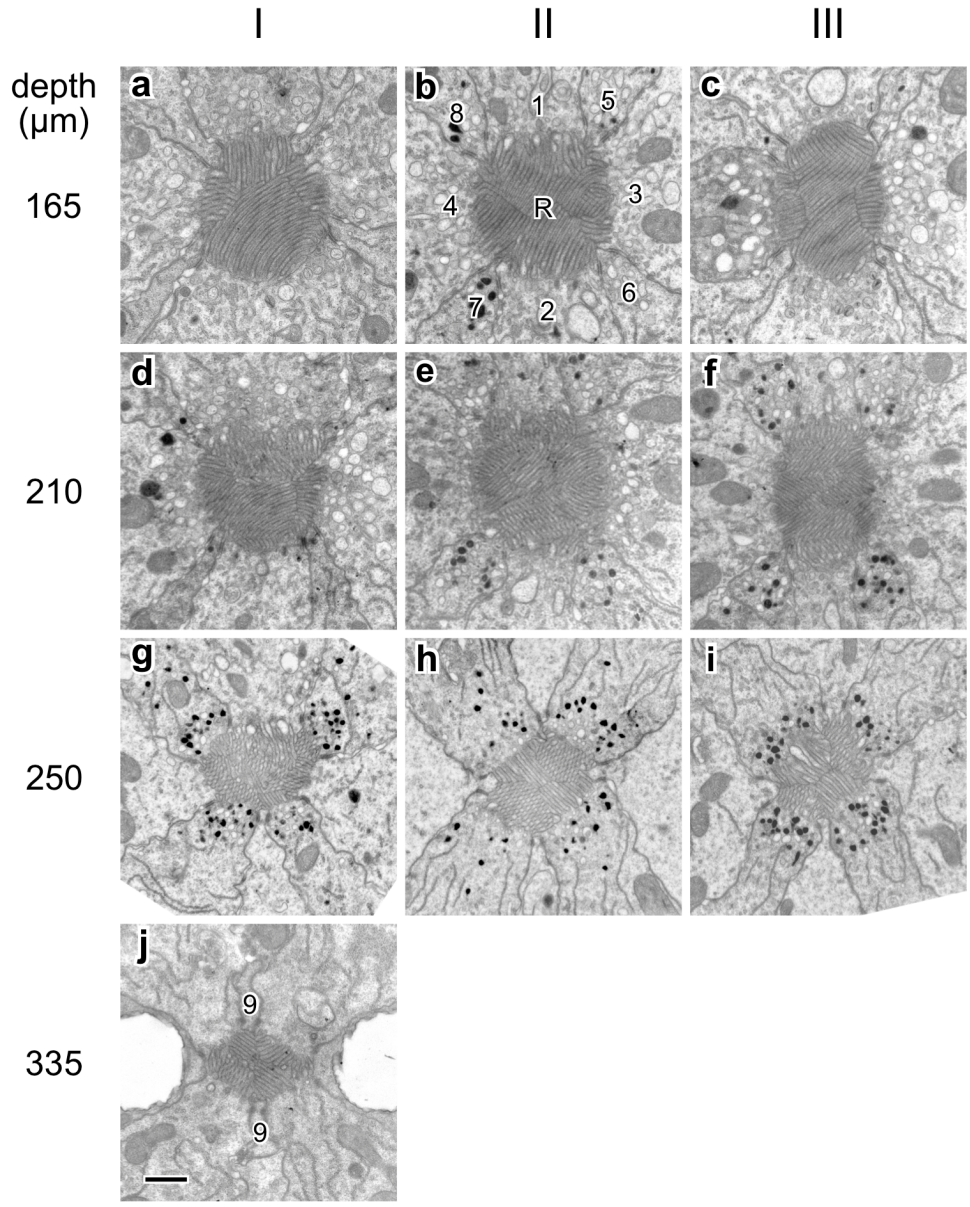

Figure 3.4 **Electron micrographs of transverse sections of female *Pieris rapae rapae* rhabdoms. (a, d, g) Ommatidial type I. (b, e, h) Ommatidial type II. (c, f, i) Ommatidial type III. (a-c) Depth from corneal surface: ~165 µm. (d-f) Depth ~210 µm. (g-i) Depth ~250 µm. (j) Depth ~335 µm. Numbers in b and j refer to the photoreceptor number. R – rhabdom. Scale bar (all panels): 1 µm**

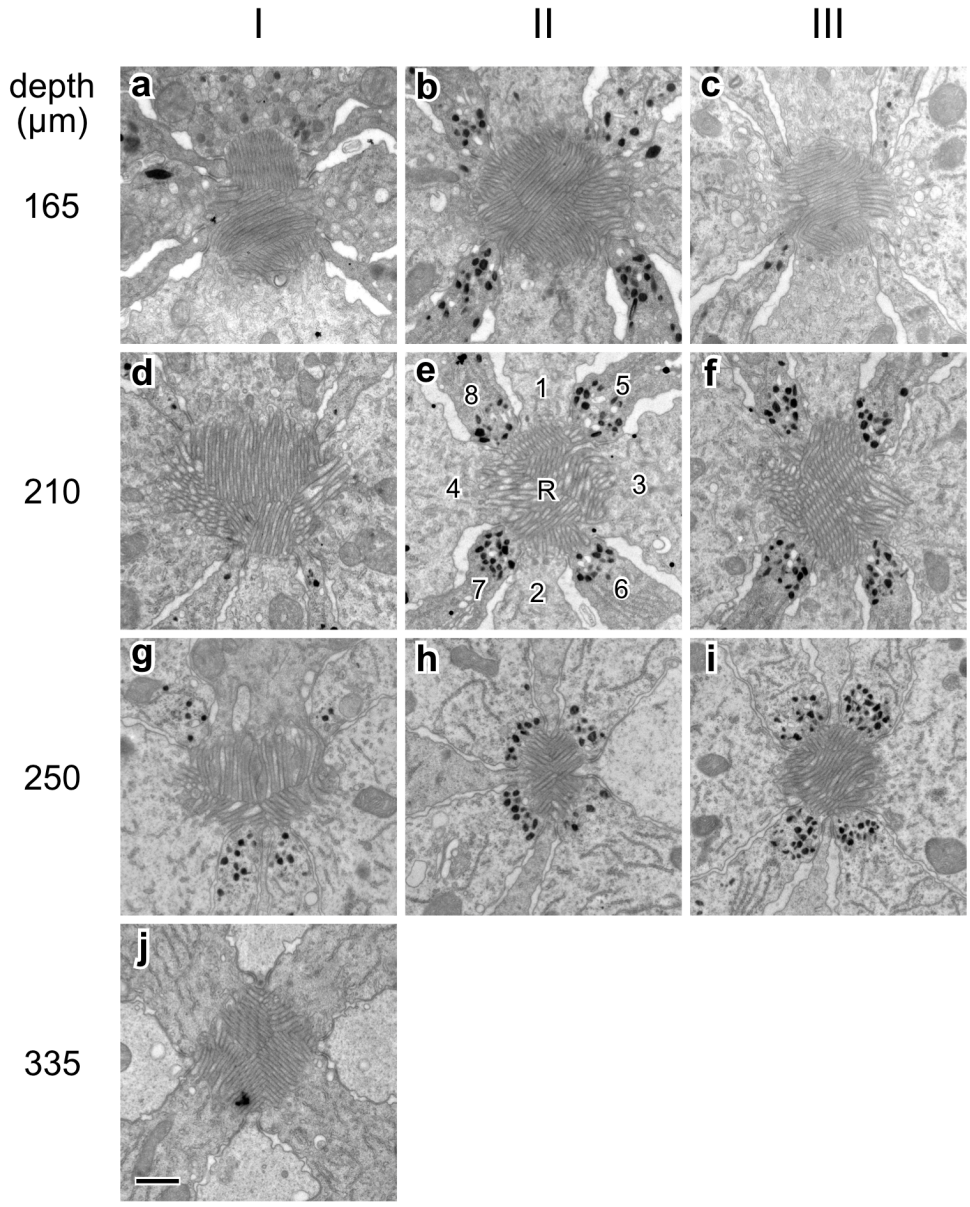

Figure 3.5 **Electron micrographs of transverse sections of male *Pieris rapae rapae* rhabdoms. (a, d, g) Ommatidial type I. (b, e, h) Ommatidial type II. (c, f, i) Ommatidial type III. (a-c) Depth: ~190 µm. (d-f) Depth ~255 µm. (g-i) Depth ~310 µm. (j) Depth ~385 µm. Numbers in e refer to the photoreceptor number. R – rhabdom. Scale bar (all panels): 1 µm**

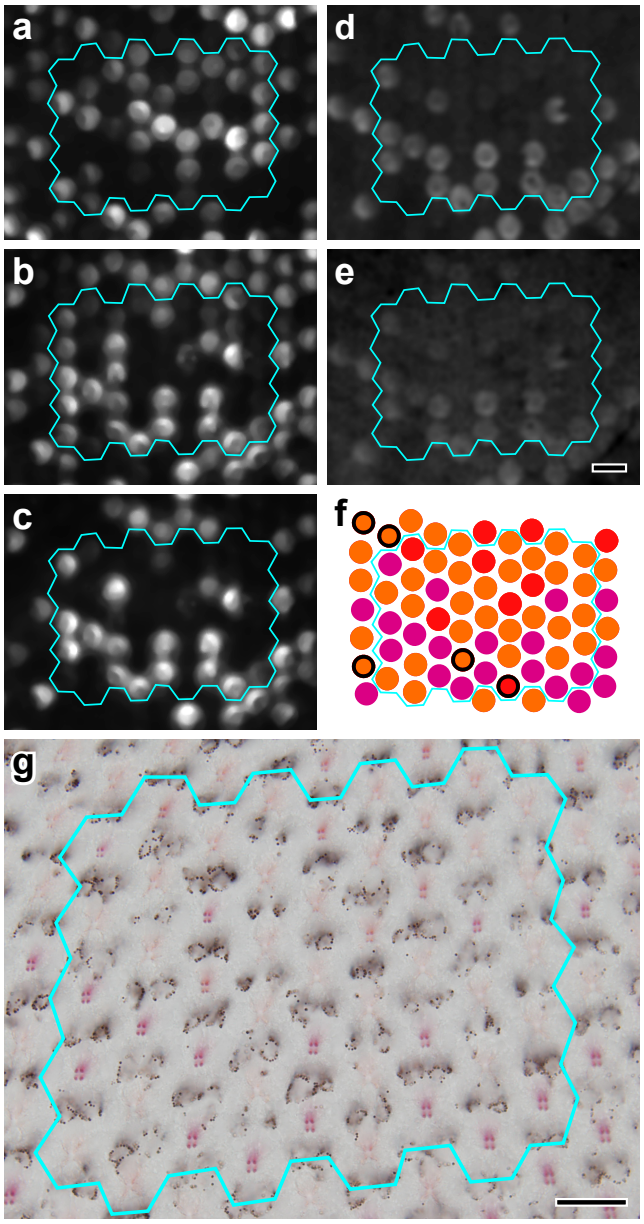

Figure 3.6 **Eyeshine, fluorescence and histology of the same set of ommatidia (encircled by the light blue polygons) of a male *Pieris rapae rapae*. (a-c) Local eyeshine elicited by epi-illumination with 620 nm, 670 nm, and 690 nm light, respectively. (d, e) Fluorescence induced by blue-violet and ultraviolet light, respectively. (f) Diagram of the arrangement of different ommatidial types: orange - type I, pink – type II, red – type III; the black circles indicate ommatidia dark in both eyeshine and fluorescence. (g) Transverse section of local ommatidia showing pigment clusters. Scale bars: 20 µm**

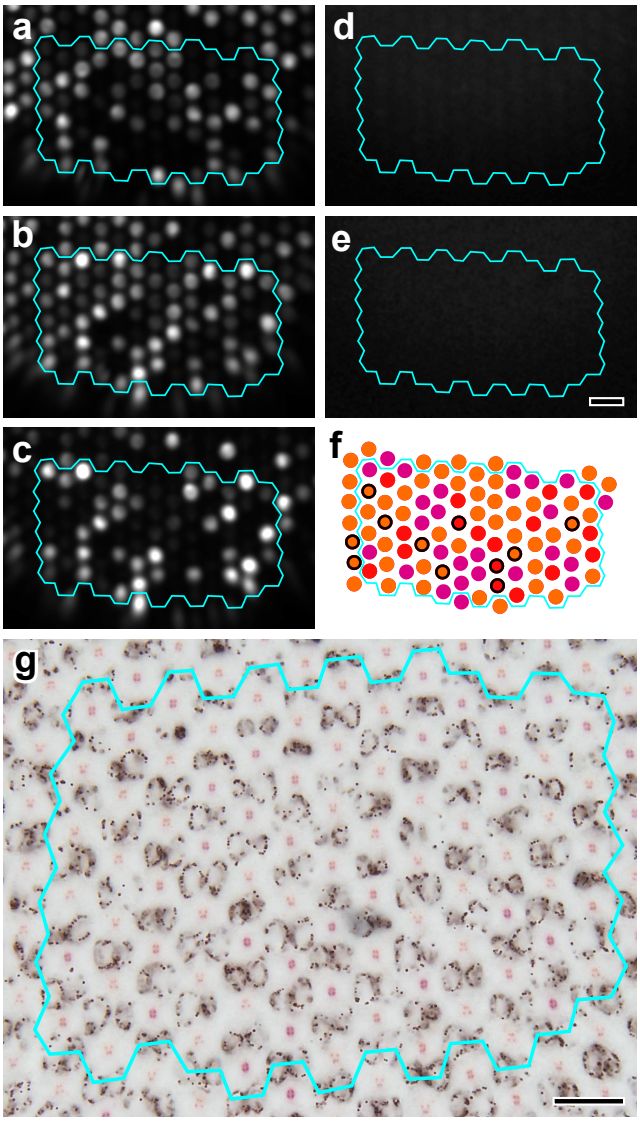

Figure 3.7 **Eyeshine, fluorescence and histology of the same set of ommatidia, encircled by the light blue polygons, of a female *Pieris rapae rapae*. (a-c) Local eyeshine elicited by epi-illumination with 620 nm, 670 nm and 690 nm light, respectively. (d, e) Fluorescence induced by blue-violet and ultraviolet light, respectively. (f) Diagram of the arrangement of ommatidial types: orange – type I, pink – type II, red – type III; the black circles indicate ommatidia dark in both eyeshine and fluorescence. (g) Transverse section of the local ommatidia showing pigment clusters. Scale bars: 20 µm**

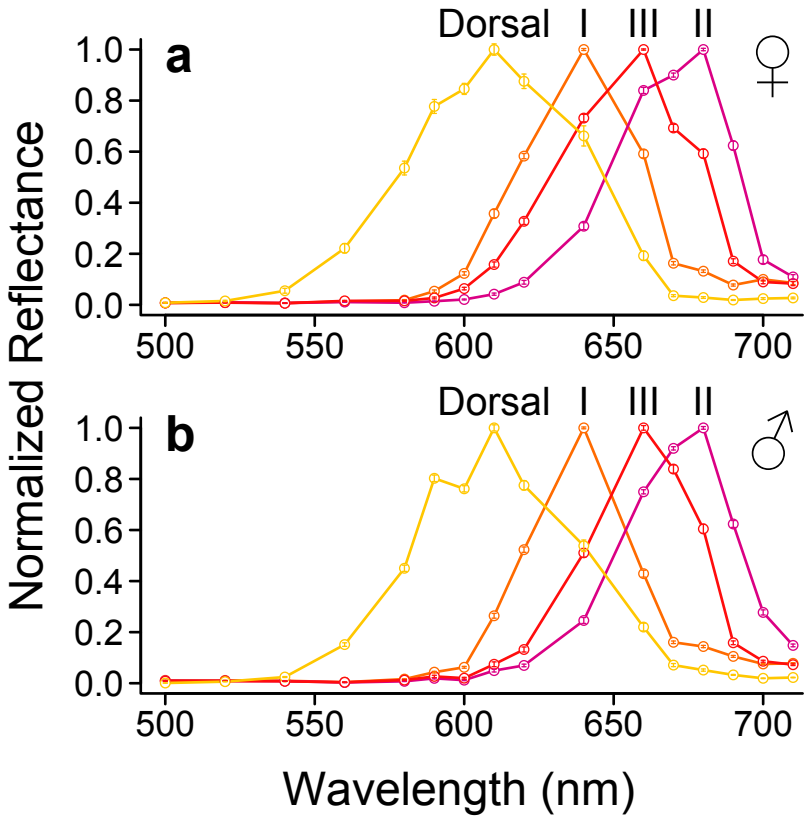

Figure 3.8 **Reflectance spectra (normalized) of *Pieris rapae rapae* ommatidia. (a, b) Mean ± the standard error of normalized reflectance spectra for ommatidial types I-III in the ventral eye region, and of ommatidia in the dorsal eye region of *P. r. rapae* females and males, respectively.**

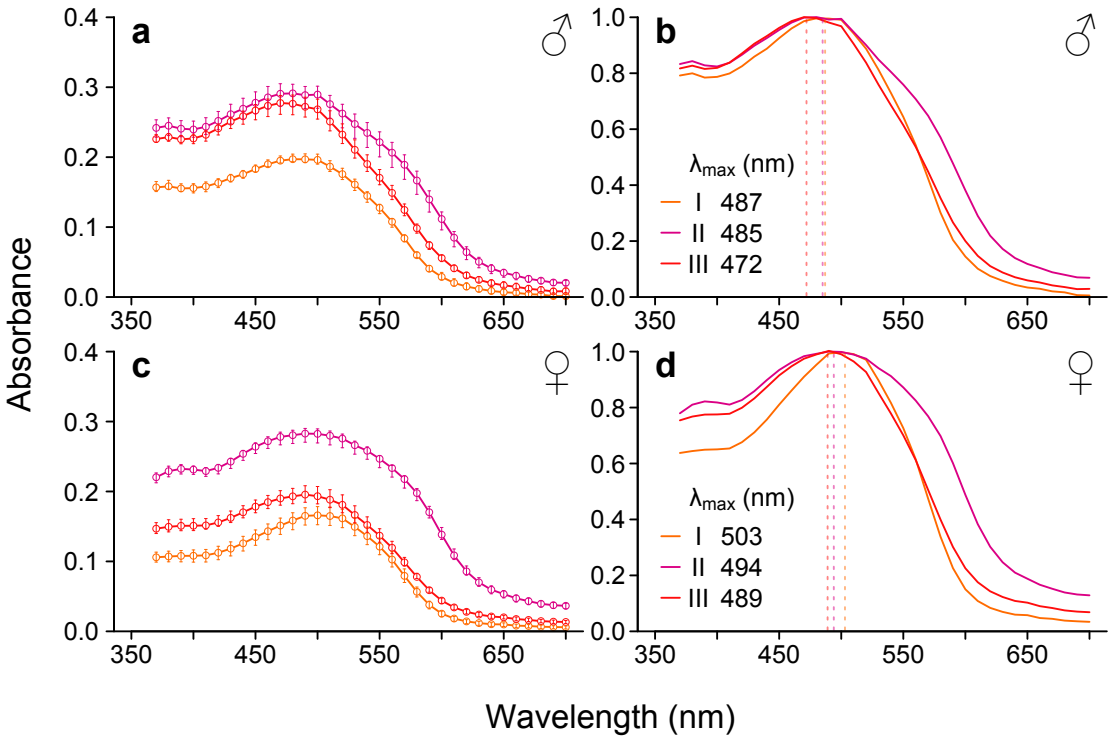

Figure 3.9 **Absorbance spectra of red screening pigments in the ommatidia of *Pieris rapae rapae*. The measurements for types I-III are from a transverse section of the compound eye at a position along the rhabdom where all three ommatidial types express screening pigments. The mean non-normalized absorbance for each ommatidial type from a male (a) and female (c) is shown on the left with error bars showing quartiles. The mean normalized absorbance along with peak wavelength (λ_{max}) is shown on the right for both male (b) and female (d).**

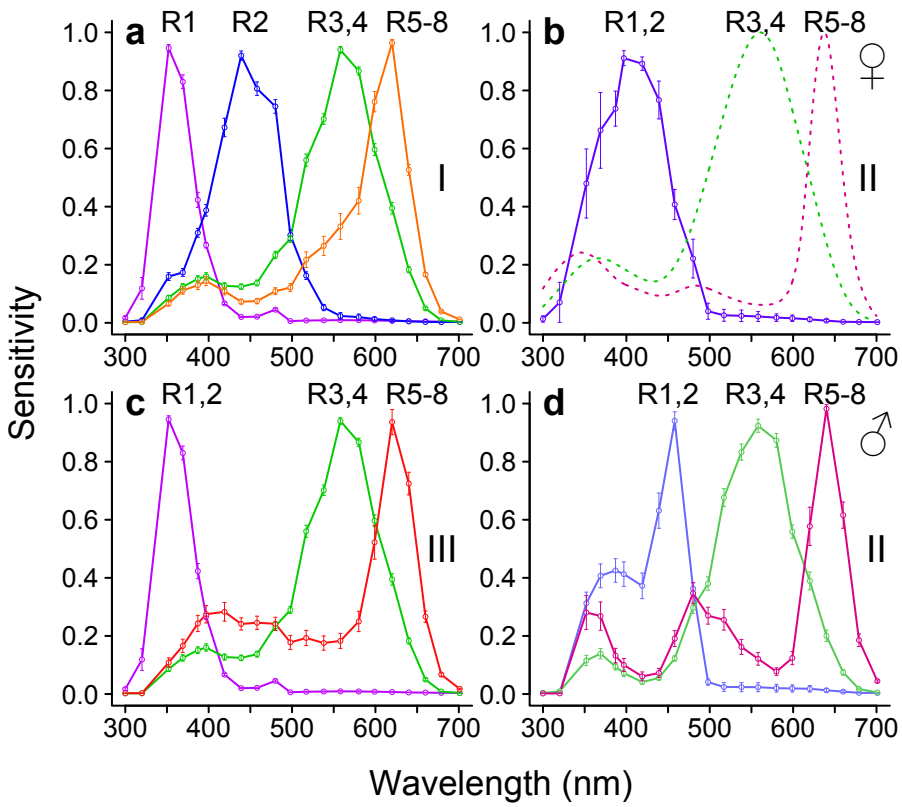

Figure 3.10 **Differences in spectral sensitivities of photoreceptors among ommatidial types in *Pieris rapae crucivora*. Lines indicate the mean spectral sensitivity among recordings ± the standard error. (a) Type I ommatidia. (b) Type II ommatidia in females. (c) Type III ommatidia. (d) Type II ommatidia in males. No electrophysiological recordings were available for female type II green or red photoreceptors; shown instead (b, *dotted lines*) are predicted spectral sensitivities from a wave-optical model of visual and screening pigment absorbance within the *Pieris rapae* ommatidium (Stavenga and Arikawa 2011).**

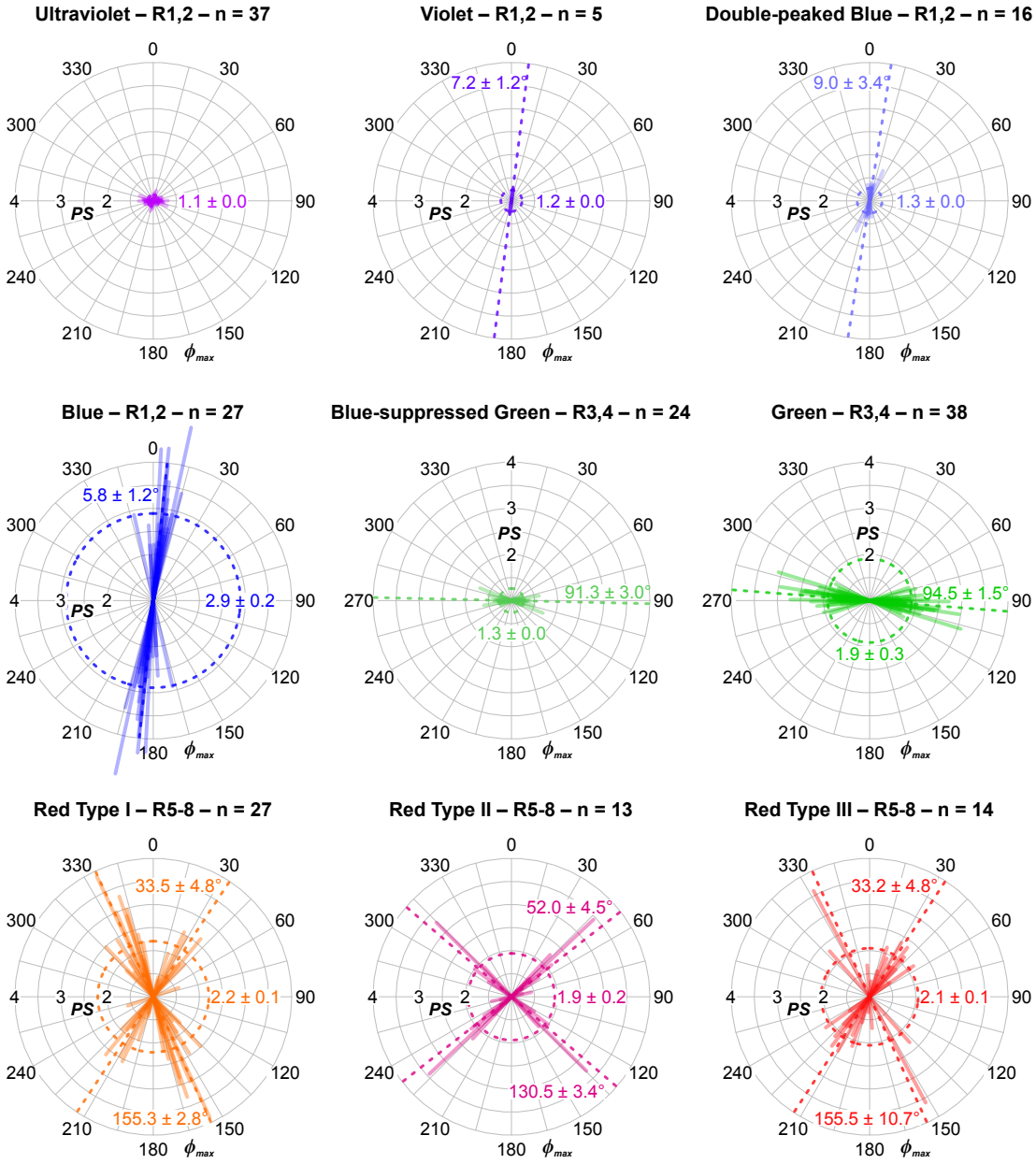

Figure 3.11 **Polarization sensitivity of photoreceptors of the different spectral classes in *Pieris rapae crucivora* as represented by a series of semi-transparent solid lines. The length of these lines indicates the polarization sensitivity (*PS*), whereas the line's rotation indicates the axis of polarization where the sensitivity is greatest (ϕ_{max}). The labeled dashed circles and lines show the mean *PS* and ϕ_{max} ± the standard error, respectively.**

Chapter 4.

Polarization of foliar reflectance: novel host plant cue for insect herbivores[1]

[1]The corresponding manuscript is published in *Proceedings of the Royal Society B: Biological Sciences* (2019, doi.org/10.1098/rspb.2019.2198) with the following authors: Blake AJ, Couture S, Go MC, Hahn G, Grey H, Gries G

4.1. Abstract

Insect herbivores exploit plant cues to discern host and non-host plants. Studies of visual plant cues have focused on color despite the inherent polarization sensitivity of insect photoreceptors and the information carried by polarization of foliar reflectance, most notably the degree of linear polarization (*DoLP*; 0-100%). The *DoLP* of foliar reflection was hypothesized to be a host plant cue for insects but was never experimentally tested. Here we show that cabbage white butterflies, *Pieris rapae* (Pieridae), exploit the *DoLP* of foliar reflections to discriminate among plants. In experiments with paired digital plant images, *P. rapae* females preferred images of the host plant cabbage with a low *DoLP* (31%) characteristic of cabbage foliage over images of a non-host potato plant with a higher *DoLP* (50%). By reversing the *DoLP* of these images, we were able to shift the butterflies' preference for the cabbage host plant image to the potato non-host plant image, indicating that the *DoLP* had a greater effect on foraging decisions than the differential color, intensity or shape of the two plant images. Although previously not recognized, the *DoLP* of foliar reflection is an essential plant cue that may commonly be exploited by foraging insect herbivores.

4.2. Introduction

Locating, feeding, and laying eggs on suitable host plants enable insect herbivores to maximize their fitness and that of their offspring (Jaenike 1990). Foraging for suitable plants, insects exploit plant cues with visual, infrared, olfactory, tactile, or gustatory characteristics (Prokopy and Owens 1983; Renwick and Radke 1988; Takács et al. 2008). Studies of visual plant characteristics have largely focused on plant color, brightness (intensity of perceived reflected light), or shape (Prokopy and Owens 1983; Renwick and Radke 1988; Takács et al. 2008; Reeves 2011). Yet, differential polarized reflections from plant foliage have long been hypothesized to guide plant-foraging insects (Kelber et al. 2001; Hegedüs and Horváth 2004).

For polarized reflections from plant foliage to serve as a host plant indicator for insect herbivores, three criteria must be met: (1) the *DoLP* of foliar reflections must differ between host and non-host plants; (2) the insects' photoreceptors must be capable of sensing and processing plant-derived polarized light, and (3) the specific *DoLP* of host plant foliage reflections must inform plant selection decisions by foraging insects. We investigated these criteria with our model organism, the cabbage white butterfly, *Pieris rapae*.

Like water or glass surfaces, plant foliage surfaces can polarize sunlight (or skylight) in a direction parallel to the surface, through specular reflection (Foster et al. 2018; Fig. 4.1a). This direction, or axis of polarization (*AoP*, 0-180°), is dependent upon the relative positions of the sun, the reflecting leaf surface, and the foraging insect (Fig. 4.1b). The *DoLP*, the fraction of the light that is polarized in the predominant *AoP* (Fig. 4.1b), is also affected by many leaf characteristics that differ among plant species, such as pigmentation, pubescence, epicuticular waxes and surface undulations, or even by viral infection (Grant et al. 1993; Maxwell et al. 2016). Females of *P. rapae*, lay eggs on brassicaceous plants including cabbage and rutabaga which possess an epicuticular wax layer giving their leaves a matte appearance (Prokopy and Owens 1983) and a lower *DoLP* compared to many other plants (Fig. 2.4).

The photoreceptors of insects and other arthropods including those of *P. rapae* can sense polarized light. Both the *AoP* and the *DoLP* of light affect photoreceptor responses through differential absorbance by photopigments (Horváth and Varjú 2004)

embedded within the cellular membrane of microvilli composing the ommatidial rhabdom (Fig. 4.1c-e). This arrangement makes these photoreceptors more sensitive to light with an *AoP* that is parallel to the microvilli (Fig. 4.1f). Increasing the *DoLP* of a stimulus light increases the differential response of photoreceptors to the *AoPs* of light. It is through these mechanisms that both the *AoP* and the *DoLP* affect the responses of insect photoreceptors. The visual system of *P. rapae* has been extensively studied (Qiu et al. 2002; Qiu and Arikawa 2003ab; Arikawa et al. 2005). Electrophysiological recordings and electron microscopy demonstrated that the blue-sensitive and red-sensitive photoreceptors, and a subset of green-sensitive photoreceptors, are sensitive to vertically, obliquely and horizontally polarized light, respectively (Blake et al. 2019b).

4.3. Results

4.3.1. Depolarizing-Filter Experiment

To investigate whether the *DoLP* of foliar reflections informs plant selection by foraging *P. rapae,* we ran a series of behavioral experiments. When we offered female *P. rapae* a choice between a live host plant (cabbage, *Brassica oleracea*) with a low *DoLP* (31%; Fig. 4.5), and a live non-host plant (potato, *Solanum tuberosum*) with a high *DoLP* (50%) in the absence of plant odor (Fig. 4.2), we observed a strong preference for the cabbage host plant (Fig. 4.6a). To determine whether the differential *DoLP* of the stimulus plants informed the females' plant choice, we added a depolarizing filter to both stimulus windows of the bioassay arena, thereby reducing and equalizing the *DoLP* of the two stimulus plants. With the information conveyed by the *DoLP* removed, *P. rapae* females failed to select their cabbage host plant (Fig. 4.6a), demonstrating the importance of the *DoLP* as an essential host plant cue.

4.3.2. LCD-Monitor-Proof-of-Concept Experiment

Digital plant images (relative to live plants) offer greatly enhanced opportunities of independently manipulating visual characteristics to tease apart their potential roles in host plant foraging. We therefore designed a novel combination of λ/4 retarder films and liquid crystal displays (LCDs) to modify and display static plant images. Previous uses of LCDs or projectors were either limited in their ability to modify *DoLP* and intensity (Foster et al. 2018) or limited in their ability to display color (Stewart et al. 2017). Our

set-up allowed for pixel-level control of color and intensity, and global control of both *AoP* and *DoLP*. We used a bioassay arena (Fig. 4.3) where LCD monitors displaying plant images replaced live plants. LCDs emit highly polarized light (>95%) due to linear polarizers used in their construction. We manipulated the *AoP* and *DoLP* of plant images by rotating the LCDs and counter rotating the images, and by changing the alignment between the λ/4 retarder film and the *AoP* of the LCD, respectively. We used photo polarimetry to both generate the potato and cabbage plant images tested in bioassays and to characterize the *AoP* and *DoLP* of both plant species. The *DoLP* of potato foliage (50%) and cabbage foliage (31%) differ markedly but the species are similar in their *AoP* (Figs. 4.5, 2.4, 2.5, 2.6, 2.7).

When we offered *P. rapae* females a choice between images of cabbage or potato plants, each matching the mean *DoLP* and the modal *AoP* of the corresponding plant species, most females selected the cabbage image (Fig. 4.6b, top bar), thus demonstrating the feasibility of testing plant images, instead of live plants, for behavioral responses of bioassay insects. Therefore, we proceeded to isolate and test the exclusive effect of the *DoLP* on the insects' responses. When we offered *P. rapae* females a choice between a cabbage image with a *DoLP* (50%) approximating that of a potato plant and a potato plant image with a *DoLP* (31%) approximating that of a cabbage plant, most females selected the potato plant image (Fig. 4.6b, middle bar). By simply reversing the *DoLP* of the two images, we were able to make the virtual non-host potato plant as attractive (47:19 preference ratio) as the virtual cabbage host plant with its typical *DoLP* (47:18 preference ratio). This result indicated that the *DoLP* was a more important cue in these bioassays than the differential color (although differences were small), intensity and shape of the two plant images. Moreover, when we kept the *DoLP* of both the cabbage and the potato plant image unnaturally low (<15%), the distinct shape and color of the cabbage host plant were insufficient to attract *P. rapae* females (Fig. 4.6b, bottom bar), emphasizing again the importance of the *DoLP* as a host plant cue.

4.3.3. Degree and Axis of Polarization Preference Experiments

To determine the range of the *AoP* and the *DoLP* of foliar reflections that remain attractive to *P. rapae* females, we offered females a choice between a cabbage image that varied in either *AoP* or *DoLP*, and a cabbage control image with a fixed *DoLP* of

31% and a fixed *AoP* of 90° (Fig. 4.7). In these experiments, cabbage images with an *AoP* at or near 45° and 135° proved repellent, whereas cabbage images with any other *AoP* were equally attractive. Furthermore, most cabbage images with a *DoLP* less than, or greater than, the *DoLP* (31%) indicative of cabbage were repellent to *P. rapae* females. Combined, these results indicate that *P. rapae* females are attracted to a *DoLP* indicative of a host plant (Fig. 2.4) but are relatively indifferent to the *AoP* of plants, except for repellency to *AoPs* near 45° and 135°. The indifference of *P. rapae* females to most *AoP*s greatly enhances the utility of the *DoLP* as a foraging cue because the *AoP* of plant reflections will vary considerably depending on the position of the insect and the sun relative to the plant. Furthermore, unlike the *DoLP*, the *AoP* is largely unaffected by foliage surface characteristics, as shown by our polarimetry (Foster et al. 2018; Figs. 2.4, 2.5, 2.6, 2.7).

4.4. Discussion

This is the first study documenting that the polarization of foliar reflectance serves as a host plant cue for insect herbivores. Based on our data, and considering the typically small differences in foliage color between plant species (Grant 1987), it seems that relative differences in *DoLP* among plants could be more informative host plant cues than plant shape, foliage color or intensity. Many insects exploit polarized light during navigation, and aquatic insects utilize horizontally polarized light to locate bodies of water for oviposition (Horváth and Varjú 2004). Most non-aquatic insects were once thought to lack polarization-sensitive photoreceptors in the ventral portion of their compound eyes. However, more recent histological and electrophysiological work indicates that this type of polarization sensitivity could be widespread among insect taxa (Wachmann 1977; Hardie 1979; Wernet et al. 2012; Mishra 2015; Ilić et al. 2016) including herbivores other than *P. rapae*.

Most of the insect visual systems studied to date are incapable of independently perceiving *DoLP* and *AoP* because these systems rely on information from a single polarization-sensitive photoreceptor or from the comparison between two such photoreceptors (Labhart 2016). To fully disentangle the effects of *DoLP*, *AoP*, intensity and color as foraging cues,, comparison among at least three photoreceptors with similar spectral sensitivity, but with sensitivity to distinct *AoPs*, would be required (How and Marshall 2014). It is therefore likely that *P. rapae* does not perceive differences in

DoLP in isolation from other characteristics of light. The neurological mechanism(s) in *P. rapae* underlying the observed discrimination of stimuli with contrasting *DoLP* remain(s) unknown. *Papilio* butterflies perceive polarization differences as color or intensity differences depending on the behavioral context (Kelber et al. 2001; Kinoshita et al. 2011). Both mechanisms are plausible for *P. rapae* but specific behavioral experiments are needed to determine the photoreceptors that are involved and how they perceive *DoLP* differences.

The fitness benefits foraging insects accrue by exploiting polarization host cues will depend upon the specificity of these cues. Our measurements (Figs. 2.4, 2.5, 2.6, 2.7) and those of a previous study (Grant et al. 1993) revealed significant variation among plant species. Species within genera (most prominently *Brassica* spp. and *Solanum* spp.) have a similar *DoLP,* whereas genera within a plant family (e.g., *Brassica* and *Sinapis* in the Brassicaceae) have distinctly different *DoLP*s. These findings suggest that polarization host cues have the greatest utility for insect herbivores that specialize on a single plant genus or on several closely related genera. However, any differences in polarization host cues among genera are not absolute in that the *DoLP* also pertains to the viewing angle of the foraging insect (Foster et al. 2018).

The complementary information conveyed by plant-derived polarization cues could help insect herbivores locate and select optimal host plants. As optimal hosts confer significant fitness benefits to plant herbivores (Gripenberg et al. 2010), it follows that there might be strong selection pressure for foraging insect herbivores to exploit plant polarization cues. The preference of *P. rapae* for *DoLP*s approximating those of both matt host plants (*Brassica* spp. ~30%) and shiny host plants (*Sinapis* ~70%) supports the concept that the additional information provided by the *DoLP*s of foliar reflections confer fitness benefits. Avoiding areas with *DoLP*s below 30% may be adaptive in that these areas are more likely to be shaded, and without direct solar illumination will lack the host information provided by polarized specular reflections. The benefits of these cues are further evident by improved larval performance on wild cabbage plants with a blueish appearance (Green et al. 2015) that presumably had a significant epicuticular wax layer and thus a low *DoLP* of foliar reflections (Grant 1987). Failure of *P. rapae* females to visually discern among cabbage host plants (Green et al. 2015), or between cabbage host plants and lettuce (*Lactuca sativa*) non-host plants

(Ikeura et al. 2010) when polarization cues were not considered, also points to the *DoLP* of foliar reflections as an important host plant cue.

A sound understanding of how polarized light cues inform host plant selection decisions by insect herbivores will present pest managers and plant breeders with new options to lower the “apparency” of host plants. For example, breeding plant lines with reduced leaf wax (Stoner 1990) or spraying plants with kaolin clay suspensions (Glenn et al. 1999) will modify foliar surface characteristics and polarizations of their reflections, thus rendering plants less apparent to specific insect herbivores. However, the many potential tradeoffs of these types of interventions (e.g., changes in leaf surface affecting water-use efficiency or resistance to generalist insect herbivores or pathogens), will require *in-situ,* system-specific investigations prior to large-scale implementations of any intervention.

4.5. Materials and Methods

4.5.1. Insect Material

Detailed electrophysiological and histological studies were previously carried out with the Asian subspecies *P. rapae crucivora* (Qiu et al. 2002; Qiu and Arikawa 2003ab; Arikawa et al. 2005). Recent work has revealed no meaningful differences in the structure and function of the compound eyes of *P. r. crucivora* and the European subspecies *P. rapae rapae* (Blake et al. 2019b), indicating that the two sub-species can be used interchangeably in future behavioral studies that investigate responses of these insects to visual cues. Because *P. r. rapae* is present in North America and can readily be field-collected or purchased from North American suppliers, we worked with *P. r. rapae* in our experiments.

Insects were obtained from a laboratory colony that was started with material purchased from the Carolina Biological Supply Company (# 144100, Burlington, NC, USA) and housed at Simon Fraser University. Additional *P. r. rapae* females (tested in the *DoLP* preference experiment) were collected in cabbage fields near Delta, BC, Canada. Maintenance of the colony followed a well-established protocol (Webb and Shelton 1988), however adult insects were housed indoors (18-25°C; photoperiod 16L:8D). Colony-raised adult females and males were held together in cages with no

access to host plants or oviposition substrates. Females tested in experiments were 3-13 days post eclosion and were assumed to be gravid (Webb and Shelton 1988). Field-collected females were used for a period of ~14 days following capture. Females were tested in multiple bioassays, each bioassay presenting a new set of experimental stimuli. These different bioassays were considered independent.

4.5.2. Plant Material

Seeds of cabbage (*Brassica oleracea* L. var. *capitata* L. f. *alba* DC., cv 'Early Jersey Wakefield') and tubers of potato (*Solanum tuberosum* L. cv 'Russet Burbank') were grown in 12.7 cm diameter pots in a greenhouse. Plants tested in experiments were 10-20 cm tall with 4-8 fully expanded true leaves (BBCH 104-108). Experimental plants for each pair were carefully selected to minimize differences in leaf area.

4.5.3. Experimental Arena – Plant Stimuli

An experimental arena with a removable acrylic plastic lid (Fig. 4.2) was built from an aquarium (31.6 cm × 76.5 cm × 32.1 cm) made of soda-lime-silica glass. The aquarium was placed on a stand and an insect inlet tube was added to the center of the arena's bottom surface, allowing for the release of a bioassay insect into the arena. The bottom of the arena and its two lateral sides were lined with a matt brown kraft paper (NCR Corp., Duluth, GA, USA) with a reflectance spectrum resembling that of soil (Fig. 4.4b). The inner surface of the arena lid was lined with matt white banner paper (NCR Corp.) to allow for illumination of the arena interior. The paper lining the interior surfaces of the arena was replaced after each bioassay replicate and the exposed glass surface was cleaned with hexane. The two end sections of the arena, each serving as a "stimulus window" and facing a test plant, were left unobstructed.

Each stimulus chamber (31 cm × 31 cm × 47 cm) was lined with the same brown kraft paper (see above) and placed with its open side facing one of the stimulus windows of the arena (Fig. 4.2). With this arrangement, only the interior of the chambers was visible to the bioassay insect from inside the arena. The lighting aperture (19 × 20 cm) in the top of the chambers was designed to enable illumination of the test plant while minimizing any attraction of bioassay insects to the illumination sources (see below), and lessening chamber wall illumination and potential polarized reflectance. Each stimulus

plant was positioned with a 30° incline towards the experimental arena so that the plant was fully visible from within the arena.

Each chamber was illuminated from above by a 400 W Hortilux® Blue metal halide lamp (Fig. 4.4c; MT400D/BUD/HTL-BLUE, EYE Lighting International, Mentor, OH) centered 55-60 cm above the lighting aperture (see above; Fig. 4.2). The height of the lamps above the stimulus chambers was carefully adjusted to minimize differences in the intensity and spectral composition of the illumination of the two experimental plants. There was no bias toward one side of the arena (side 1 prop. = 50%, $\chi = 0.0$, df = 1, $n = 124$, $p = 1.0$).

In each bioassay replicate, a female *P. r. rapae* was allowed 5 min to choose between a host cabbage plant and a non-host potato plant. If, at the end of the 5 min bioassay period, a female was present within 10 cm of a stimulus window, she was considered to have responded to the plant behind that window. Females not responding within 5 min were considered non-responders. The positions of stimuli were alternated so that they appeared equally often on either side of the arena.

4.5.4. Experimental Arena – Image Stimuli

The arena described above (Fig. 4.2) was subsequently modified to bioassay responses of female *P. rapae* to plant images instead of live plants. Unless otherwise specified below, the same general experimental design and protocols were used to bioassay responses to plant images as were used to bioassay responses to live plants. Plant images were displayed on paired liquid crystal display (LCD) monitors (Fig. 4.3; 1707FPt, Dell Inc., Round Rock, TX) calibrated to minimize any differences between the monitors in the displayed irradiance spectra of pixels with identical Red/Green/Blue (RGB) values (Fig. 4.4e). The monitors displayed images of cabbage host plants and potato non-host plants generated through polarimetry (see below) of the live plants tested in the depolarizing-filter experiment (see below). We used photo polarimetry to ensure that the color of the displayed image stimuli were representative of the original plant stimuli. There may still have been differences in perceived color due to differences in background illumination. We also resized the plant images, so that when displayed on the monitors all plants occupied an equal pixel area. That these plant images lack the UV light typically found in plant reflectance was deemed acceptable because

prescreening testing revealed that the females' preference for cabbage plants remained unchanged when the illumination spectrum was altered to exclude UV wavelengths. Each monitor was positioned against the wall of the stimulus chamber opposite the stimulus window (Fig. 4.3), facing the experimental arena. In this wall was a 22 cm octagonal display aperture which was covered with a removable kraft paper mask with a hole in the shape of the plant image. This arrangement ensured that only the portion of the LCD displaying the plant image was visible to the bioassay insect. The top of each stimulus chamber had a lighting aperture (27 × 26 cm) covered with the same white banner paper as the arena lid, thus affording similar illumination of the arena and the stimulus chambers. The arena and the chambers were lit by a florescent lamp (Fig. 4.4d; F32T8/SPX50/ECO GE, Boston, MA) centered 15 cm above the arena. In 5 min bioassays, a camera mounted at the top rear of each stimulus chamber recorded the movements of each *P. rapae* female. The first approach towards a stimulus window and its associated plant image was recorded as a response. If a female made no approach, she was considered a non-responder. Images were displayed equally often on both monitors/sides of the arena. There was no bias towards one side of the arena over the course of all experiments (side 1 prop. = 49.8%, $\chi = 0.017$, df = 1, $n = 592$, $p = 0.97$).

4.5.5. Polarimetry of Experimental Plants

We used photo polarimetry (Horváth and Varjú 2004; Foster et al. 2018) to measure the *DoLP* and the *AoP* for all cabbage and potato plants used in the depolarizing-filter experiment. Photo polarimetry gives a *DoLP* and a *AoP* value for the red (575-700 nm), green (455-610 nm), blue (410-530 nm) and ultraviolet (330-395 nm) (UV) bands of the electromagnetic spectrum. All pixel values were then averaged to give a whole plant mean or modal value for the *DoLP* and the *AoP,* respectively. We utilized an Olympus E-PM1 camera (Olympus, Tokyo, Japan), modified for expanded spectral sensitivity covering both the UV (< 400 nm) and human-visible light range (400-700 nm) (Fig 4.4f; Dr. Klaus Schmitt, Weinheim, Germany, uvir.eu). We used an ultra-broadband linear polarizing filter (68-751, Edmund Optics, USA) in combination with a UV/IR filter (Baader Planetarium, Mammendorf, Germany) or a U-filter (Baader Planetarium) for human-visible (red, green, and blue) and UV images, respectively. The experimental plants were positioned and lit the same way as described for experimental plants in the experimental arena (see above). All other plants were photographed upright inside a

black velvet-lined box lit from above by a metal halide lamp (see above) through a circular opening in the top of the box. White-balance, aperture, and other exposure controls were manually set and remained constant among exposures, with all images captured in a raw image format before decoding with DCRAW (Coffin 2019) in a manner that preserved sensor linearity. Required color corrections, determined through photographing a 99% Spectralon reflectance standard (SRS-99-010, Labsphere, NH, USA) under similar lighting conditions, were then applied to ensure accurate color representation. Images were then aligned (Thévenaz et al. 1998) before stokes parameters, *DoLP,* and *AoP* were calculated.

4.5.6. Depolarizing-Filter Experiment

Depolarizing filters were made from two sheets of optically anisotropic mylar (Dura-Lar 0.003, Grafix, Maple Heights, OH). Oriented at 45° to each other (Sweeney et al. 2003), these mylar sheets partially circularly polarize light, effectively depolarizing the incident light (Shashar et al. 2000) by reducing *DoLP* to below 4-15% depending upon wavelength, as measured through photo polarimetry. Depolarizing filters were placed on the exterior wall of the stimulus widows completely covering them so that all light reflected from plants entered the arena through these filters. The transmission spectra of stimulus windows with or without the depolarizing filter are shown in Fig. 4.4a. In 200 bioassay replicates, 14 pairs of a cabbage and a potato plant matched in size were presented. In half of the replicates, depolarizing filters were in place on both stimulus windows and in the remaining half no filter was present.

4.5.7. LCD-Monitor-Proof-of-Concept Experiment

We designed a novel combination of λ/4 retarder films and LCD monitors to display static images (in this case plant images). This design allowed for greater control of image attributes than reported in previous methods (Foster et al. 2018). By manipulating the rotation of the monitor's display and the alignment of the λ/4 retarder film (Fig. 4.4a; #88-253, Edmund Optics, Barrington, NJ) relative to the display's *AoP*, we were able to mimic the mean *DoLP* and the modal *AoP*, as determined through photo polarimetry, of both the cabbage plants (31% *DoLP*, 90° *AoP*) and the potato plants (50% *DoLP*, 90° *AoP*), as they appeared in the depolarizing filter experiment (Fig. 4.3). LCDs emit highly polarized light (>95% *DoLP*) due to the use of polarizers in their assembly. We

manipulated the *AoP* of the plant image by rotating the monitor's display and counter rotating the image. The *DoLP* was manipulated through the use of a λ/4 retarder film (Blake et al. 2019a). When the *AoP* of the LCD monitor is aligned with either the slow or the fast axis of the retarder film, the *DoLP* is unchanged by the retarder film. As the *AoP* of the LCD monitor is aligned at an increasing angle to the axes of the retarder film, the light becomes less linearly polarized and increasingly elliptically polarized until this angle is 45° and most of the light becomes circularly polarized and the *DoLP* is minimized. When the entire human visible spectrum is considered, the λ/4 retarder film also shifts *AoP* in a clockwise direction by an amount approximating the rotation angle of the film relative to the monitor (Blake et al. 2019a), necessitating an equal counter-clockwise rotation of the monitor. Using these methods, we were able to replicate the depolarizing filter experiment using virtual plants instead of live plants as test stimuli. A cabbage host plant image with a cabbage *DoLP* was tested *versus* a potato non-host plant image with a potato *DoLP,* and the same images were tested with the *DoLP* minimized. Additionally, the LCD monitor setup allowed us to reverse the *DoLP* of the two plant images and to present a cabbage host plant image with a potato *DoLP* and *vice versa*. We ran 80 bioassay replicates for each of the three comparisons, using 10 matched pairs of cabbage and potato plant images.

4.5.8. Degree and Axis of Polarization Preference Experiments

To determine how the *AoP* and *DoLP* of plants (or their images) affect host plant choices by *P. rapae* females*,* we presented a series of choices between a control cabbage image and an identical treatment image differing in either *AoP* or *DoLP.* The control image in both experiments was presented with a *DoLP* of 31% and a *AoP* of 90°. In the *AoP* preference experiment, the treatment image had an *AoP* of 0°, 30°, 45°, 60°, 105°, 120°, 135°, or 150° (Fig. 4.7a) with a *DoLP* of 31%. In the *DoLP* experiment, the treatment image had a *DoLP* of 10%, 21%, 41%, 50%, 70% with an *AoP* of 90° (Fig. 4.7b). We ran 50 and 73 bioassay replicates for the *AoP* and the *DoLP* treatments, respectively, using a total of 14 different cabbage images.

4.5.9. Statistical Analysis

Chi-square tests were used to analyze whether the proportion of *P. rapae* females responding to live experimental plants, or plant images, differed from 0.5. Further, chi-

square tests were used to compare the proportion of females responding among experimental treatments. Females not responding to test stimuli (live plants or plant images) were excluded from statistical analyses.

4.6. References

Arikawa K, Wakakuwa M, Qiu X, et al (2005) Sexual dimorphism of short-wavelength photoreceptors in the small white butterfly, *Pieris rapae crucivora*. J Neurosci 25:5935–5942. https://doi.org/10.1523/JNEUROSCI.1364-05.2005

Blake AJ, Go MC, Hahn GS, Grey H, Couture S, Gries G (2019a) λ/4 Retarder Film Measurement from: Polarization of foliar reflectance – novel host plant cue for insect herbivores. v7, Dryad, Dataset. https://doi.org/10.5061/dryad.xgxd254bs

Blake AJ, Pirih P, Qiu X, Arikawa K, Gries G (2019b) Compound eyes of the small white butterfly *Pieris rapae* have three distinct classes of red photoreceptors. J Comp Physiol A 205:553–565. https://doi.org/10.1007/s00359-019-01330-8

Coffin D (2019) Decoding raw digital photos in Linux. https://www.dechifro.org/dcraw/. Accessed 23 Dec 2019

Foster JJ, Temple SE, How MJ, et al (2018) Polarisation vision: overcoming challenges of working with a property of light we barely see. Sci Nat 105:27. https://doi.org/10.1007/s00114-018-1551-3

Glenn DM, Puterka GJ, Vanderzwet T, et al (1999) Hydrophobic particle films: a new paradigm for suppression of arthropod pests and plant diseases. J Econ Entomol 92:759–771. https://doi.org/10.1093/jee/92.4.759

Grant L (1987) Diffuse and specular characteristics of leaf reflectance. Remote Sens Environ 22:309–322. https://doi.org/10.1016/0034-4257(87)90064-2

Grant L, Daughtry CST, Vanderbilt VC (1993) Polarized and specular reflectance variation with leaf surface features. Physiol Plant 88:1–9. https://doi.org/10.1111/j.1399-3054.1993.tb01753.x

Green JP, Foster R, Wilkins L, et al (2015) Leaf colour as a signal of chemical defence to insect herbivores in wild cabbage (*Brassica oleracea*). PLoS One 10:e0136884. https://doi.org/10.1371/journal.pone.0136884

Gripenberg S, Mayhew P, Parnell M, Roslin T (2010) A meta-analysis of preference–performance relationships in phytophagous insects. Ecol Lett 13:383–393

Hardie RC (1979) Electrophysiological analysis of fly retina. I: Comparative properties of R1-6 and R 7 and 8. J Comp Physiol 129:19–33. https://doi.org/10.1007/BF00679908

Hegedüs R, Horváth G (2004) Polarizational colours could help polarization-dependent colour vision systems to discriminate between shiny and matt surfaces, but cannot unambiguously code surface orientation. Vision Res 44:2337–2348. https://doi.org/10.1016/j.visres.2004.05.004

Horváth G, Varjú D (2004) Polarized Light in Animal Vision: Polarization Patterns in Nature. Springer, New York

How MJ, Marshall NJ (2014) Polarization distance: a framework for modelling object detection by polarization vision systems. Proc R Soc B Biol Sci 281:20131632. https://doi.org/10.1098/rspb.2013.1632

Ikeura H, Kobayashi F, Hayata Y (2010) How do *Pieris rapae* search for Brassicaceae host plants? Biochem Syst Ecol 38:1199–1203. https://doi.org/10.1016/j.bse.2010.12.007

Ilić M, Pirih P, Belušič G (2016) Four photoreceptor classes in the open rhabdom eye of the red palm weevil, *Rynchophorus ferrugineus* Olivier. J Comp Physiol A 202:203–213. https://doi.org/10.1007/s00359-015-1065-9

Jaenike J (1990) Host specialization in phytophagous insects. Annu Rev Ecol Syst 21:243–273. https://doi.org/10.1146/annurev.es.21.110190.001331

Kelber A, Thunell C, Arikawa K (2001) Polarisation-dependent colour vision in *Papilio*. J Exp Biol 204:2469–2480

Kinoshita M, Yamazato K, Arikawa K (2011) Polarization-based brightness discrimination in the foraging butterfly, *Papilio xuthus*. Philos Trans R Soc B Biol Sci 366:688–696. https://doi.org/10.1098/rstb.2010.0200

Labhart T (2016) Can invertebrates see the e-vector of polarization as a separate modality of light? J Exp Biol 219:3844–3856. https://doi.org/10.1242/jeb.139899

Maxwell DJ, Partridge JC, Roberts NW, et al (2016) The effects of plant virus infection on polarization reflection from leaves. PLoS One 11:e0152836-18. https://doi.org/10.1371/journal.pone.0152836

Mishra M (2015) An eye ultrastructure investigation of a plant pest *Acyrthosiphon pisum* (Harris) (Insecta: Hemiptera: Aphididae). Open Access Insect Physiol 5:41–46. https://doi.org/10.2147/OAIP.S84633

Prokopy R, Owens E (1983) Visual detection of plants by herbivorous insects. Annu Rev Entomol 28:337–364. https://doi.org/10.1146/annurev.en.28.010183.002005

Qiu X, Arikawa K (2003a) Polymorphism of red receptors: sensitivity spectra of proximal photoreceptors in the small white butterfly *Pieris rapae crucivora*. J Exp Biol 206:2787–2793. https://doi.org/10.1242/jeb.00493

Qiu X, Arikawa K (2003b) The photoreceptor localization confirms the spectral heterogeneity of ommatidia in the male small white butterfly, *Pieris rapae crucivora*. J Comp Physiol A 189:81–88. https://doi.org/10.1007/s00359-002-0380-0

Qiu X, Vanhoutte K, Stavenga DG, Arikawa K (2002) Ommatidial heterogeneity in the compound eye of the male small white butterfly, *Pieris rapae crucivora*. Cell Tissue Res 307:371–379. https://doi.org/10.1007/s00441-002-0517-z

Reeves JL (2011) Vision should not be overlooked as an important sensory modality for finding host plants. Environ Entomol 40:855–863. https://doi.org/10.1603/EN10212

Renwick JAA, Radke CD (1988) Sensory cues in host selection for oviposition by the cabbage butterfly, *Pieris rapae*. J Insect Physiol 34:251–257. https://doi.org/10.1016/0022-1910(88)90055-8

Shashar N, Hagan R, Boal JG, Hanlon RT (2000) Cuttlefish use polarization sensitivity in predation on silvery fish. Vision Res 40:71–75. https://doi.org/10.1016/S0042-6989(99)00158-3

Stewart FJ, Kinoshita M, Arikawa K (2017) A novel display system reveals anisotropic polarization perception in the motion vision of the butterfly *Papilio xuthus*. Integr Comp Biol 57:1130–1138. https://doi.org/10.1093/icb/icx070

Stoner KA (1990) Glossy leaf wax and plant resistance to insects in *Brassica oleracea* under natural infestation. Environ Entomol 19:730–739. https://doi.org/10.1093/ee/19.3.730

Sweeney A, Jiggins C, Johnsen S (2003) Insect communication: Polarized light as a butterfly mating signal. Nature 423:31–32. https://doi.org/10.1038/423031a

Takács S, Bottomley H, Andreller I, et al (2008) Infrared radiation from hot cones on cool conifers attracts seed-feeding insects. Proc R Soc B Biol Sci 276:649–655. https://doi.org/10.1098/rspb.2008.0742

Thévenaz P, Ruttimann UE, Unser M (1998) A pyramid approach to subpixel registration based on intensity. IEEE Trans Image Process Publ IEEE Signal Process Soc 7:27–41. https://doi.org/10.1109/83.650848

Wachmann E (1977) Vergleichende Analyse der feinstrukturellen Organisation offener Rhabdome in den Augen der Cucujiformia (Insecta, Coleoptera), unter besonderer Berücksichtigung der Chrysomelidae. Zoomorphologie 88:95–131. https://doi.org/10.1007/BF01880649

Webb S, Shelton AM (1988) Laboratory rearing of the imported cabbageworm. New Yorks Food Life Sci Bull 122:1–6

Wernet MF, Velez MM, Clark DA, et al (2012) Genetic dissection reveals two separate retinal substrates for polarization vision in *Drosophila*. Curr Biol 22:12–20. https://doi.org/10.1016/j.cub.2011.11.028

4.7. Figures

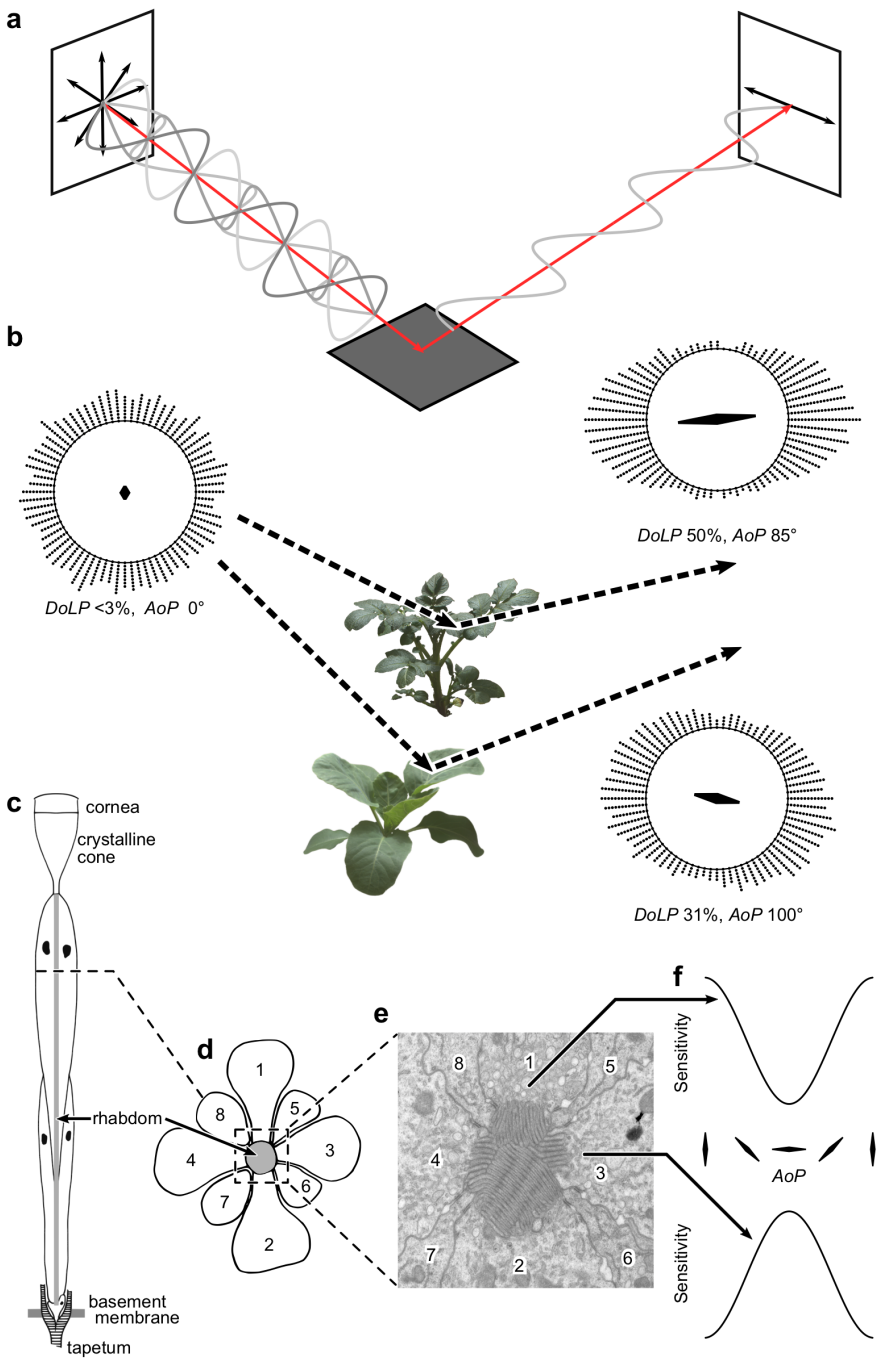
a
b
DoLP <3%, AoP 0°
DoLP 50%, AoP 85°
DoLP 31%, AoP 100°
c
cornea
crystalline cone
rhabdom
basement membrane
tapetum
d
e
f
Sensitivity
AoP
Sensitivity

Figure 4.1 **Diagrams depicting polarization by reflectance and an ommatidium (photoreceptor unit) of the *P. rapae* compound eye. (a) Unpolarized light (light vibrating equally in all directions) from the sun is polarized via reflection from surfaces such as water or plant foliage. Light vibrating in the direction parallel to the surface is preferentially reflected resulting in polarization. (b) Light reflections from cabbage (bottom) or potato (top) foliage (note color and shape differences); associated compass diagrams show the distribution in vibration direction of waves composing each light ray. The predominate direction of vibration, or *AoP* (0-180°), is represented by the direction of the compass needles. The *DoLP* as a measure of the anisotropy of vibration directions is depicted as the amount of spread around this predominate direction and by the size of the compass needle. (c) Diagram of an ommatidium. (d) Cross sectional diagram of an ommatidium showing the eight photoreceptors (R1-8). Diagrams in c and d modified from (Qiu et al 2002). (e) Electron micrograph showing the parallel microvilli of photoreceptors R1-4 composing the rhabdom. (f) The resulting modulations in sensitivity, with changes in the *AoP* of incident light, of the indicated photoreceptors. *AoP* = Axis of Polarization; *DoLP* = Degree of Linear Polarization**

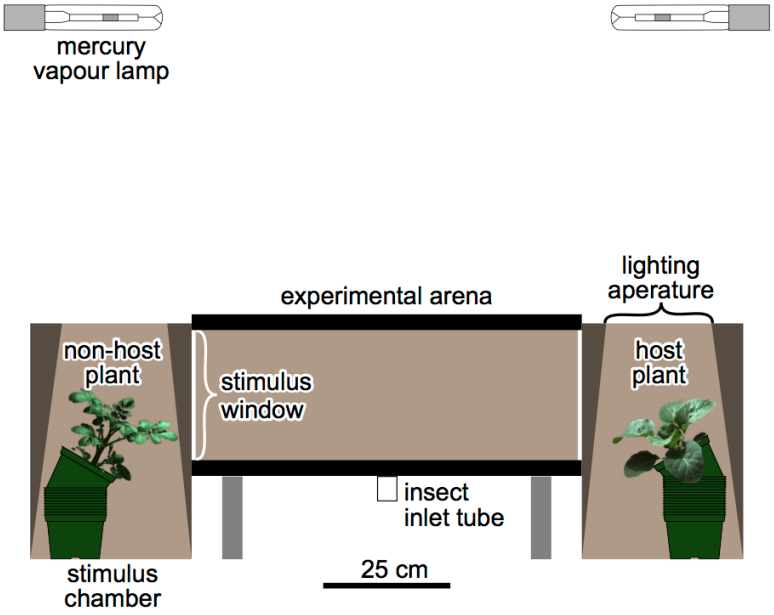

Figure 4.2 **Bioassay setup to test behavioral responses of female *P. rapae* to live potato non-host plants (left) and live cabbage host plants (right).**

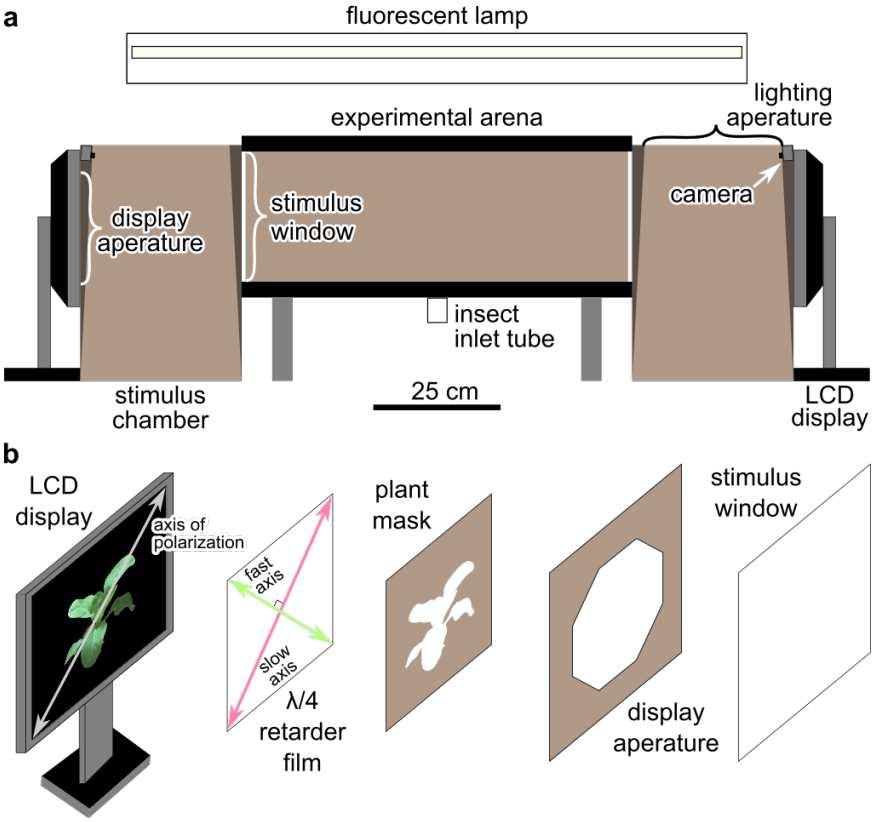

Figure 4.3 **Bioassay setup to test behavioral responses of female *P. rapae* to image stimuli. (a) Diagram of experimental arena. (b) Exploded view of the arrangement of components between the LCD monitor and the stimulus windows. LCD = Liquid Crystal Display**

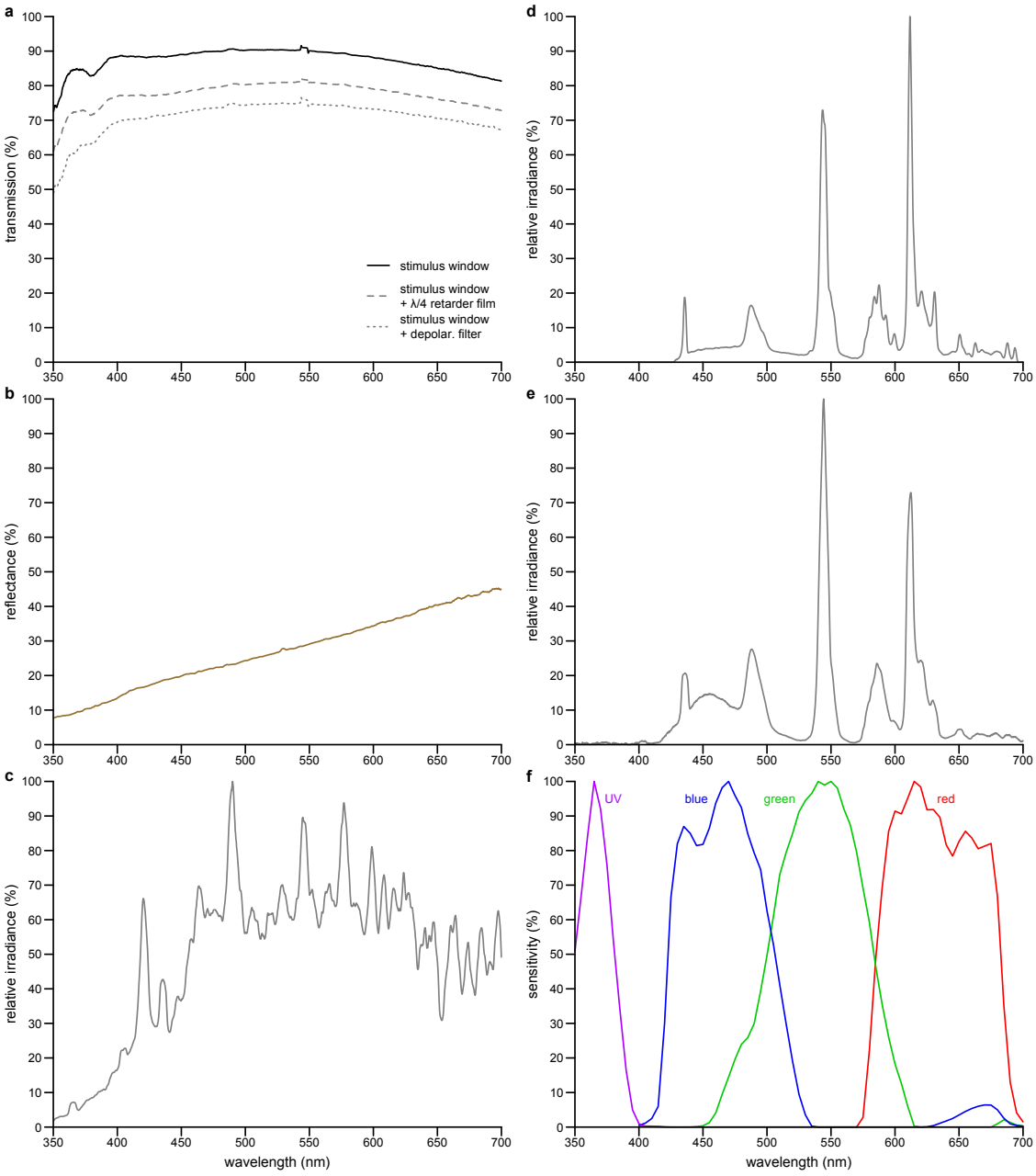

Figure 4.4 **Spectra of filters, background, illumination sources, and camera sensitivity. (a) Transmission spectra of the stimulus windows of the experimental arena, and the same windows with a depolarizing filter or a λ/4 retarder film. (b) Reflection spectrum of the brown kraft paper. (c, d) Relative irradiance of the metal halide and fluorescent lamps. (e) Relative irradiance of white pixels (mean of both LCD monitors). (f) Spectral sensitivity of the modified Olympus E-PM1 camera in the UV, blue, green and red bands of the electromagnetic spectrum**

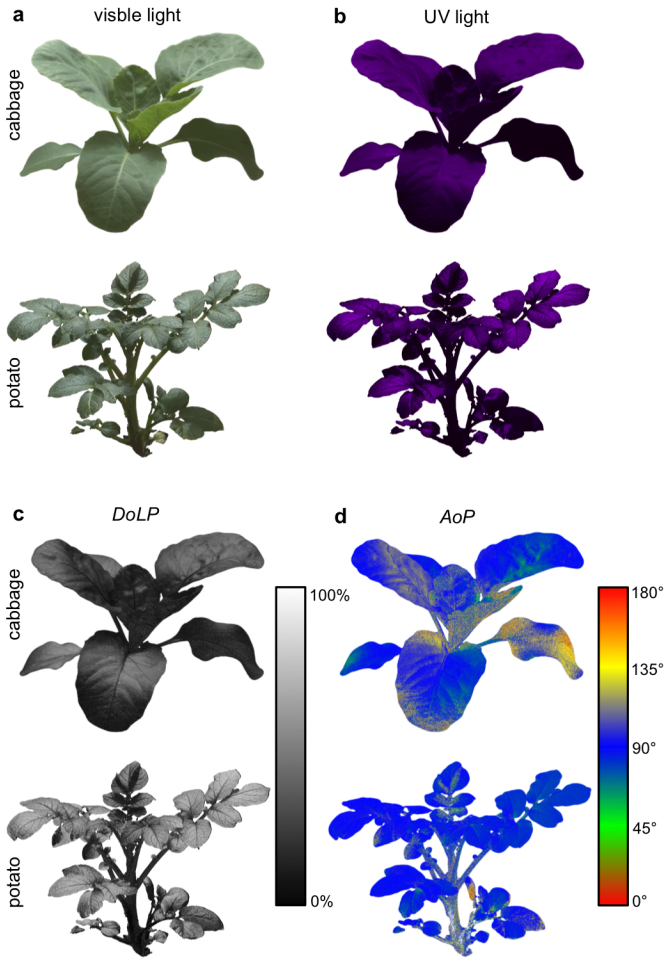

e

	Cabbage	Potato
UV *DoLP* (%)	55 ± 1	85 ± 1
Blue *DoLP* (%)	31 ± 1	49 ± 1
Green *DoLP* (%)	16 ± 1	25 ± 1
Red *DoLP* (%)	19 ± 1	30 ± 1
UV *AoP* (°)	90 ± 1	88 ± 1
Blue *AoP* (°)	90 ± 1	87 ± 1
Green *AoP* (°)	89 ± 1	87 ± 1
Red *AoP* (°)	89 ± 1	87 ± 1

Figure 4.5 **Polarimetry of experimental host (cabbage) and non-host (potato) plants. (a, b) Human-visible light images (red, green, blue) and false-color UV light (330-395 nm) images, respectively. (c, d) Images showing the *DoLP* and the *AoP* that were calculated using the blue band (575 to 700 nm) of the human visible spectrum. Other bands (Fig. 4.4) showed similar patterns in *DoLP* and *AoP*. (e) The mean ± s.e. *DoLP* and *AoP* of experimental plants in the UV, blue, green, and red bands of the electromagnetic spectrum. These means are a multi-plant average of the mean *DoLP* or modal *AoP* of all pixels from one plant. UV = Ultraviolet; *AoP* = Axis of Polarization; *DoLP* = Degree of Linear Polarization**

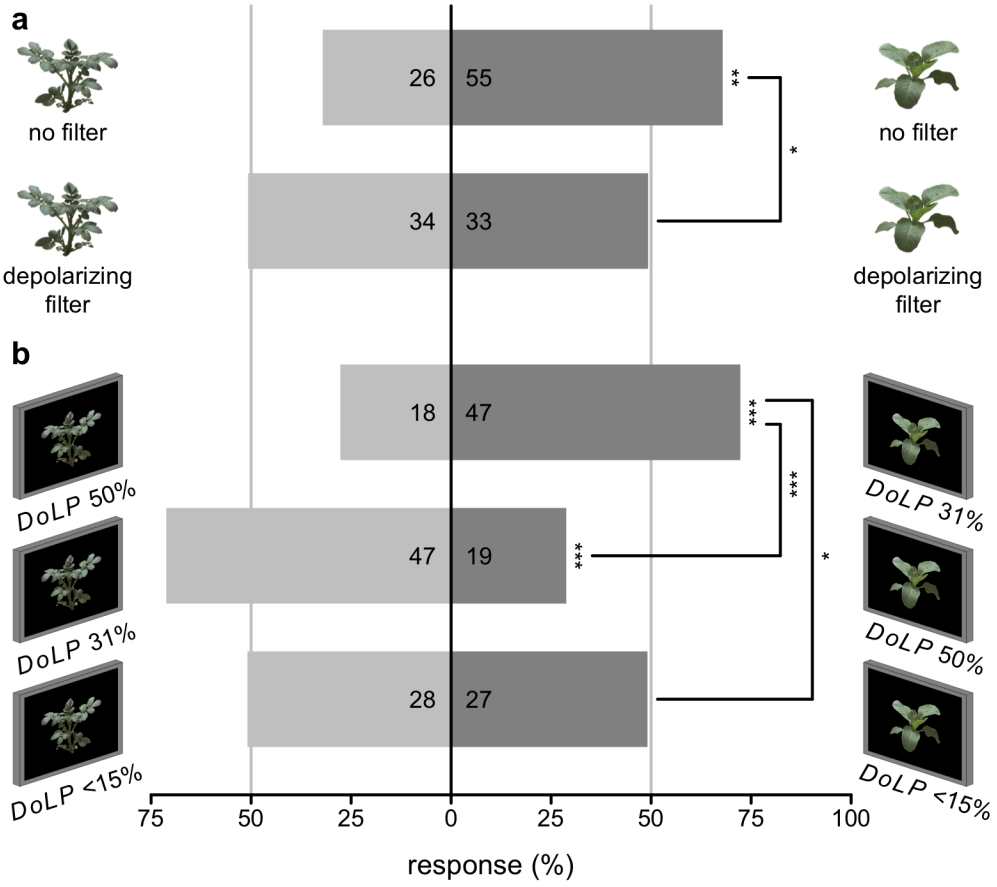

Figure 4.6 ***DoLP* affects plant choice by *P. rapae*. (a) Without access to plant odors, females prefer a live cabbage host plant (right) over a live potato non-host plant (left) when polarized light cues are intact (top bar). This preference disappears when these cues are removed with a depolarizing filter (bottom bar). (b) Females also prefer the image of a cabbage host plant (right) over the image of a potato non-host plant (left) when presented with a *DoLP* matching that of live plants. The preference could be removed (bottom row) or even reversed (middle row) by changing the *DoLP* of the images. Numbers of females responding to each stimulus are shown within bars. The asterisk(s) either indicate(s) a percentage deviating from 50% or a significant difference between two percentages (χ^2 test, * $p < 0.05$, ** $p < 0.01$, *** $p < 0.001$). *DoLP* = Degree of Linear Polarization**

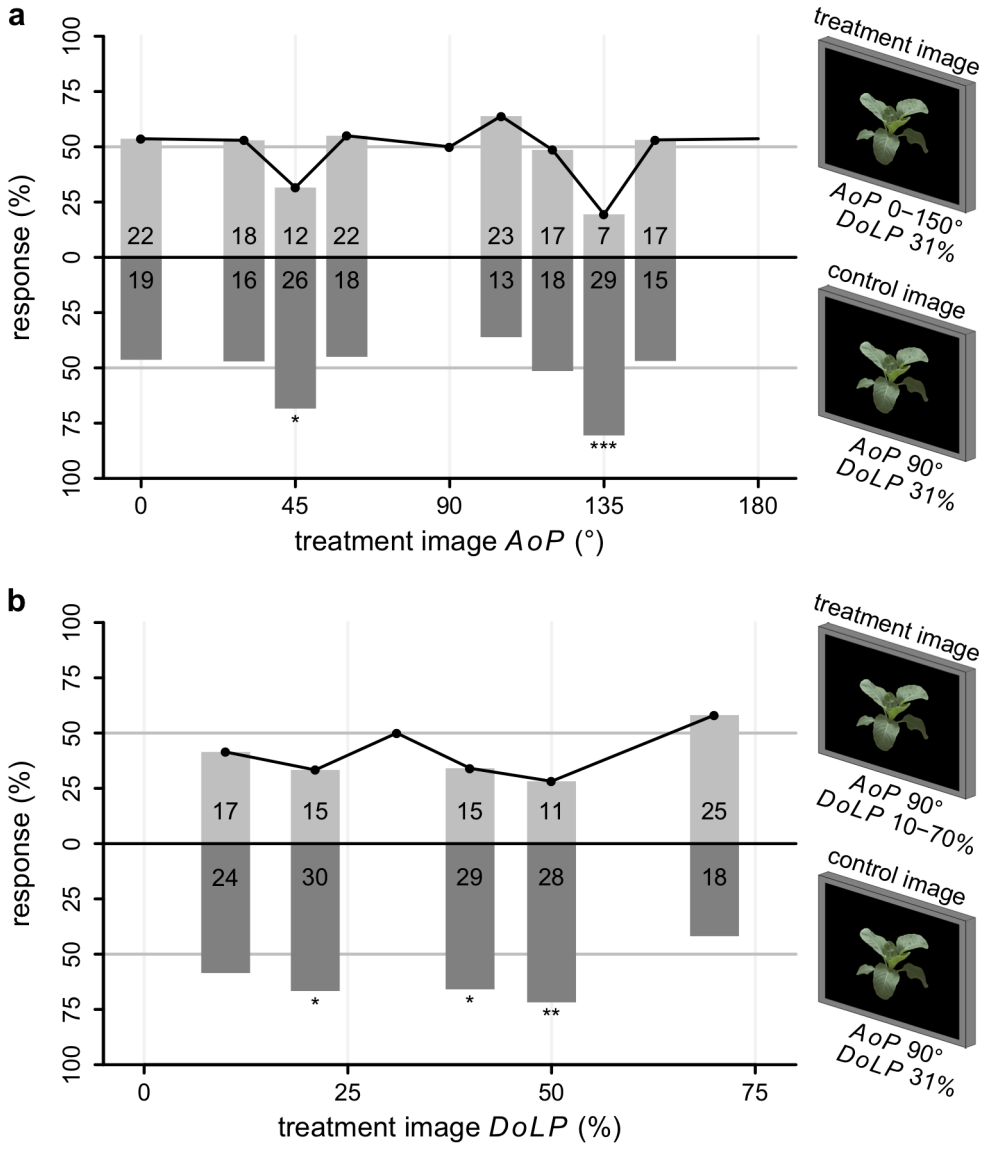

Figure 4.7 **Both the *DoLP* and the *AoP* affect plant choice by *P. rapae*. (a), A cabbage image with a *AoP* of 45° or 135° was repellent to females. (b), Most images with a *DoLP* above or below that typical of cabbage (31%) were discriminated against by females. Responses to a treatment image with a *DoLP* and an *AoP* identical to those of the control image were assumed to be 50%. Numbers of females responding to each treatment are shown within bars. The asterisk(s) indicate(s) either a proportion deviating from 50% or a significant difference between two percentages (χ^2 test, $p < 0.10$, * $p < 0.05$, ** $p < 0.01$, *** $p < 0.001$). *AoP* = Axis of Polarization; *DoLP* = Degree of Linear Polarization**

Chapter 5.

Polarized light sensitivity in *Pieris rapae* is dependent on both color and intensity[1]

[1]The corresponding manuscript is published in the *Journal of Experimental Biology* (2020, doi.org/10.1242/jeb.220350) with the following authors: Blake AJ, Hahn G, Grey H, Kwok SA, McIntosh D, Gries G

5.1. Abstract

There is an ever increasing number of arthropod taxa shown to have polarization sensitivity throughout their compound eyes. However, the downstream processing of polarized reflections from objects is not well understood. The small white butterfly, *Pieris rapae,* has been demonstrated to exploit foliar polarized reflections, specifically the degree of linear polarization (*DoLP*), to recognize host plants. The well-described visual system of *P. rapae* includes several photoreceptor types (red, green, blue) that are sensitive to polarized light. Yet, the roles and interaction among photoreceptors underlying the behavioral responses of *P. rapae* to stimuli with different *DoLPs* remain unknown. To investigate potential neurological mechanisms, we designed several two-choice behavioral bioassays, displaying plant images on paired LCD monitors which allowed for independent control of polarization, color and intensity. When we presented choices between stimuli that differed in either color or *DoLP*, both decreasing and increasing the intensity of the more attractive stimulus reduced the strength of preference. This result suggests differences in color and *DoLP* are perceived in a similar manner. When we offered a *DoLP* choice between plant images manipulated to minimize the response of blue, red, or blue and red photoreceptors, *P. rapae* shifted its preference for *DoLP*, suggesting a role for all of these photoreceptors. Modeling of *P. rapae* photoreceptor responses to test stimuli suggests that differential *DoLP* is not perceived solely as a color difference. Our combined results suggest that *P. rapae* females process and interpret polarization reflections in a way different from that described for other polarization-sensitive taxa.

5.2. Introduction

Polarized light cues are used by many arthropods but apart from polarized skylight navigation little is known about how these organisms perceive polarized reflections (Heinloth et al. 2018). All organisms with rhabdomeric photoreceptors have the potential to sense polarized light (Horváth and Varjú 2004). The tubular structure of the microvilli forming the rhabdom results in photopigments aligning more along the long axis of the microvilli. This alignment, in turn, causes these photopigments to be more sensitive to light vibrating in the plane parallel to the long axis of the microvilli (Johnsen 2011). The plane of polarization with the greatest photoreceptor sensitivity is referred to as ϕ_{max} and typically aligns with the microvillar orientation (Horváth and Varjú 2004). The size of this difference in sensitivity is referred to as polarization sensitivity (*PS*) and is defined as the the ratio of sensitivity to light vibrating at ϕ_{max}, and to light vibrating orthogonal to ϕ_{max}. Photoreceptors with a high *PS* are typically found in a specialized area of the compound eye known as the dorsal rim allowing for polarized skylight navigation (Labhart and Meyer 1999). The microvilli of these photoreceptors are aligned, and non-twisted, along the length of their relatively short rhabdom, thereby enhancing *PS*. Additionally, these high *PS* photoreceptors involved in skylight navigation, which differ in ϕ_{max}, all share similar spectral sensitivities. If these photoreceptors differed in both spectral sensitivity and ϕ_{max}, the perceived color of an object would depend on both its reflection spectrum and its polarization (Wehner and Bernard 1993). Many insects avoid polarization-induced false colors by twisting the direction of these microvilli along the length of the rhabdom, because otherwise the perceived color of objects would change as insects navigate through the environment. However, many other insects, especially those in aquatic and semi-aquatic habitats (Horváth and Csabai 2014), possess photoreceptors with moderate *PS* throughout their compound eyes and some of these insects do experience these polarization-induced false colors (Kelber et al. 2001). Histological and electrophysiological work has also revealed evidence for *PS* in many herbivorous insects (Wachmann 1977; Mishra 2015; Ilić et al. 2016).

Recently, *P. rapae* females have been shown to discriminate among potential host plants based on the polarization of light reflected from their foliage (Blake et al. 2019a). Like any shiny surface, the leaf surface preferentially reflects light oscillating parallel to that surface (Shashar et al. 1998; Horváth et al. 2002). This axis of

polarization (*AoP*, 0-180°), as well as the degree to which the foliar reflection is polarized (degree of linear polarization, *DoLP*, 0-100%), are both strongly dependent upon the viewing angle and the location of the light source. However, *AoP* (unlike *DoLP*) is largely independent of leaf surface characteristics (Blake et al. 2019a). As only the specular component of the reflection is polarized, any leaf characteristics that affect the relative shininess or mattness also affect the *DoLP*. Decreasing the diffuse reflection through absorbance by pigments, scattering the specular reflection with epicuticular waxes or pigments, or undulations of the plane of the leaf's surface can all affect the *DoLP* of foliar reflections (Grant et al. 1993). Being dependent on these leaf characteristics, foliar *DoLP* can convey information about the host plant not conveyed by its color or intensity. Female *P. rapae* are able to discern cabbage host plants and potato non-host plants based on the lower *DoLP* of cabbage leaf reflections (Blake et al. 2019a). In choice bioassays, which presented manipulated host plant images, *P. rapae* females rejected most images with a *DoLP* dissimilar to that of their cabbage host plant (*DoLP* of 31%). The informative value of this cue during host plant selection is enhanced by a relative insensitivity of *P. rapae* females to all but *AoP*s very near to 45° or 135°. Both the underlying neurological mechanism and the photoreceptors involved in this discrimination remain unknown.

The visual system of *P. rapae* resembles that of other butterflies in that each ommatidium contains nine photoreceptors and the three ommatidial types are arranged in a random mosaic throughout the compound eye (Fig. 5.1a). Similar to the ommatidia of *Papilio* butterflies (Kelber 2001), the shortwave-sensitive (UV, violet, blue) R1,2 photoreceptors, with the exception of the polarization-insensitive UV photoreceptor, respond most strongly to vertically polarized light, whereas the longwave-sensitive R3-9 photoreceptors respond most strongly to horizontally polarized light (R3,4) and obliquely polarized light (R5-8) (Blake et al., 2019b; Fig. 5.1b,c). In the ventral portion of the eye, the sensitivity of the R5-8 photoreceptors, which like R3,4 express a green-sensitive opsin, are modified by perirhabdomal filtering pigments into three classes of red photoreceptors distinct to the three ommatidial types, with more variation in *PS* among ommatidial types than reported in *Papilio* (Fig. 5.1c). Of the shortwave receptors, only the type I blue photoreceptors show significant *PS*. There is also a lower *PS* in type II R3,4 receptors, whose polarization filtering effects on more basal photoreceptors (Snyder 1973) may explain the difference in the axis of maximal polarization sensitivity

(ϕ_{max}) of red photoreceptors among ommatidial types (Blake et al. 2019c). The R9 receptor is thought to be red-sensitive (Shimohigashi and Tominaga 1991), and likely has low *PS* due to its bidirectional microvillar arrangement (Qiu et al. 2002).

The compound eye of *P. rapae* has been extensively characterized, but there is no obvious mechanism that would explain how *P. rapae* processes the signals from its suite of photoreceptors to discriminate among stimuli with different *DoLP*s. To determine whether *P. rapae* perceives differential *DoLPs* as differences in stimulus intensity or color, we sought to emulate the work of Kinoshita et al. (2011). In two-choice bioassays, we examined the responses of *P. rapae* to differences in *DoLP* or color between stimuli to determine whether intensity differences between the stimuli affected preference in a similar manner. We also determined the photoreceptors involved in *DoLP* discrimination by minimizing the blue, red, or blue and red light of cabbage images that we presented to *P. rapae* in bioassays. This type of manipulation is possible through use of our novel monitor bioassay (Blake et al. 2019a). We predicted that if a photoreceptor were involved in *DoLP* discrimination, then image manipulations of stimuli reducing the photoreceptor's stimulation should alter the behavioral response of *P. rapae* to *DoLP* differences. We also modeled the catch of all *P. rapae* photoreceptors aiming to explain the observed behavioral bioassay responses of *P. rapae*.

5.3. Methods

5.3.1. Insect Material

Our laboratory colony of *P. r. rapae* originated from eggs obtained from the Carolina Biological Supply Company (# 144100, Burlington, NC, USA) and later from adults collected from cabbage fields near Delta, BC, Canada. Using a well-established protocol (Webb and Shelton 1988), larvae were maintained on either a wheat-germ diet or on cabbage plants grown in a greenhouse. We housed both male and female adults in indoor cages (60 × 60 × 60 cm, BugDorm 2120, MegaView Science Co. Ltd., Taichung, Taiwan) kept at 18-25 °C and a photoperiod of 16L:8D. The females we tested in experiments were randomly selected from cohorts of adults 3-14 days post eclosion and were assumed to be gravid. We tested females in multiple bioassays, each bioassay presenting a new pair of experimental plant images. These different bioassays were considered independent.

5.3.2. General Experimental Setup

We used the same experimental arena (31.6 cm × 76.5 cm × 32.1 cm) and LCD monitor setup as recently described (Blake et al., 2019c; Fig. 4.3a). The inner surface of the removable arena lid was lined with matt white banner paper (NCR Corp., Duluth, GA, USA). We left the two end sections of the arena facing the monitors (stimulus windows) unobstructed but lined all the other inner surfaces of the arena with a matt brown kraft paper (NCR Corp.). To prevent build-up of any olfactory cues in the arena, we replaced the paper lining the interior surfaces and cleaned exposed glass surfaces with hexane daily.

In all experiments, we displayed cabbage plant images, created through photo polarimetry, as detailed in a recent publication (Blake et al. 2019a). In summary, we photographed cabbage plants, corrected the image color balance using a reflectance standard (SRS-99-010, Labsphere, NH, USA), removed the image background, and then standardized the plant size in each image such that all plant images presented an equal number of pixels. The pixel values of these Red/Green/Blue (RGB) images were then manipulated to create versions which differed in intensity or color (Table 5.1; Fig. 5.2d-f). These images were presented on paired liquid crystal display (LCD) monitors (1707FPt, Dell Inc., Round Rock, TX) calibrated to minimize any differences between monitors in the displayed irradiance spectra of pixels with identical RGB values (Fig. 5.2c). These monitors lack UV irradiance but the absence of UV wavelengths did not affect *DoLP*-based host plant preferences (Blake et al. 2019a). As LCD monitors produce highly polarized light, we manipulated the *AoP* by rotating the display and counter rotating the image. Using a λ/4 retarder film (#88-253, Edmund Optics, Barrington, NJ), we were also able to manipulate the plant image *DoLP* by changing the alignment of the *AoP* of the display relative to the retarder film (Blake et al. 2019b, a). Using LCD monitors also enabled us to readily manipulate both the plant image's color and/or intensity.

The monitors were separated from the stimulus windows of the experimental arena by a stimulus chamber (31 cm × 31 cm × 47 cm) lined with the same kraft paper as the arena. This separation limited the range of viewing angles of the monitor from within the arena. In order to limit the visible portion of the LCD to that displaying the plant image, we placed a kraft paper plant mask over the display aperture in each stimulus

chamber (Fig. 4.3b). The top of each stimulus chamber had a lighting aperture (27 × 26 cm) covered with the same white banner paper as the arena lid, thus affording similar illumination of the arena and the stimulus chambers. The arena and the chambers were lit from a fluorescent lamp (Fig. 5.2b; F32T8/SPX50/ECO GE, Boston, MA) centered 15 cm above the arena.

Using a camera mounted at the top rear of each stimulus chamber, we monitored the response of *P. rapae* females introduced into the arena. We allowed each female up to 5 min to approach one of the stimulus windows and recorded this approach as a behavioral response to the associated plant image. We considered females making no response non-responders. Image stimuli were alternated so they appeared equally often on both monitors/sides of the arena. To help minimize any time-of-day effects (Lazopulo et al. 2019), day/weather effects (Roitberg et al. 1993; Pellegrino et al. 2013), or cohort-of-butterflies effects, we ran bioassays in blocks that included all stimuli comparisons using butterflies from a single cohort. There were two exceptions to this blocking: (1) The color removal experiments commenced comparing R+G+B and G bioassay treatments at *AoP* 90° and only later included the remaining *AoP* 90° treatments; and (2) the *AoP* 0° bioassays in the color-removal experiment were a follow-up to the *AoP* 90° experiments and did not proceed concurrently.

5.3.3. Intensity-*vs*-Color Discrimination Experiment

To determine whether *P. rapae* females perceive differential *DoLP* as differential color or intensity, we performed experiments similar to those of Kinoshita et al. (2011). We presented females with paired stimuli consisting of the same cabbage image but modified to create differences in intensity (A), color and intensity (B), or *DoLP* and intensity (C) between the two images (Fig. 5.3; Table 5.1). The paired stimuli we presented were (A) two unmodified images both with a *DoLP* of 31%; (B) one unmodified (treatment) image and one red-shifted (control) image each at a *DoLP* of 31% (Table 5.1; Fig. 5.2d,e); and (C) two unmodified images presented with a *DoLP* of either 31% (treatment) or 50% (control). The image whose intensity remained constant in each sub-experiment was designated the control, but this control image was not identical in each sub-experiment. In A-C, we presented the treatment image at intensities lower (44%, 87%), equal (100%) and greater (130%) than the original

intensity (Table 5.1; Fig. 5.2d,e). In (A), we did not present a choice between two unmodified images (*DoLP* 31%, 100% intensity) assuming no preference in response.

5.3.4. Color-Removal Experiment

To determine the photoreceptors involved in polarized light discrimination, we modified the color of cabbage images and offered *P. rapae* females a series of choices between these modified images presented at a *DoLP* of either 31% or 50%, with both images presented at an *AoP* of both 0° and 90°. To minimize the stimulation of the butterflies' red photoreceptors, blue photoreceptors or both simultaneously (within the limits inherent in the RGB color space where each color channel stimulates multiple photoreceptor classes; Fig. 5.2c), we respectively set the red, blue, or red and blue values of all pixels in both stimulus images to 0 (Table 5.1; Fig. 5.2f). As a control, we also offered a choice between images with no modification to any pixel values.

5.3.5. Statistical Analysis

We used two-tailed chi-square tests to determine whether the proportion of *P. rapae* females responding to plant images differed from 0.5, and whether the proportion of females responding differed among the experimental treatments. We excluded non-responding females from statistical analyses.

5.3.6. Modeling Photoreceptor Quantum Catches

Unless otherwise noted, all spectra were measured with a calibrated spectrophotometer (HR-4000, Ocean Optics Inc., Dunedin, FL, USA) and were recently reported (Blake et al. 2020). To allow us to calculate the quantum catch of the background, we measured the ambient irradiance of the fluorescent lamps within the arena, the transmission of the arena wall and the λ/4 retarder film, and the reflectance of the brown kraft paper (Fig. 5.2a,b). We measured reflectance with a JAZ spectrometer (Ocean Optics) calibrated with a 99% Spectralon reflectance standard (SRS-99-010, Labsphere, NH, USA). Using photo polarimetry of the arena's interior (Foster et al. 2018), we approximated the mean *DoLP* and modal *AoP* of the background across the human visible spectrum (400-700 nm) to be 10% and 90°, respectively.

We also used this spectrometer to measure the irradiance produced by the monitors at a range of 8-bit RGB values including pure red, green and blue spectra ([255, 0, 0], [0, 255, 0], [0, 0, 255], respectively, Fig. 5.2c) in order to estimate the monitor's decoding gamma (γ = 1.90) and the intensity at a RGB value of 0 (0.0055). Using equation 1, a modified gamma correction incorporating a non-zero intercept (Burger and Burge 2009), we could appropriately scale and sum the pure spectra $I_C(\lambda)$ (where C is red, green or blue) using the red, green or blue pixel value PV_C to estimate the displayed irradiance spectra across all wavelengths (λ) from 300 to 750 nm for any combination of RGB values. Using the mean RGB pixel values of the stimulus image, we could then create a mean spectrum for all pixels displayed in the image. The resulting spectrum was corrected for the transmission spectrum of the aquarium wall and the λ/4 retarder film (Fig. 5.2a).

$$I(\lambda) = \sum_{C \in (R,G,B)} I_C(\lambda) \left(\frac{1}{1 + 0.0055}\right) \left(\frac{PV_C}{255}\right)^{\gamma + 0.0055} \quad (1)$$

Using wavelength-specific effects of the λ/4 retarder film along with measurements of a photoreceptor's *PS*, and the *AoP* of greatest sensitivity (ϕ_{max}) taken from Blake et al. (2019a), we could use equation 2 to calculate the wavelength-specific effect of polarization on the photoreceptor's response ($P_i(\lambda)$ for photoreceptor type *i*). This effect along with the previously mentioned intensity spectrum, and the reported spectral sensitivities of *P. rapae* photoreceptors (R_i) (Blake et al. 2019c), allowed us to model the quantum catch (Q_i) of all photoreceptor types with equation 3, with dλ being the spectral resolution of the spectrometer used to measure $I(\lambda)$, and with all other variables interpolated to match this resolution (Blake et al. 2020). The quantum catch of the background (Q_{ib}) was similarly calculated, with irradiance $I(\lambda)$ being determined from the irradiance spectra of fluorescence lamps and the reflectance spectra of the kraft paper. However, the measured values of *DoLP* and *AoP* (10% and 90°, respectively) determined from photo polarimetry were assumed to be uniform across 300-750 nm. As photoreceptors adapt to the background illumination, we then calculated the quantum catch relative to the background (q_i) (equation 4).

$$P_i(\lambda) = \frac{1}{PS_i} + \frac{PS_i - 1}{PS_i} \cdot \left[\frac{1 - DoLP(\lambda)}{2} + DoLP(\lambda) \cdot \cos^2(AoP(\lambda) - \phi_{\max}) \right] \quad (2)$$

$$Q_i = \int_{300}^{750} I(\lambda) R_i(\lambda) P_i(\lambda) \mathrm{d}\lambda \quad (3)$$

$$q_i = Q_i / Q_{ib} \quad (4)$$

5.4. Results

5.4.1. Intensity-*vs*-Color Discrimination Experiment

In general, when treatment and control stimuli differed only in intensity, *P. rapae* females preferred the more intense stimulus (Fig. 5.3a). This preference was statistically significant only when the intensity of treatment stimuli was <50% of that of the control stimuli (χ^2 = 8.70, *N* = 1, *P*=0.0032). When the treatment stimulus had an intensity of 87% relative to the control stimulus, females did not discriminate between these stimuli.

When we presented a choice between a red-shifted cabbage image (control) and an unmodified (treatment) image of varying intensity, females significantly preferred the treatment image only with an intensity of 87% relative to the control image (χ^2 = 12.30, *N* = 1, *P* = 0.0005; Fig. 5.3b). Treatment images of a higher or a lower intensity were not significantly preferred, although there was a marginal preference for the treatment image when it had an intensity equal to, or greater than, that of the control image.

Similarly, when the treatment and control image differed in *DoLP*, females significantly preferred the treatment image (*DoLP* 31%) only when it had an intensity equal to that of the control image (*DoLP* 50%; χ^2 = 8.32, *N* = 1, *P* = 0.0039; Fig. 5.3c). Treatment images of a lower intensity were as attractive as the control image while there was a non-significant preference for the control image when it was more intense.

5.4.2. Color-Removal Experiment

When cabbage images were presented with all color channels intact (R+G+B), *P. rapae* females preferred the image with the lower *DoLP* both at an *AoP* of 0° and 90° (*AoP* of

0°: χ^2 =7.36, *N* = 44, *P* = 0.0067; *AoP* of 90°: χ^2 = 15.25, *N* = 63, *P* = 0.0001; Fig. 5.4). When the blue color channel was removed (R+G), females shifted their preference towards the image with a higher *DoLP*, but only at an *AoP* of 0° (χ^2 = 18.75, *N*=86, *P*<0.0001). When the red color channel was removed (G+B), females preferred images with the higher *DoLP* at both *AoP*s (*AoP* of 0°: χ^2 = 11.72, *N* = 53, *P* = 0.0006; *AoP* of 90°: χ^2 = 7.41, *N* = 39, *P* = 0.0064). When only the green color channel of the image was included, females did not discriminate between images with a high or a low *DoLP*, when presented at an *AoP* of 90°. However, when these images were presented at an *AoP* of 0°, females chose the lower *DoLP* images (χ^2 = 9.28, *N* = 57, *P* = 0.0023) similar to their response when all color channels were intact.

5.5. Discussion

Our study refines the possible neurological processing mechanisms for *DoLP*-based host plant discrimination by female *P. rapae*. According to our data, *P. rapae* females are likely not perceiving differences in *DoLP* as differences in purely intensity or in color. Rather, our data suggest that perception of color, intensity and polarization, at least in the context of host-plant discrimination, are all linked and contingent upon one another.

The intensity-*vs*-color discrimination experiment revealed that females preferred the plant image with greater intensity when all other factors were equal (Fig. 5.3). In our study, color preferences shifted in response to intensity changes in one of the two test stimuli, contrasting with results obtained in similar studies with *Papilio* butterflies (Kelber and Pfaff 1999; Kinoshita et al. 2011). While it is possible that *P. rapae* lacks true color vision (the ability to discriminate between colors independent of intensity), this explanation seems unlikely given the shared evolutionary history of *Papilio* and *Pieris* butterflies as members of Papilionoidea (Wahlberg et al. 2005), and the similarities of their respective compound eyes (Kelber et al. 2001). Although our colored stimuli lacked an appreciable UV component (unlike many stimuli tested with *Papilio*), these stimuli should provide adequate stimulation of the UV photoreceptors to distinguish between stimuli in the color-removal experiment (Fig. 5.6b). Training of bioassay insects offers a more likely explanation for these contrasting results. While we tested the innate preferences of *P. rapae* females, corresponding studies with *Papilio* involved rewarded training (Kelber and Pfaff 1999; Kinoshita et al. 2011). The spontaneous color choices of *P. brassicae* also shift in accordance with stimulus intensity (Scherer and Kolb 1987),

however increases in intensity always have a positive effect on preference, contrasting our color preference data (Fig. 5.3b). When paired images were similar in color and *DoLP,* we observed a positive linear relationship between the intensity of the treatment image and the preference of female *P. rapae* for this image (Fig. 5.3a). In contrast, when image pairs were dissimilar in color or dissimilar in *DoLP,* female preference for the treatment image declined when the intensity of the treatment image was greater than that of the control image (Fig. 5.3b,c). Like in experiments with *Papilio*, these results suggest that *P. rapae* butterflies perceive differences in *DoLP* in a manner similar to their perception of differences in color, albeit not independent of intensity.

The color-removal experiment revealed that blue, green and red photoreceptors are involved in the perception of differential *DoLP*. This conclusion is based on data showing (*i*) preferential responses to images with a lower *DoLP* (*AoP*: 0° and 90°) when all color channels were present; (*ii*) a preference shift for images (*AoP*: 0° or 90°) where either the blue or the red channel was removed; and (*iii*) the reversal of preferences with the green-only channel images (*AoP*: 90°) as compared with R+G or G+B images (*AoP*: 90°).

Contrary to results of the intensity-*vs*-color discrimination experiment, modeling of photoreceptor catch does not support the concept that differences in *DoLP* are perceived as color differences, at least not when modeled as a linear interaction among photoreceptors (Kelber 1999, 2001). The color triangles represent the modeled *P. rapae* color space and depict the relative quantum catch of the red, green and shortwave (omitting UV in type I) photoreceptors of the three ommatidial types disregarding intensity (Fig. 5.5, 5.6). In modeling the catch of the red photoreceptors, we assumed the catch of R5-8 are pooled negating much of *PS* of these photoreceptors. If *DoLP* discrimination could be explained through linear interactions between different photoreceptors, as seen in *Papilio* and in *P. rapae* with unpolarized stimuli, we would expect a consistent direction of preference between stimuli. For example, using existing linear color models for *Papilio* and *Pieris*, with the catch of green photoreceptors having a positive effect and blue and red receptors having a negative effect, we would expect the stimuli closest to the upper green vertex to be preferred. In our modeling, stimuli differing only in polarization characteristics largely align along the blue to green axis, with the direction of preference among paired stimuli tested converging on no one region of the color space (Fig. 5.5). This inconsistency applied to all ommatidial types (Fig. 5.6),

albeit with smaller separations among low and high *DoLP* stimuli due to lower *PS* of the photoreceptors. It is unlikely that this inconsistency could be resolved even if downstream opponent processing was considered (Chen et al. 2019) or if photoreceptors were to be compared among different ommatidial types (Takemura and Arikawa 2005).

Other plausible mechanisms also fail to explain our bioassay results. If polarization discrimination by *P. rapae* were to be dependent on comparisons between any two polarization-sensitive photoreceptors, or between one polarization-sensitive and one insensitive photoreceptor, we would expect *AoP* to have a strong effect on preference (Fig. 5.7a; How and Marshall, 2014), similar to how *Papilio* butterflies strongly prefer horizontally over vertically polarized light (Kelber 2001). We would also expect such comparisons among photoreceptors to result in either a linear increase or decrease in preferential response as *DoLP* increased (Fig. 5.7b; How and Marshall, 2014). Yet, we found that the attractiveness of test stimuli was not affected by *AoP* outside regions near 45° and 135°, and that images with a *DoLP* similar to that of their cabbage host plants (*DoLP* of 31%) are preferred, with the appeal of stimuli declining both above and below this 31% value (Blake et al. 2019a). Comparisons between two or more pairs of photoreceptors are also unlikely to explain the observed *DoLP* preferences of *P. rapae* (Fig. 5.7ef). Models that incorporated the absolute value of the differences in responses between photoreceptors (Fig. 5.7cd; Meglič et al., 2019) could explain observed *AoP* preferences in *P. rapae*, but again would fail to explain *DoLP* preferences. The results of the color-removal experiment preclude true polarization vision (the ability to discriminate among stimuli independent of color or intensity), as changes in color prompted large shifts in polarization preference.

Our combined results suggest that a new and as of yet undescribed mechanism for the processing of polarized reflections underlying *DoLP* discrimination in *P. rapae*. The mechanism likely involves blue, green and red photoreceptor classes, and is affected by intensity, color and polarization. If true, this would be yet another example of unique neural processing of polarization information from object-reflected light. The systems for processing such information differ between all taxa thus far studied, including crabs (Smithers et al. 2019), fruit flies (Wernet et al. 2012), horse flies (Meglič et al. 2019), and backswimmers (Schwind 1984). There are even as many as three different systems at work in *Papilio* butterflies depending on the behavioral context

(Kelber et al. 2001; Kinoshita et al. 2011; Stewart et al. 2019). This information seems to show that different arthropod taxa have utilized the polarization sensitivity inherent in rhabdomeric photoreceptors to create visual subsystems tuned in accordance to their particular ecology. Further investigations into different arthropod taxa will almost certainly reveal novel combinations and processing of photoreceptor inputs using polarized light for object recognition.

5.6. References

Blake AJ, Go MC, Hahn GS, Grey H, Couture S, Gries G (2019a) Polarization of foliar reflectance: novel host plant cue for insect herbivores. Proc R Soc B Biol Sci 286:20192198. https://doi.org/10.1098/rspb.2019.2198

Blake AJ, Go MC, Hahn GS, Grey H, Couture S, Gries G (2019b) λ/4 Retarder Film Measurement from: Polarization of foliar reflectance – novel host plant cue for insect herbivores. Dryad. https://doi.org/10.5061/dryad.xgxd254bs

Blake AJ, Pirih P, Qiu X, Arikawa K, Gries G (2019c) Compound eyes of the small white butterfly *Pieris rapae* have three distinct classes of red photoreceptors. J Comp Physiol A 205:553–565. https://doi.org/10.1007/s00359-019-01330-8

Burger W, Burge MJ (2009) Digital image processing: an algorithmic introduction using Java, 1st edn. Springer, New York

Chen P-J, Belušič G, Arikawa K (2019) Chromatic information processing in the first optic ganglion of the butterfly *Papilio xuthus*. J Comp Physiol A. https://doi.org/10.1007/s00359-019-01390-w

Foster JJ, Temple SE, How MJ, et al (2018) Polarisation vision: overcoming challenges of working with a property of light we barely see. Sci Nat 105:27. https://doi.org/10.1007/s00114-018-1551-3

Grant L, Daughtry CST, Vanderbilt VC (1993) Polarized and specular reflectance variation with leaf surface features. Physiol Plant 88:1–9. https://doi.org/10.1111/j.1399-3054.1993.tb01753.x

Heinloth T, Uhlhorn J, Wernet MF (2018) Insect responses to linearly polarized reflections: orphan behaviors without neural circuits. Front Cell Neurosci 12:50. https://doi.org/10.3389/fncel.2018.00050

Horváth G, Csabai Z (2014) Polarization Vision of Aquatic Insects. In: Horváth G (ed) Polarized Light and Polarization Vision in Animal Sciences. Springer Berlin Heidelberg, Berlin, Heidelberg, pp 113–145

Horváth G, Gál J, Labhart T, Wehner R (2002) Does reflection polarization by plants influence colour perception in insects? Polarimetric measurements applied to a polarization-sensitive model retina of *Papilio* butterflies. J Exp Biol 205:3281–3298

Horváth G, Varjú D (2004) Polarized Light in Animal Vision: Polarization Patterns in Nature. Springer, New York

How MJ, Marshall NJ (2014) Polarization distance: a framework for modelling object detection by polarization vision systems. Proc R Soc B Biol Sci 281:20131632. https://doi.org/10.1098/rspb.2013.1632

Ilić M, Pirih P, Belušič G (2016) Four photoreceptor classes in the open rhabdom eye of the red palm weevil, *Rynchophorus ferrugineus* Olivier. J Comp Physiol A 202:203–213. https://doi.org/10.1007/s00359-015-1065-9

Johnsen S (2011) The Optics of Life. Princeton University Press, New Jersey

Kelber A (2001) Receptor based models for spontaneous colour choices in flies and butterflies. Entomol Exp Appl 99:231–244. https://doi.org/10.1046/j.1570-7458.2001.00822.x

Kelber A (1999) Ovipositing butterflies use a red receptor to see green. J Exp Biol 202:2619–2630

Kelber A, Pfaff M (1999) True colour vision in the orchard butterfly, *Papilio aegeus*. Naturwissenschaften 86:221–224. https://doi.org/10.1007/s001140050601

Kelber A, Thunell C, Arikawa K (2001) Polarisation-dependent colour vision in *Papilio*. J Exp Biol 204:2469–2480

Kinoshita M, Yamazato K, Arikawa K (2011) Polarization-based brightness discrimination in the foraging butterfly, *Papilio xuthus*. Philos Trans R Soc B Biol Sci 366:688–696. https://doi.org/10.1098/rstb.2010.0200

Labhart T, Meyer EP (1999) Detectors for polarized skylight in insects: a survey of ommatidial specializations in the dorsal rim area of the compound eye. Microsc Res Tech 47:368–379. https://doi.org/10.1002/(SICI)1097-0029(19991215)47:6<368::AID-JEMT2>3.0.CO;2-Q

Lazopulo S, Lazopulo A, Baker JD, Syed S (2019) Daytime colour preference in *Drosophila* depends on the circadian clock and TRP channels. Nature 574:108–111. https://doi.org/10.1038/s41586-019-1571-y

Meglič A, Ilić M, Pirih P, et al (2019) Horsefly object-directed polarotaxis is mediated by a stochastically distributed ommatidial subtype in the ventral retina. Proc Natl Acad Sci 116:21843–21853. https://doi.org/10.1073/pnas.1910807116

Mishra M (2015) An eye ultrastructure investigation of a plant pest *Acyrthosiphon pisum* (Harris) (Insecta: Hemiptera: Aphididae). Open Access Insect Physiol 5:41–46. https://doi.org/10.2147/OAIP.S84633

Pellegrino AC, Peñaflor MFGV, Nardi C, et al (2013) Weather forecasting by insects: Modified sexual behaviour in response to atmospheric pressure changes. PLoS ONE 8:e75004. https://doi.org/10.1371/journal.pone.0075004

Qiu X, Vanhoutte K, Stavenga DG, Arikawa K (2002) Ommatidial heterogeneity in the compound eye of the male small white butterfly, *Pieris rapae crucivora*. Cell Tissue Res 307:371–379. https://doi.org/10.1007/s00441-002-0517-z

Roitberg BD, Sircom J, Roitberg CA, et al (1993) Life expectancy and reproduction. Nature 364:108–108. https://doi.org/10.1038/364108a0

Scherer C, Kolb G (1987) Behavioral experiments on the visual processing of color stimuli in *Pieris brassicae* L. (Lepidoptera). J Comp Physiol A 160:645–656. https://doi.org/10.1007/BF00611937

Schwind R (1984) Evidence for true polarization vision based on a two-channel analyzer system in the eye of the water bug, *Notonecta glauca*. J Comp Physiol A 154:53–57. https://doi.org/10.1007/BF00605390

Shashar N, Cronin TW, Wolff LB, Condon MA (1998) The polarization of light in a tropical rain forest. Biotropica 30:275–285. https://doi.org/10.1111/j.1744-7429.1998.tb00061.x

Shimohigashi M, Tominaga Y (1991) Identificaton of UV, green and red receptors, and their projection to lamina in the cabbage butterfly, *Pieris rapae*. Cell Tissue Res 263:49–59. https://doi.org/10.1007/BF00318399

Smithers SP, Roberts NW, How MJ (2019) Parallel processing of polarization and intensity information in fiddler crab vision. Sci Adv 5:eaax3572. https://doi.org/10.1126/sciadv.aax3572

Snyder AW (1973) Polarization sensitivity of individual retinula cells. J Comp Physiol A 83:331–360. https://doi.org/10.1007/BF00696351

Stewart FJ, Kinoshita M, Arikawa K (2019) Monopolatic motion vision in the butterfly *Papilio xuthus*. J Exp Biol 222:jeb191957. https://doi.org/10.1242/jeb.191957

Takemura SY, Arikawa K (2005) Ommatidial type-specific interphotoreceptor connections in the lamina of the swallowtail butterfly, *Papilio xuthus*. J Comp Neurol 494:663–672. https://doi.org/10.1002/cne.20830

Wachmann E (1977) Vergleichende Analyse der feinstrukturellen Organisation offener Rhabdome in den Augen der Cucujiformia (Insecta, Coleoptera), unter besonderer Berücksichtigung der Chrysomelidae. Zoomorphologie 88:95–131. https://doi.org/10.1007/BF01880649

Wahlberg N, Braby MF, Brower AVZ, et al (2005) Synergistic effects of combining morphological and molecular data in resolving the phylogeny of butterflies and skippers. Proc R Soc B Biol Sci 272:1577–1586. https://doi.org/10.1098/rspb.2005.3124

Webb S, Shelton AM (1988) Laboratory rearing of the imported cabbageworm. New Yorks Food Life Sci Bull 122:1–6

Wehner R, Bernard GD (1993) Photoreceptor twist: a solution to the false-color problem. Proc Natl Acad Sci 90:4132–4135. https://doi.org/10.1073/pnas.90.9.4132

Wernet MF, Velez MM, Clark DA, et al (2012) Genetic dissection reveals two separate retinal substrates for polarization vision in *Drosophila*. Curr Biol 22:12–20. https://doi.org/10.1016/j.cub.2011.11.028

5.7. Tables

Table 5.1 **The mean RGB pixel values of plant images along with the corrections necessary to generate these images from the unmodified originals. The mean values were calculated from individual RGB means of each image. Also included are the degree of linear polarization (*DoLP*) and axis of polarization (*AoP*) of stimuli used in each experiment.**

intensity-*vs*-color discrimination experiment (A) - intensity difference

treatment image						control image					
	R	G	B	*DoLP*	*AoP*		R	G	B	*DoLP*	*AoP*
	72 ± 1 (0.64×R)	82 ± 2 (0.64×G)	64 ± 2 (0.64×G)	31%	90°		112 ± 2 (1.00×R)	129 ± 3 (1.00×G)	100 ± 3 (1.00×G)	31%	90°
	105 ± 2 (0.93×R)	120 ± 3 (0.93×G)	93 ± 2 (0.93×G)	31%	90°		112 ± 2 (1.00×R)	129 ± 3 (1.00×G)	100 ± 3 (1.00×G)	31%	90°
	129 ± 3 (1.15×R)	148 ± 3 (1.15×G)	115 ± 3 (1.15×G)	31%	90°		112 ± 2 (1.00×R)	129 ± 3 (1.00×G)	100 ± 3 (1.00×G)	31%	90°

intensity-*vs*-color discrimination experiment (B) - color difference

treatment image						control image					
	R	G	B	*DoLP*	*AoP*		R	G	B	*DoLP*	*AoP*
	72 ± 1 (0.64×R)	82 ± 2 (0.64×G)	64 ± 2 (0.64×G)	31%	90°		237 ± 1 (0.38×R+195)	93 ± 2 (0.72×G)	82 ± 2 (0.82×G)	31%	90°
	105 ± 2 (0.93×R)	120 ± 3 (0.93×G)	93 ± 2 (0.93×G)	31%	90°		237 ± 1 (0.38×R+195)	93 ± 2 (0.72×G)	82 ± 2 (0.82×G)	31%	90°
	112 ± 2 (1.00×R)	129 ± 3 (1.00×G)	100 ± 3 (1.00×G)	31%	90°		237 ± 1 (0.38×R+195)	93 ± 2 (0.72×G)	82 ± 2 (0.82×G)	31%	90°
	129 ± 3 (1.15×R)	148 ± 3 (1.15×G)	115 ± 3 (1.15×G)	31%	90°		237 ± 1 (0.38×R+195)	93 ± 2 (0.72×G)	82 ± 2 (0.82×G)	31%	90°

intensity-*vs*-color discrimination experiment (C) - *DoLP* difference

treatment image						control image					
	R	G	B	*DoLP*	*AoP*		R	G	B	*DoLP*	*AoP*
	72 ± 1 (0.64×R)	82 ± 2 (0.64×G)	64 ± 2 (0.64×G)	31%	90°		112 ± 2 (1.00×R)	129 ± 3 (1.00×G)	100 ± 3 (1.00×G)	50%	90°
	105 ± 2 (0.93×R)	120 ± 3 (0.93×G)	93 ± 2 (0.93×G)	31%	90°		112 ± 2 (1.00×R)	129 ± 3 (1.00×G)	100 ± 3 (1.00×G)	50%	90°
	112 ± 2 (1.00×R)	129 ± 3 (1.00×G)	100 ± 3 (1.00×G)	31%	90°		112 ± 2 (1.00×R)	129 ± 3 (1.00×G)	100 ± 3 (1.00×G)	50%	90°
	129 ± 3 (1.15×R)	148 ± 3 (1.15×G)	115 ± 3 (1.15×G)	31%	90°		112 ± 2 (1.00×R)	129 ± 3 (1.00×G)	100 ± 3 (1.00×G)	50%	90°

color-removal experiment

	R	G	B	*DoLP*	*AoP*		R	G	B	*DoLP*	*AoP*
	112 ± 2 (1.00×R)	129 ± 3 (1.00×G)	100 ± 3 (1.00×G)	50%	90°		112 ± 2 (1.00×R)	129 ± 3 (1.00×G)	100 ± 3 (1.00×G)	31%	90°
	112 ± 2 (1.00×R)	129 ± 3 (1.00×G)	0 ± 0 (0.00×G)	50%	90°		112 ± 2 (1.00×R)	129 ± 3 (1.00×G)	0 ± 0 (0.00×G)	31%	90°
	0 ± 0 (0.00×R)	129 ± 3 (1.00×G)	100 ± 3 (1.00×G)	50%	90°		0 ± 0 (0.00×R)	129 ± 3 (1.00×G)	100 ± 3 (1.00×G)	31%	90°
	0 ± 0 (0.00×R)	129 ± 3 (1.00×G)	0 ± 0 (0.00×G)	50%	90°		0 ± 0 (0.00×R)	129 ± 3 (1.00×G)	0 ± 0 (0.00×G)	31%	90°

5.8. Figures

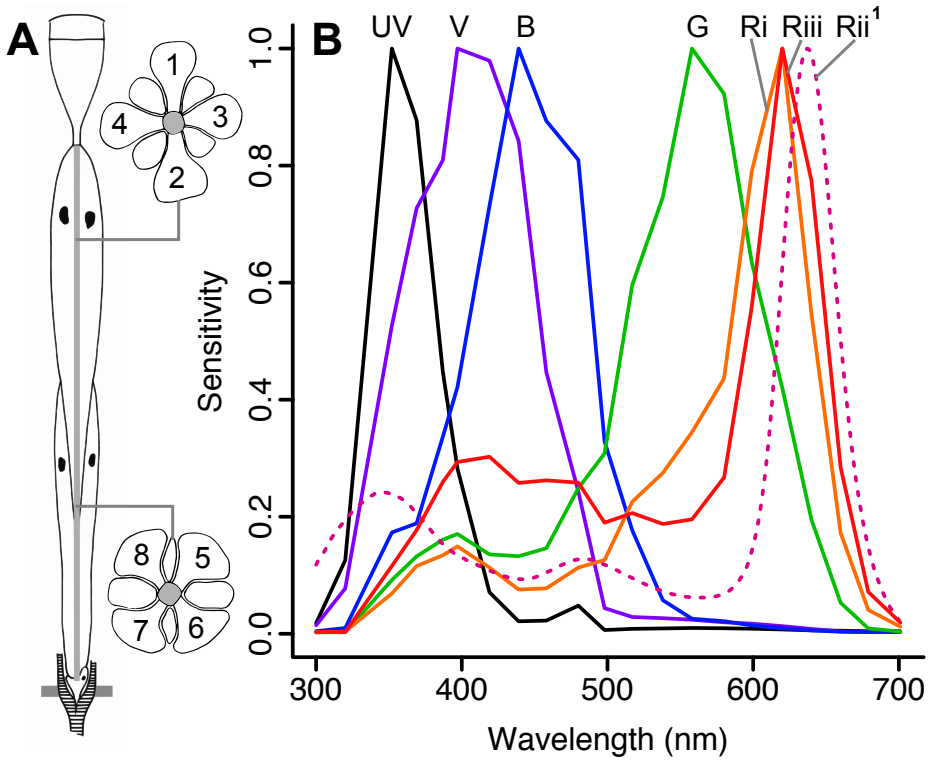

C

		I[2]			II[2]			III[2]		
		S(λ)	*PS*	ϕ_{max}(°)	*S*(λ)	*PS*	ϕ_{max}(°)	*S*(λ)	*PS*	ϕ_{max}(°)
photoreceptor	R1	UV[3]	1.1	NA	V	1.2	7	UV	1.1	NA
	R2	B[3]	2.9	6	V	1.2	7	UV	1.1	NA
	R3,4	G	1.9	95	G	1.3[4]	91[4]	G	1.9	95
	R5,7	Ri	2.2	155	Rii[1]	1.9[4]	131[4]	Riii	2.1	156
	R6,8	Ri	2.2	34	Rii[1]	1.9[4]	52[4]	Riii	2.1	33
	R9	R?	?	?	R?	?	?	R?	?	?

Figure 5.1 **Visual system of female *Pieris rapae*. (A) Diagram of ommatidium showing the arrangement of the nine photoreceptors (R1-9). (B) Spectral sensitivities, S(λ), of the various photoreceptor spectral classes. Ultraviolet (UV), violet (V), blue (B), green (G), type I-III red (Ri-Riii). [1]Spectral sensitivity predicted from a model of the female ommatidium (Stavenga and Arikawa 2011). (C) Table summarizing the spectral class and polarization characteristics (polarization sensitivity: *PS*; axis of maximal polarization sensitivity: ϕ_{max}) of photoreceptors R1-9 in [2]ommatidial types I-III. [3]UV and blue photoreceptors are positioned opposite each other but are equally likely to be in the R1 or R2 position. [4]Values inferred from electrophysiological recordings of male butterflies.**

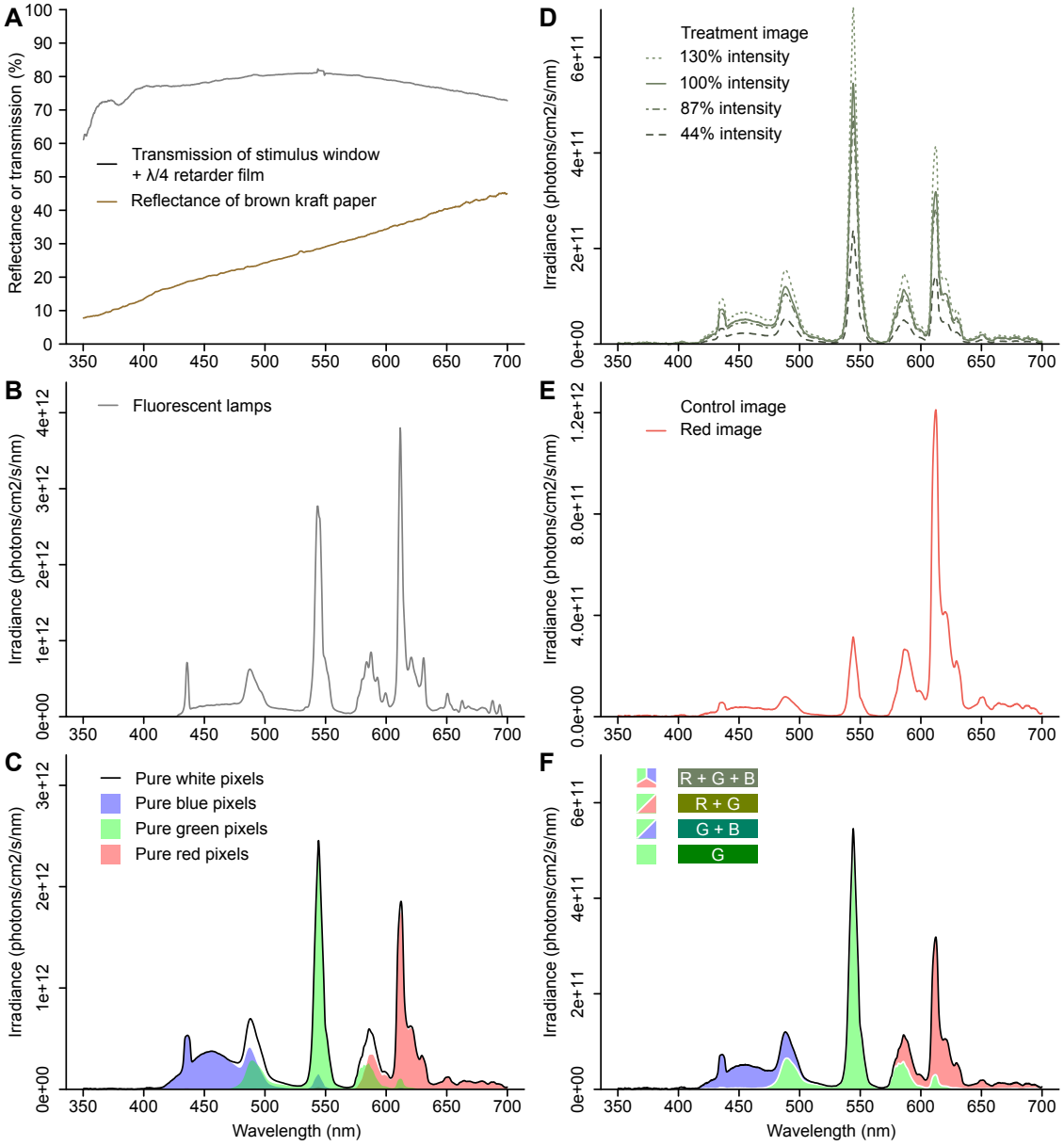
A
Reflectance or transmission (%)
Transmission of stimulus window
+ λ/4 retarder film
Reflectance of brown kraft paper
B
Irradiance (photons/cm2/s/nm)
Fluorescent lamps
C
Irradiance (photons/cm2/s/nm)
Pure white pixels
Pure blue pixels
Pure green pixels
Pure red pixels
Wavelength (nm)
D
Irradiance (photons/cm2/s/nm)
Treatment image
130% intensity
100% intensity
87% intensity
44% intensity
E
Irradiance (photons/cm2/s/nm)
Control image
Red image
F
Irradiance (photons/cm2/s/nm)
R + G + B
R + G
G + B
G
Wavelength (nm)

Figure 5.2 **Spectra of filters, background, and illumination sources. (A) Transmission spectrum of the stimulus windows of the experimental arena (Fig. 4.3) with a λ/4 retarder film and the reflectance spectrum of the background brown kraft paper. (B) Irradiance of the fluorescent lamps measured from within the arena at its center. (C) Irradiance of white (RGB: 255, 255, 255), blue (0, 0, 255), green (0, 255, 0), or red pixels (0, 0, 255) as measured from the other surface of the display of the bioassay monitors (mean of both LCD monitors). (D) Differences in irradiance spectra among different control image intensities used in the intensity-*vs*-color discrimination experiment. (E) Spectra of the red control image in the color difference portion of the intensity-*vs*-color discrimination experiment. (F) Spectra of stimuli tested in the color-removal experiment, where the red, blue, or red and blue, pixel values were set to 0. The spectra in D-F were calculated using equation 1 from the mean pixel values in Table 5.1.**

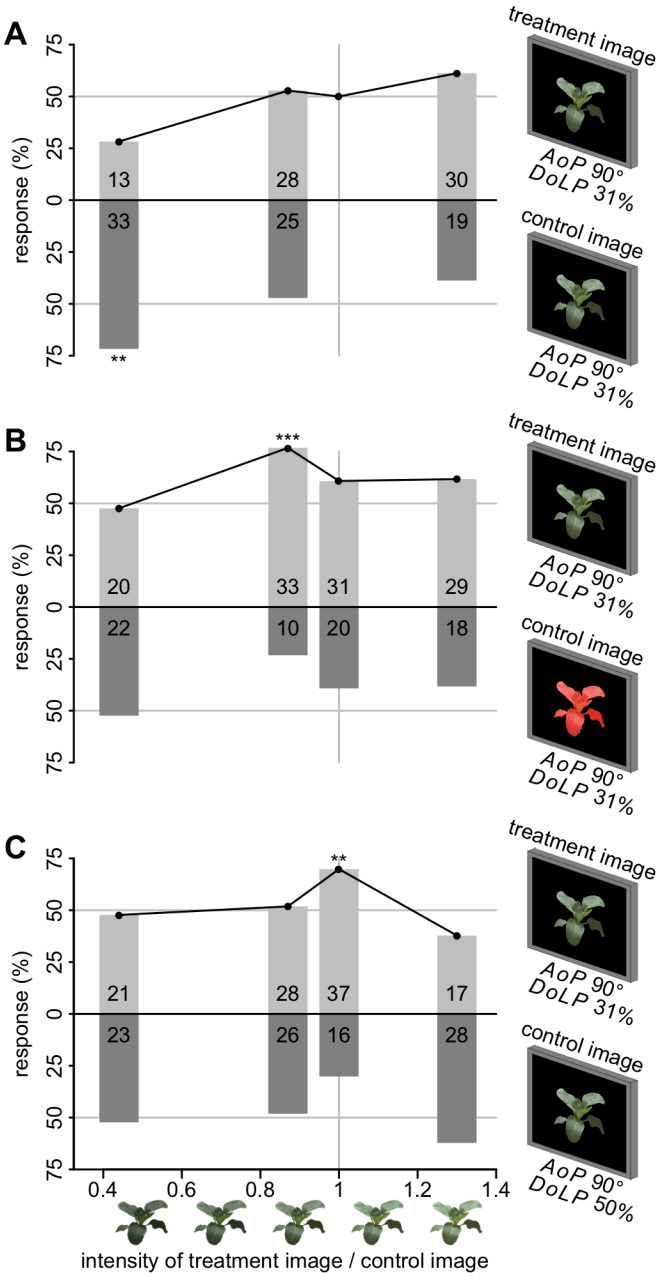

Figure 5.3 **Intensity-vs-color discrimination experiment. Effect of relative increase in intensity of the treatment image on the preference of *Pieris rapae* females when treatment and control images differ only in intensity (A), in both color and intensity (B), and in both *DoLP* and intensity (C). The responses in (A) to treatment and control images of equal brightness were assumed to be 50%. Numbers of females responding to each stimulus are shown within bars. The asterisk(s) indicate(s) a proportion deviating from 50% (χ^2 test, * p < 0.05, ** p < 0.01, *** p < 0.001). *AoP* = Axis of Polarization; *DoLP* = Degree of Linear Polarization**

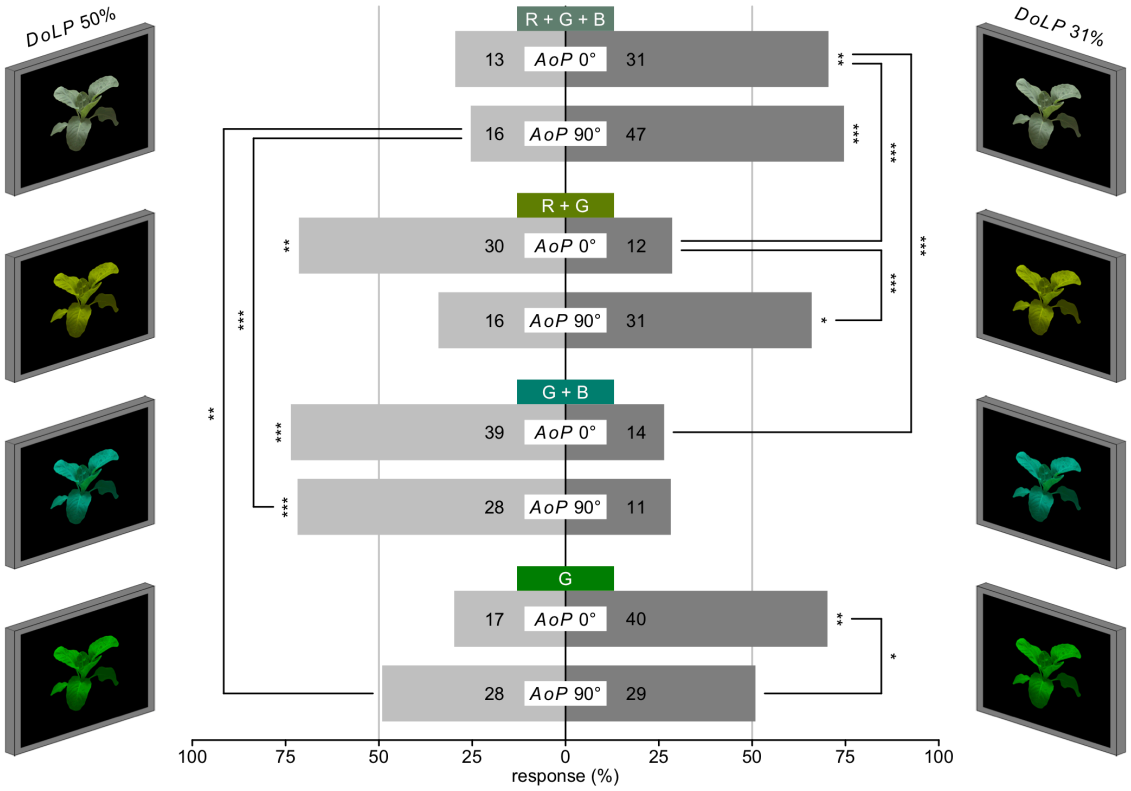

Figure 5.4 **Color-removal experiment. Changes in the preference of *P. rapae* females for cabbage plant images differing in *DoLP*, with removal of RGB color channels. The stimulus images display unmodified RGB pixel values or have the red, blue, or red and blue values of all pixels in both stimulus images set to 0 (top to bottom). Numbers of females responding to each stimulus are shown within bars. The asterisk(s) indicate(s) a proportion deviating from 50% or a significant difference between two proportions (χ^2 test, * $p < 0.05$, ** $p < 0.01$, *** $p < 0.001$). Note: the 31% *DoLP* is typical of cabbage plants. *AoP* = Axis of Polarization; *DoLP* = Degree of Linear Polarization**

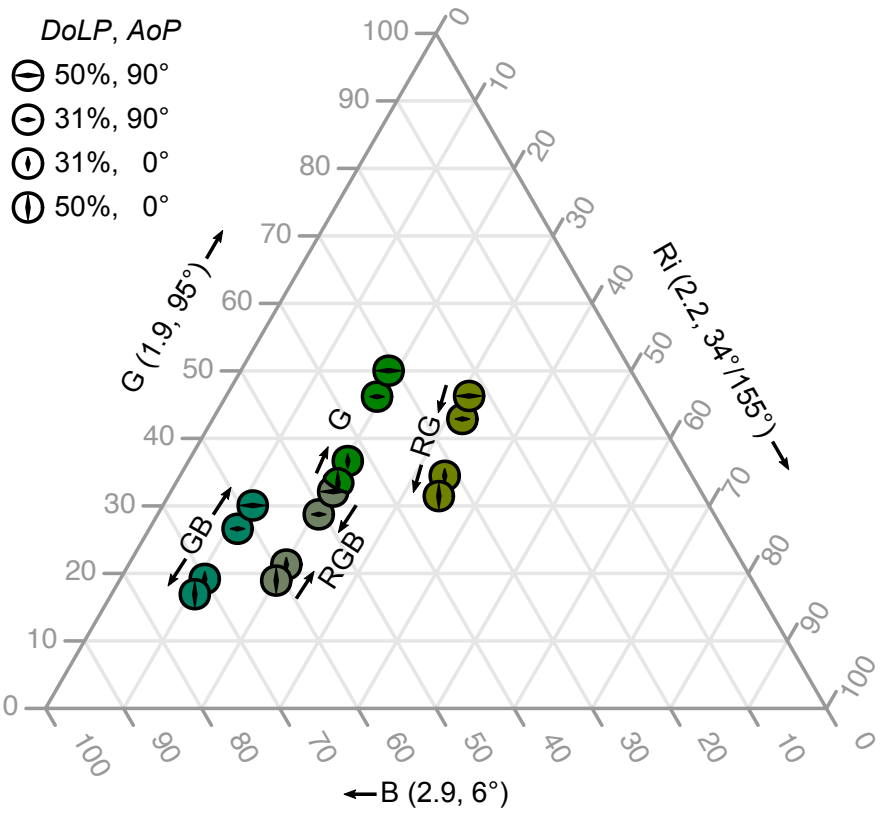

Figure 5.5 **Color triangle representing the modeled color space of *Pieris rapae* females. This triangle shows a model of relative blue (B), green (G) and red photoreceptors' (Ri) quantum catch in type I ommatidia. This color does not include the ultraviolet (UV) photoreceptor which was deemed acceptable due to the low levels of illumination in the UV range and the low *PS* of UV photoreceptors. The numbers in parentheses show the *PS* and ϕ_{max} of each receptor. The colored circles show the stimuli in the color-removal experiment. Arrows indicate the stimuli preferred by female *P. rapae*.**

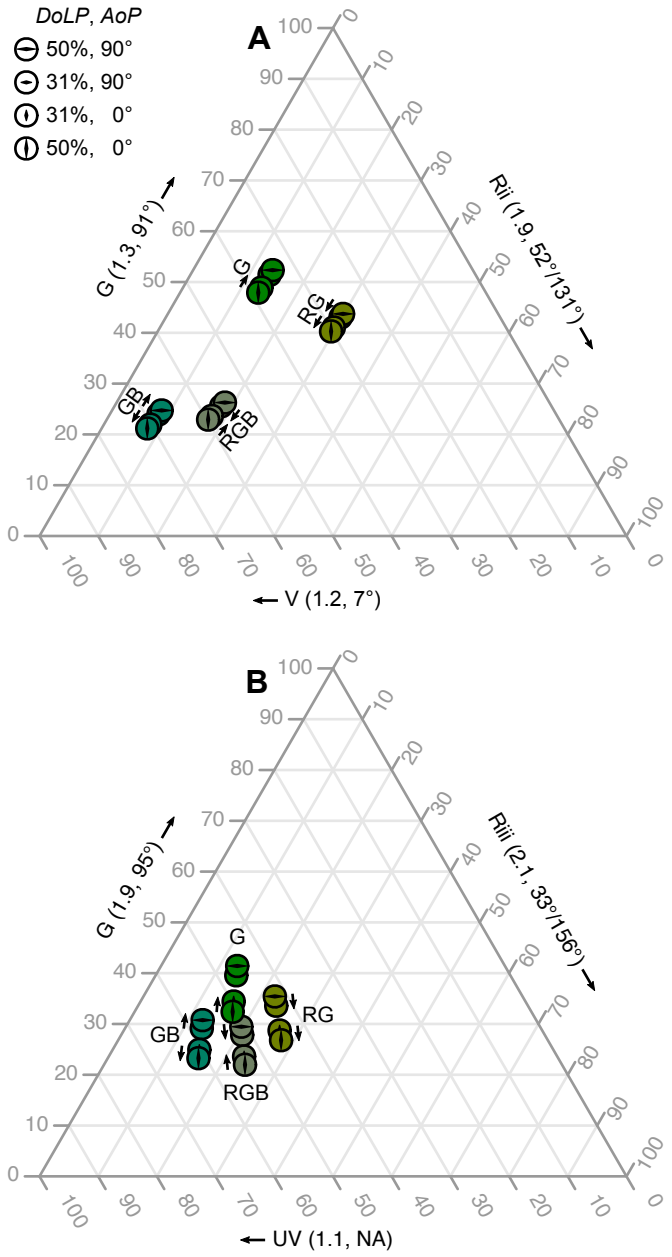

Figure 5.6 **Color triangles representing the modeled color space of *Pieris rapae* females. Triangles show a model of relative ultraviolet (UV), violet (V), green (G) and red photoreceptors' (Rii or Riii) quantum catch in type II (A) and III (B) ommatidia. The numbers in parentheses show the polarization sensitivity (PS) and axis of maximal polarization sensitivity (ϕ_{max}) of each receptor. The colored circles show the stimuli tested in the color-removal experiment. Arrows indicate the stimuli preferred by female *P. rapae*. DoLP, degree of linear polarization. AoP, axis of polarization.**

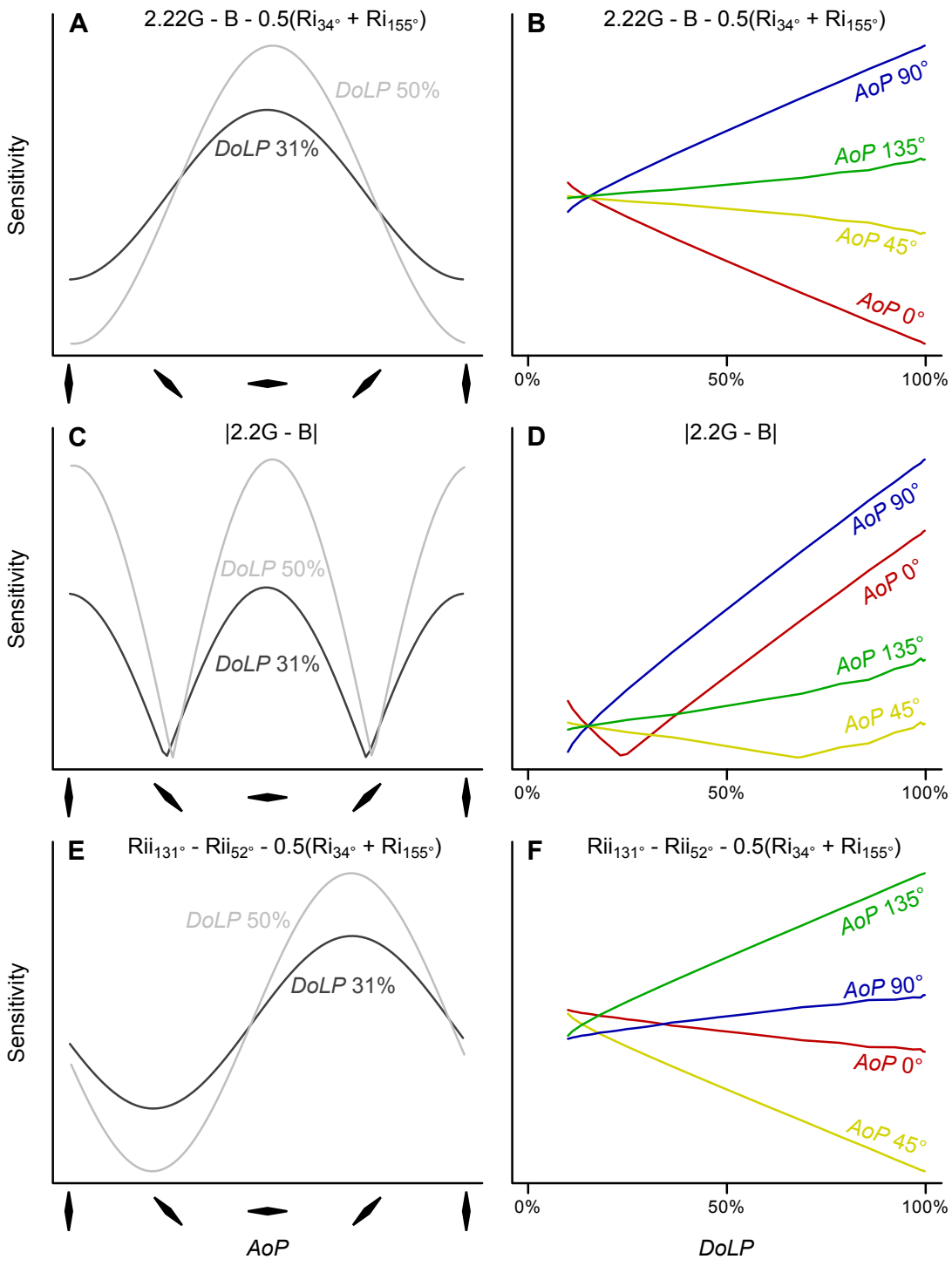
A
2.22G - B - 0.5(Ri34° + Ri155°)
DoLP 50%
DoLP 31%
Sensitivity
B
2.22G - B - 0.5(Ri34° + Ri155°)
AoP 90°
AoP 135°
AoP 45°
AoP 0°
0%
50%
100%
C
|2.2G - B|
DoLP 50%
DoLP 31%
Sensitivity
D
|2.2G - B|
AoP 90°
AoP 0°
AoP 135°
AoP 45°
0%
50%
100%
E
Rii131° - Rii52° - 0.5(Ri34° + Ri155°)
DoLP 50%
DoLP 31%
Sensitivity
AoP
F
Rii131° - Rii52° - 0.5(Ri34° + Ri155°)
AoP 135°
AoP 90°
AoP 0°
AoP 45°
0%
50%
100%
DoLP

Figure 5.7 **Effect of AoP and DoLP image manipulations on models combining photoreceptor catch from *Pieris rapae* females. (A,C,E), Effect of AoP on models at DoLPs of 31% and 50%. (B,D,F), Effect of DoLP on models at AoPs of 0°, 45°, 90°, and 135°. (A,B), Color model involving red, green and blue photoreceptors from type I ommatidia (Fig. 5.5) which would also be representative of any comparisons between polarization-sensitive photoreceptors, or between one polarization-sensitive and one polarization-insensitive photoreceptor. (C,D), Model calculating the absolute difference between two photoreceptors. (E,F), Model comparing more than two photoreceptors. AoP = Axis of Polarization; DoLP = Degree of Linear Polarization**

Chapter 6.

Concluding summary

For this chapter, I review my findings in bullet form and emphasize their impact.

- There are large differences in the degree of linear polarization (*DoLP*) of leaf-reflected light among plant species generally and between host and non-host plants of *Pieris rapae* specifically.
- These differences are most pronounced in the blue and ultraviolet (UV) color bands.
- UV polarimetry data closely resemble those of the human-visible color bands, especially blue.
- Recorded reflections from entire plants, rather than single leaves, reveal several emergent phenomena related to the effects of observer and light source position on the polarization of foliar reflections.
- Plants that are lit more from the side than from above (greater ψ) have a relatively greater leaf area shadowed by their own leaves. These shadowed areas have a lower *DoLP*, lowering the plants' overall *DoLP* even when the reflections are at the Brewster's angle.
- Modeling the data from photo polarimetry measurements of entire plants under a range of light source and observer positions, revealed that certain approach trajectories are optimal for foraging insects to discriminate between plant species on the basis of the *DoLP* of leaf-reflected light.
- These differences among plant species show that the *DoLP* of foliar reflection carries information about potential hosts and that this information could be used as a host plant cue by insect herbivores.
- Comparisons of the compound eyes of the two subspecies of *P. rapae* using genetic, microscopical, spectrographic and histological methods show no differences that would meaningfully affect photoreceptor sensitivity.
- My investigations of the compound eye further revealed that the peri-rhabdomal reddish-screening pigments differ among the three ommatidial types, with each ommatidial type exhibiting a unique class of red photoreceptor with a distinct spectral peak.
- Electrophysiological recordings show that the blue, green, and red photoreceptors of *P. rapae* exhibit a polarization sensitivity (PS) > 2, confirming the ability of *P. rapae* to perceive polarized light.

- Females of *P. rapae* preferred digital images of their cabbage host plant with a low *DoLP* (31%; characteristic of cabbage foliage) to images of a non-host potato plant with a higher *DoLP* (50%).

- When these images were presented with the *DoLP*s reversed, we were able to make the virtual potato non-host plant image as attractive as the cabbage host plant image with its typical *DoLP*, indicating that the *DoLP* had a greater effect on foraging decisions than color, intensity or shape.

- Additional bioassays determined the attractive range of *DoLP* and axis of polarization (*AoP*), showing that *P. rapae* females discriminate against *DoLP*s outside the range typical of their host plants (31%), but that females are relatively indifferent to the AoP of plants, except for *AoP*s near 45° and 135° which are repellent.

- These behavioral experiments demonstrate that *P. rapae* females discriminate between plants, or plant images, on the basis of their *DoLP*.

- When I presented *P. rapae* females choices between plant image stimuli that differed in either color or *DoLP*, both decreasing and increasing the intensity of the more attractive stimulus reduced the strength of preference. This result suggests that differences in color and *DoLP* are perceived in a similar manner.

- In similar bioassays, When I offered *P. rapae* females a *DoLP* choice between plant images manipulated to minimize the response of blue, red, or blue and red photoreceptors, females shifted their preference for *DoLP*, suggesting a role for all of these photoreceptors.

- Modeling of *P. rapae* photoreceptor responses to test stimuli suggests that differential *DoLP* is not perceived solely as a color difference.

- The combined results of behavioral bioassays and this modeling indicate that *P. rapae* females process and interpret polarization reflections in a way different from that described for other polarization-sensitive taxa.

- My findings (1) that the *DoLP* differs between host and non-host plants of *P. rapae*, (2) that *P. rapae* females possess several photoreceptor classes capable of perceiving differences in polarization, and (3) that these differences affect host plant selection behaviour by *P. rapae* females, all support earlier predictions that insect herbivores exploit foliar *DoLP* to recognize host plants. The given the prevalence polarization sensitivity among insects, exploitation of these cues may be widespread among herbivorous insects.